BEYOND THE CROAK:

DECODING THE SILENT COMMUNICATION OF FROGS

JHAEL ALEJANDRA ORTEGA PAEZ

A THESIS SUBMITTED TO THE FACULTY OF GRADUATE STUDIES IN PARTIAL FULFILLMENT OF THE REQUIREMENTS FOR THE DEGREE OF MASTER OF SCIENCE

GRADUATE PROGRAM IN BIOLOGY

YORK UNIVERSITY

TORONTO, ONTARIO

August, 2025

©Jhael Alejandra Ortega Paez, 2025

Abstract

Frogs rely on vocal signals for social interactions, which depend on a functional auditory system. Yet multiple lineages have independently lost critical auditory structures, raising questions about how communication is maintained. We hypothesized that visual adaptations could compensate for reduced auditory capacity. To test this, we measured eye and corneal size across 264 anuran species and assessed associations with ecological traits and auditory condition. We also sequenced the genome of *Pristimantis brevicrus*, an earless species, to examine the molecular evolution of visual opsins. Species with auditory reductions had smaller eyes, but non-fossorial taxa exhibited enlarged corneas, enhancing light sensitivity at lower metabolic cost. Analyses of RH1, SWS1, SWS2, and LWS revealed predominant purifying selection, while species with auditory loss showed relaxed constraint and positive selection, particularly in SWS1 and LWS. These findings suggest that visual adaptations compensate for auditory loss, highlighting sensory trade-offs as drivers of anuran communication and evolution.

Dedication

To Rashin and Joaquin,
you both healed me in every possible way.
Never leave me.

Acknowledgements

I would like to thank my supervisor, Dr. Ryan Schott, for welcoming me into his lab and for giving me the freedom to develop and pursue my own research ideas. I am also deeply grateful to Dr. Elizabeth Clare, a member of my project committee, who has supported me from the beginning of this work with thoughtful feedback and detailed suggestions. I also thank my thesis committee as a whole for their guidance throughout this process.

I am grateful to Dr. Santiago Ron and Dr. Omar Torres, curators of the Herpetology Museum QCAZ at the Pontificia Universidad Católica del Ecuador, for granting me access to specimens in the collection and for their invaluable logistical support during fieldwork. Their help with permit applications and the exportation of tissue samples used in this thesis was essential.

I also want to thank the students in my lab for their collaboration and contributions during my time in the program.

To my parents, thank you for being the most wonderful people I know, for always supporting my decisions, and for being present even from afar. I am deeply thankful to my sisters, who are the best part of my life, and to my younger siblings, whose love, support, and kindness have always lifted my spirits. To my grandparents, these achievements are also yours. I would not be here without your constant care and love.

To Joaquin, thank you for all your love, patience, support, and strength throughout this journey. I truly could not have done it without you.

To my dear friend Rashin, thank you for being such a constant and caring presence, and for the little family we built together, with our two cats, during my time in Canada.

Finally, I am grateful to my extended family and my friends in Ecuador, especially Gaby, Andrés, Felipe, Francisca, and Kari, for their love and encouragement from afar.

Pursuing a degree so far from home has been challenging, but the support and kindness of each of you made it possible.

Table of Contents

Chapter I: General Introduction

Communication in nature has long been a central focus of scientific inquiry due to its fundamental role in organismal biology and evolutionary dynamics. It occurs across all levels of biological organization, and its complexity often scales with the sophistication of the organism. This complexity is reflected in the diversity of signals produced, the sensory systems that detect them, and the behavioral or physiological responses they elicit (1,2). Signals may be visual, acoustic, chemical, or tactile, and often involve multiple modalities. Effective communication requires both the transmission of information and the capacity to trigger a response in a receiver, enabling organisms to interact with their environment and with conspecifics. This ability is essential for locating food, avoiding predators, defending territory, finding and assessing mates, reproducing, and caring for offspring. As such, studies of communication systems offer critical insight into the evolutionary processes that shape behavior, morphology, and life histories across taxa (3,4).

Amphibians, particularly anurans, stand out as exceptional models for exploring these dynamics due to their evolutionary antiquity and ecological diversity. As one of the earliest vertebrate groups to colonize both aquatic and terrestrial environments, amphibians exhibit a remarkable array of morphological, physiological, and behavioral adaptations (5,6). Their capacity to thrive in diverse and changing habitats has fostered extraordinary species richness, currently exceeding 8,600 described species with new taxa continually being discovered, especially in tropical regions (7–9). This diversity reflects key life history traits such as limited dispersal ability, environmental specialization, and high sensitivity to abiotic factors like temperature and humidity. Moreover, amphibians display wide variation in activity patterns and reproductive modes, ranging from strictly diurnal or nocturnal behaviors to flexible temporal strategies, and encompassing more than thirty reproductive modes with varied developmental pathways and parental care strategies (10,11). These features have driven the evolution of complex communication systems finely tuned to their ecological contexts, making amphibians invaluable for understanding the evolution of communication and its role in shaping biodiversity.

In anuran species, calling emerges as a fundamental communication mechanism. Acoustic communication plays a central role in the social and reproductive biology of anurans and is widely considered a major driver of their evolutionary diversification. Frogs and toads rely

predominantly on vocal signals to mediate a range of behaviors, especially those related to courtship, mating, and territory defense (2). These vocalizations are diverse and context-dependent, broadly categorized into reproductive, aggressive, and defensive calls, each encompassing multiple subtypes (12,13). Advertisement calls, in particular, are the most widespread and taxonomically informative, typically produced by males to attract females to breeding sites, and are key to species recognition, mate choice, and the reinforcement of reproductive isolation (2,12,14). Through vocal signals, individuals convey information about their location, body size, and identity, allowing for effective social and reproductive interactions (2,12,15–19). Given the centrality of acoustic communication in anuran biology, it is especially surprising that many species appear to thrive despite lacking the conventional capacity for perceiving, and sometimes producing, vocalizations.

Investigations into the developmental and genetic bases underlying the loss of vocal and auditory structures in anurans have been notably limited, resulting in substantial gaps in knowledge. Vocal structures, which function as secondary sexual traits and are closely linked to sexual maturity, typically develop alongside fully formed and functional testes, marking the onset of sexual activity. In some species, these vocal structures develop independently of metamorphosis, occurring before, during, or after this critical developmental stage (20). However, the genetic pathways regulating the coexistence of fully developed testes with incomplete or absent vocal structures remain largely unknown.

Similarly, knowledge regarding the ontogeny of the middle ear in anurans is scarce. Normal middle ear development begins in the later stages of metamorphosis and often extends into postmetamorphic phases (21–23). Disruptions or heterochronies during these stages may result in the underdevelopment or complete loss of middle ear structures (23,24). Despite these insights, the specific genetic mechanisms governing middle ear formation and loss in amphibians remain elusive, though genes implicated in these processes in other vertebrates offer promising avenues for investigation (25).

Recent studies have revealed that the loss of auditory structures specifically has independently occurred at least 38 times across various anuran clades, often without close phylogenetic relationships. These auditory losses appear particularly prevalent within the Bufonidae and Strabomantidae families, with a higher frequency observed among Andean

species (9,24). Furthermore, the incidence of auditory loss tends to increase with elevation, although it is not restricted exclusively to high-altitude habitats. This pattern may be driven by the presence of small populations with narrow altitudinal ranges, which could facilitate genetic drift leading to trait loss. Additionally, variation in communication modalities related to differing acoustic environments likely contributes to this phenomenon. Notably, earless species frequently share geographic distributions and microhabitats with their eared relatives, indicating that environmental factors alone do not fully explain these evolutionary patterns (9).

In contrast, a distinguishing characteristic of earless species is their predominantly diurnal activity. Approximately eighty percent of earless anurans exhibit strictly diurnal behavior, lacking nocturnal activity, whereas nearly sixty percent of eared species are exclusively nocturnal, with very few exhibiting diurnality (9). This suggests that increased exposure to predation during daylight hours may have exerted directional selection against loud, high-frequency calls in earless species, concurrently relaxing selective pressures on airborne hearing. The concurrent absence of vocal sacs and warning calls in many earless species further supports this pattern. However, the temporal sequence of these losses remains unclear; it is unknown whether the reduction of vocal structures preceded the loss of auditory components or vice versa (9,26). Regardless, these structural reductions might result in a reliance on non-acoustic communication channels. For example, *Atelopus zeteki*, an earless species, predominantly utilizes visual displays for communication, highlighting the potential for compensatory evolution in other sensory modalities such as vision (9,27,28).

Considering the possibility that the loss or reduction of middle ear and vocal structures may result from selection favoring other, yet unidentified, adaptive traits crucial for communication, and acknowledging the role of such traits in mate selection and reproduction, a central question emerges: How do frogs lacking auditory and/or vocal structures communicate? One plausible explanation is a sensory trade-off, a phenomenon in which the reduction in one sensory modality drives compensatory enhancement in another. This pattern is well documented in nature. For instance, in the bat *Rhinolophus hipposideros*, lineages with highly specialized echolocation systems optimized for target detection and tracking exhibit smaller eyes and altered spectral sensitivity. These changes are linked to habitat-specific foraging demands, illustrating how sensory modalities co-evolve to meet ecological requirements (29). *Python bivittatus*,

despite having simple duplex retinas, compensates with infrared-sensitive pit organs that detect thermal radiation, enabling effective prey detection and predator avoidance (30). Among mole rats, adaptation to subterranean life has driven a reduction in vision alongside heightened reliance on tactile, chemical, and vibrational cues for navigation and foraging (31).

In most documented cases of sensory trade-offs, the enhancement of one modality compensates for a diminished reliance on vision. This reflects a broad evolutionary trend in which species reduce investment in vision as they adopt alternative sensory strategies, such as echolocation, infrared perception, or mechanoreception. In contrast, in this thesis we propose an inverse scenario: enhancement of the visual system may represent an adaptive response to the reduction or loss of auditory input. In frogs that have diminished or lost the ability to detect airborne sounds, visual cues could assume a central role in communication, especially in reproductive contexts.

The visual system is a crucial and extensively studied sensory modality, notable for its capacity to deliver extensive, real-time information essential for animal perception and behavior. The visual system has evolved to meet the communicative requirements of animals by enhancing the detection and discrimination of light waves relevant to various behaviors and life histories (32,33). There are numerous examples of these adaptations across vertebrates, both at the molecular and morphological levels.

At the molecular scale, variation in opsins and associated phototransduction genes reflect ecological specialization. In lampreys, the southern species *Geotria australis* shows ontogenetic shifts in opsin gene expression between migratory stages and expresses four cone-associated opsins, enabling tetrachromacy in broad-spectrum shallow waters. In contrast, the northern lamprey *Petromyzon marinus*, adapted to dim, deep-water habitats, expresses only two opsins, limiting its color discrimination (34–37). In cichlids, visual system diversification has paralleled their adaptive radiation. Opsin gene duplications and shifts in gene expression correlate with ecological and behavioral variation, including habitat and mating strategies (35,38). Ontogenetic tuning is also seen in species such as *Acanthopagrus butcheri*, where larval stages are sensitive to short wavelengths in clear waters, while adults shift toward long-wavelength sensitivity in tannin-rich environments (39). Similarly, the European eel, *Anguilla anguilla*, modulates opsin expression throughout its complex life cycle spanning diverse photic environments (35).

Morphological adaptations also play a crucial role in tuning visual capacity. In *Latimeria chalumnae*, the retina is composed of rods and specialized ganglion cells adapted for scotopic vision in the deep sea, consistent with its limited opsin complement (40,41). In caecilians, the visual system is highly regressed, with degenerate eyes, a single photoreceptor type, and reduced brain regions involved in visual processing, in accordance with a fossorial lifestyle (42,43). In contrast, most frogs and salamanders possess more complex retinal arrangements, often including a secondary rod (SWS2), enabling broader spectral sensitivity even under low light conditions (33,44).

Altogether, these examples illustrate how the vertebrate visual system adapts through integrated genetic, morphological, and physiological modifications in response to diverse ecological and behavioral pressures. Building on this framework, this thesis investigates sensory trade-offs in anurans by examining the visual system as a potential compensatory modality in lineages that have independently experienced reductions or losses of auditory structures.

To address these sensory trade-offs comprehensively, two complementary approaches are employed. The first approach quantifies morphological investment by measuring key traits of the eye and cornea across species that differ in auditory system integrity, testing whether reductions in auditory structures correspond with increased visual investment. The second approach applies molecular evolutionary analyses to opsin genes, encoding the light-sensitive proteins essential for vision, to detect signatures of natural selection and molecular adaptation associated with sensory reductions. The overarching objective of this thesis is to evaluate sensory compensation between auditory and visual systems in anurans, determining whether morphological and molecular traits of the visual system exhibit adaptive changes linked to reductions in auditory and vocal structures.

This thesis is organized into three data chapters followed by a conclusions chapter. Chapter 2 presents comparative analyses of eye and corneal morphology across anuran species varying in auditory traits. Chapter 3 details the assembly and characterization of a high-quality genome for a representative earless species, providing a genomic foundation for molecular investigations. Chapter 4 explores molecular evolutionary patterns in opsin genes among species with differing auditory and vocal traits, testing for potential adaptive signals related to sensory loss. Together, these chapters provide an integrated and multidisciplinary perspective on the

evolution of sensory systems in anurans, advancing understanding of sensory trade-offs and the evolutionary dynamics of communication.

Chapter II: Eyes wide open: Frogs with reduction of auditory communication ability show lower eye, but higher corneal, investment

Jhael A. Ortega[1,2,], Kate N. Thomas[3,4], Santiago R. Ron[2], Rayna C. Bell[5,6], Matthew K. Fujita[3], David J. Gower[4], Jeffery W. Streicher[4], Ryan K. Schott*[1]

[1]Department of Biology and Centre for Vision Research, York University, Toronto, Ontario, Canada

[2]Museo de Zoología, Escuela de Biología, Pontificia Universidad Católica del Ecuador, Quito, Pichincha, Ecuador

[3]Department of Biology, Amphibian and Reptile Diversity Research Center, University of Texas at Arlington, Arlington, USA

[4]Department of Life Sciences, Natural History Museum, London, UK

[5]Department of Herpetology, California Academy of Sciences, San Francisco, USA

[6]Department of Vertebrate Zoology, National Museum of Natural History, Smithsonian Institution, Washington DC USA

*Corresponding author email: schott@yorku.ca

Key words

Auditory and vocalization reductions, corneal enlargement, corneal investment, sensory system losses, sensory trade-offs.

Abstract

Vocal communication, characterized by species-specific advertisement calls, is the primary mechanism of mate attraction in frogs and relies on a complex integration of the vocal and auditory systems. However, some species have lost key auditory structures that are needed to hear airborne sounds, raising the question of how they communicate in their absence. We hypothesize that frog species with reductions in the auditory system will have compensated through enhanced visual ability, specifically through enlargement of the eyes. To test this, we analyzed relative investment in eye and corneal size across 264 anuran species spanning all 55 recognized families, testing for correlations with six ecological traits, including for the first time, the condition of the auditory system. Contrary to our expectation that sensory reductions would favour larger eyes, we found that species with auditory reductions had smaller eye size and lower investment. Instead, we found that non-fossorial species with auditory reductions had significantly greater corneal investment, after controlling for habitat-based variation. Enlarged corneas enhance light sensitivity but are expected to have a lower metabolic cost than larger eyes. Relatively larger corneas in frogs with auditory reductions may, in combination with other changes, allow these frogs to rely more on vision for communication, navigation, and social interactions, while at the same time minimizing metabolic costs in small animals that are already metabolically constrained. Our findings suggest that the visual system plays an adaptive role in response to the reduction of auditory communication and highlights the condition of sensory systems as an important ecological factor shaping anuran evolution.

Introduction

Acoustic communication plays a central role in the social and reproductive biology of frog and toads (Anura; here collectively referred to as frogs) and is widely considered a major driver of their evolutionary diversification. Frogs rely predominantly on vocal signals to mediate a range of behaviors, especially those related to courtship, mating, and territory defense (1). These vocalizations are diverse and context-dependent, broadly categorized into reproductive, aggressive, and defensive calls, each encompassing multiple subtypes (2,3). Advertisement calls, in particular, are the most widespread and taxonomically informative, typically produced by males to attract females to breeding sites, and are key to species recognition, mate choice, and

the reinforcement of reproductive isolation (1,3–7). Through vocal signals, individuals convey information about their location, body size, and identity, allowing for effective social and reproductive interactions (1,3,5,8–11). Given the centrality of acoustic communication in frog biology, it is especially surprising that many species appear to thrive despite lacking the conventional capacity for perceiving vocalizations.

Because acoustic signals are so pivotal in frog communication, their perception depends on a suite of specialized auditory structures, including the tympanic membrane, tympanic annulus, middle ear bones, and inner ear (12–15). Remarkably, despite their importance in detecting vocal signals, these auditory components have been independently lost at least 38 times across the frog phylogeny (16). These losses are phylogenetically widespread but non-random: they are disproportionately found in lineages that are ground- dwelling, diurnal, and miniaturized, with many species also exhibiting restricted geographic distributions and occupying high-elevation habitats (16,17). Despite these associations, the mechanisms driving the reduction of auditory structures remain poorly understood. One hypothesis suggests that these losses may reflect selection favoring alternative, yet unidentified traits or behaviors that compensate for the diminished capacity for acoustic communication (16). Such compensatory traits are presumed to be especially critical in mating contexts, where effective signaling remains essential (14,16). A plausible explanation is that the reduction of one sensory modality may be accompanied by enhancements in another, a sensory trade-off that could enable species to maintain functional signaling despite the absence of conventional auditory mechanisms (18–21).

Several cases of sensory trade-offs have been documented among different lineages. One well-characterized example is the bat *Rhinolophus hipposideros*, which has relatively small eyes and altered spectral sensitivity, consistent with adaptations to specialized echolocation (19). Similarly, boas and pythons exhibit a simple duplex retina composed of single cones and rods, in contrast to the more complex retinal structure of caenophidian snakes (22). This visual simplicity, however, is compensated by the evolution of a specialized infrared (IR) detection system: thermoreceptors located in the labial pits allow the snake to detect thermal radiation emitted by warm objects, facilitating prey capture, predator avoidance, and thermoregulation (20). Another example is found in subterranean mammals, such as mole rats. These animals have reduced visual systems and instead rely heavily on other sensory modalities, including tactile

input, olfaction, and bone-conducted vibration, which are essential for navigation and foraging in dark, subterranean environments (23).

In most documented cases of sensory trade-offs, the enhancement of one modality compensates for a diminished reliance on vision. This reflects a broad evolutionary trend in which species reduce investment in vision as they adopt alternative sensory strategies, such as echolocation, infrared perception, or mechanoreception. In contrast, our study proposes an inverse scenario: enhancement of the visual system may represent an adaptive response to the reduction or loss of auditory input. In frogs that have diminished or lost the ability to detect airborne sounds, visual cues could assume a central role in communication, especially in reproductive contexts.

The visual system is a crucial and extensively studied sensory modality, notable for its capacity to deliver extensive, real-time information essential for animal perception and behavior. Eye size and shape directly influence optical properties, affecting both the quantity and quality of visual input (22,24). Because improvements in sensitivity, acuity, and temporal resolution often involve trade-offs, increasing eye size is generally required to enhance overall visual performance without sacrificing specific functions (24,25). Therefore, investigating variation in eye size across frogs adapted to diverse ecological niches offers valuable insights into sensory evolution and the adaptive trade-offs shaping visual systems.

Previous studies in vertebrates have demonstrated that the evolution of eye size is strongly influenced by ecological factors (21,25–33), a trend also observed in frogs (24). This suggests that frogs adapted to distinct ecological niches face unique optical constraints linked to variations in eye size. For instance, arboreal frogs tend to invest more in their eyes, exhibiting larger absolute and relative eye sizes, which are proposed to accommodate rapid visual processing during jumps and to achieve high visual precision in complex arboreal settings (24). In contrast, fossorial species exhibit minimal investment in eye size, presumably reflecting adaptations to dark or abrasive subterranean environments (24). Other ecological factors, such as activity period and reproductive strategies, also play a role. Nocturnal species often develop larger eyes to improve their sensitivity to dim light, while those breeding in vegetation or near lotic water may benefit from enhanced vision to overcome auditory challenges caused by the noise of rushing water (24,34).

Beyond anatomical investment, visual cues are critical in mediating both interspecific and intraspecific interactions, serving as essential signals across a wide range of ecological and social contexts (34), and may carry increased functional importance in species where other sensory modalities are reduced. Many frogs use conspicuous displays, such as posture changes, limb movements, or exposure of colored body surfaces, to deter predators, attract prey, or communicate with conspecifics (34–38). These behaviors are often context-dependent and particularly prominent during courtship and agonistic encounters, with their form and frequency often modulated by whether the target is a potential mate or a rival (34). In species with limited auditory capacities, visual signals may compensate for the loss of acoustic communication, serving as a complementary channel for mate attraction and social interaction. This behavioral reliance on vision could impose selective pressures favoring increased investment in the visual system, particularly in lineages with auditory reductions.

Building on this premise, we assess variation in visual system investment among frogs exposed to different ecological pressures, incorporating for the first time data on the condition of the auditory system. We hypothesize that the visual system compensates, at least in part, for the reduction of auditory perception. Accordingly, we predict that frog species with reduced or absent auditory structures will exhibit greater investment in their visual system, including the evolution of larger eyes to enhance visual capability and maintain effective communication and environmental perception in the absence of "conventional" hearing.

Methodology

Sampling and morphometric measurements

We examined 468 adult frog specimens from the amphibian collection at the QCAZ Museum of Zoology, Pontificia Universidad Católica del Ecuador. Specimens were assigned to 55 species across nine families: Aromobatidae, Bufonidae, Centrolenidae, Ceratophryidae, Craugastoridae, Hemiphractidae, Hylidae, Microhylidae, and Strabomantidae (see Tables S1 and S2). Specimens were fixed using formaldehyde following the museum's internal protocol and are preserved in 70% ethanol. For analysis, we selected only well-preserved individuals, prioritizing hydrated specimens with intact and undamaged eyes to ensure the reliable assessment of morphological

traits. Adulthood was determined by gonadal inspection: males were classified as adult if they had well-developed testes, and females if they had developed oocytes and/or convoluted oviducts (39). For each specimen, we recorded body mass (RM), snout–vent length (SVL), eye diameter (ED), and cornea diameter (CD) using a digital caliper (±0.01 mm) and a precision scale (±0.01 g), following Thomas et al. (2020). Mean ED and CD were calculated per individual prior to analysis. These morphometric data allowed us to evaluate visual system investment in the context of auditory reduction and ecological variation. We complemented this dataset with morphometric data from Thomas et al. (2020), adding 220 additional species. This integration yielded a comprehensive dataset of 264 species spanning all 55 frog families, ensuring broad ecological and phylogenetic representation (Table S3).

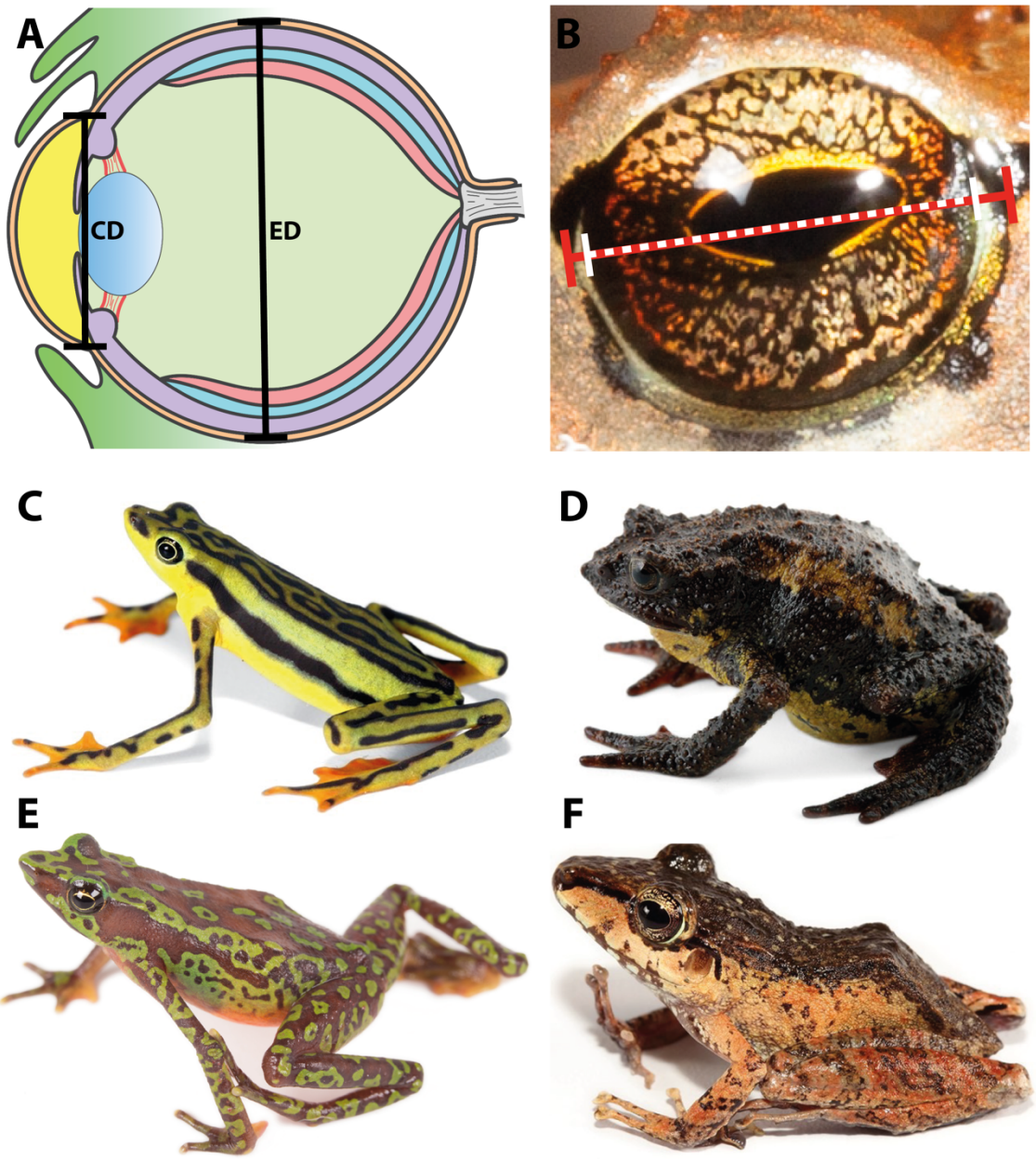

Figure 1. Examples of frogs with varying sensory system states. **(*A*)** Diagram of an frog eye illustrating the measured parameters: CD = Cornea Diameter; ED = Eye Diameter. **(*B*)** Eye measurements: red line indicates eye diameter; dashed white line, corneal diameter. **(*C*)** *Atelopus elegans*, with reduction of the auditory system only. **(*D*)** *Osornophryne guacamayo*, lacking auditory and vocalization systems. **(*E*)** *Atelopus palmatus*, with reduction of the auditory system only. **(*F*)** *Pristimantis lanthanites*, with no sensory system reductions. Photos: Santiago R. Ron - Bioweb.

Phylogeny and ecological classification

To account for phylogenetic signal in our analysis, we aligned species with the most recent and comprehensive molecular phylogeny for amphibians (40), pruning it to include only the 264 species in our dataset. For 13 species not present in the tree, we substituted their closest congeneric relatives using the *ape* package in R (41). These replacements were incorporated as polytomies and subsequently resolved using the *chronos* function in *ape* (42–44). To maintain phylogenetic consistency, all substitutions and polytomies were restricted to species within the same genus.

We classified species according to six ecological traits: (1) status of the auditory system for hearing airborne sounds (maintained or lost); and five traits from Thomas et al. (2020), (2) adult habitat (semiaquatic, aquatic, scansorial, ground-dwelling, fossorial, subfossorial), (3) activity period (diurnal, nocturnal, or both), (4) mating habitat (lotic water, lentic water, plants, or ground), (5) life-history strategy (presence or absence of free-living larvae), and (6) sexual dichromatism (present or absent).

Trait data were gathered from AmphibiaWeb, Bioweb, and primary literature, including species descriptions (see Table S1). Auditory system status was determined based on Womack & Hoke (2023), who defined "earless" taxa as those lacking the columella, tympanic membrane, tympanic annulus, and middle ear cavity. The activity period classification was also updated following Womack & Hoke (2023).

Allometric patterns and ecological correlates in frog eye size

We first tested whether previously described allometric patterns (Thomas et al., 2020) held when expanding the dataset to include more species with auditory reductions. We then examined whether auditory system loss correlated with increased investment in the visual system, and how this relationship might vary across ecological contexts.

We used phylogenetic generalized least squares (PGLS) models from the *caper* package version 1.0.3 (45) in R to assess allometric relationships between log-transformed species means of ED, CD, RM, and SVL. Specifically, we fit maximum-likelihood estimations of lambda (λ) to

log-transformed species means for eye diameter (ED) *vs* snout-vent length (SVL), ED *vs* relative mass (RM), corneal diameter (CD) *vs* ED, CD *vs* SVL, CD *vs* RM, and SVL *vs* RM. To further evaluate allometric patterns, we performed ordinary least-squares (OLS) regressions using the *stats* package (version 4.4.2) (46) and standardized major axis (SMA) regressions using the *smatr* package (version 3.4-8) (47) in R, all based on the same log-transformed dataset.

To test differences in visual investment across ecological states, we used Wilcoxon rank sum tests or, for traits with more than two categories, Kruskal–Wallis tests using the *stats* package (v.4.4.2) (46). We also implemented phylogenetic ANCOVAs via PGLS models using *caper* (v.1.0.1) to examine the effect of each ecological trait on ED and CD while controlling for body size (RM or SVL). Separate models were run for each ecological variable to avoid overparameterization. Finally, two-way ANCOVAs via PGLS were used to evaluate the combined effects of two ecological traits on eye and cornea investments. Visualizations of eye size, corneal size, and ecological states on the phylogeny were generated using *ape* (v.5.8) (41) and *phytools* (48). A full script to reproduce the analyses is available on Github (*link tbd*).

Results

Species with auditory reductions exhibit reduced absolute and relative eye size

Our analyses reveal that frogs with auditory reductions have consistently smaller eyes compared to species without auditory reduction, contrary to our initial prediction. This pattern holds true for both absolute eye diameter and eye size relative to body mass (eye investment). These differences remain significant even after controlling for confounding factors such as habitat (Fig. 3, Figs. S2–S4). Mean absolute eye diameter was 4.02 mm in species with auditory loss, compared to 5.98 mm in those without (Wilcoxon test: $W = 3040.5$, $p < 0.001$). Relative eye size, scaled by body mass and phylogenetically corrected, was also reduced in species with auditory loss (Wilcoxon test: $W = 3144$, $p < 0.001$), averaging 0.89× the expected value versus 1.07× in other species. Phylogenetic ANCOVA confirmed significant effects of both body mass ($F_{1,257} = 1047.108$, $p < 0.001$) and auditory loss ($F_{1,257} = 20.365$, $p < 0.001$) on eye size.

Because habitat strongly influences eye morphology, with fossorial and aquatic species typically exhibiting reduced eye size and investment (24), we tested whether these ecological factors could

explain the observed pattern. A two-way phylogenetic ANCOVA revealed significant main effects of auditory system reduction ($F_{1,248} = 20.462$, $p < 0.001$) and adult habitat ($F_{1,248} = 3.421$, $p = 0.005$) on absolute eye size, but not significant interaction between them ($F_{1,248} = 0.42$, $p = 0.833$). Likewise, for relative eye size, both auditory loss ($F_{1,236} = 27.428$, $p < 0.001$) and adult habitat ($F_{5,236} = 8.939$, $p < 0.001$) had significant effects, with body mass exerting the strongest influence overall ($F_{1,236} = 1307.736$, $p < 0.001$). In addition, interactions between body mass and auditory reduction ($F_{1,236} = 6.891$, $p = 0.009$), as well as between auditory reduction and adult habitat ($F_{5,236} = 3.412$, $p = 0.005$) were also significant.

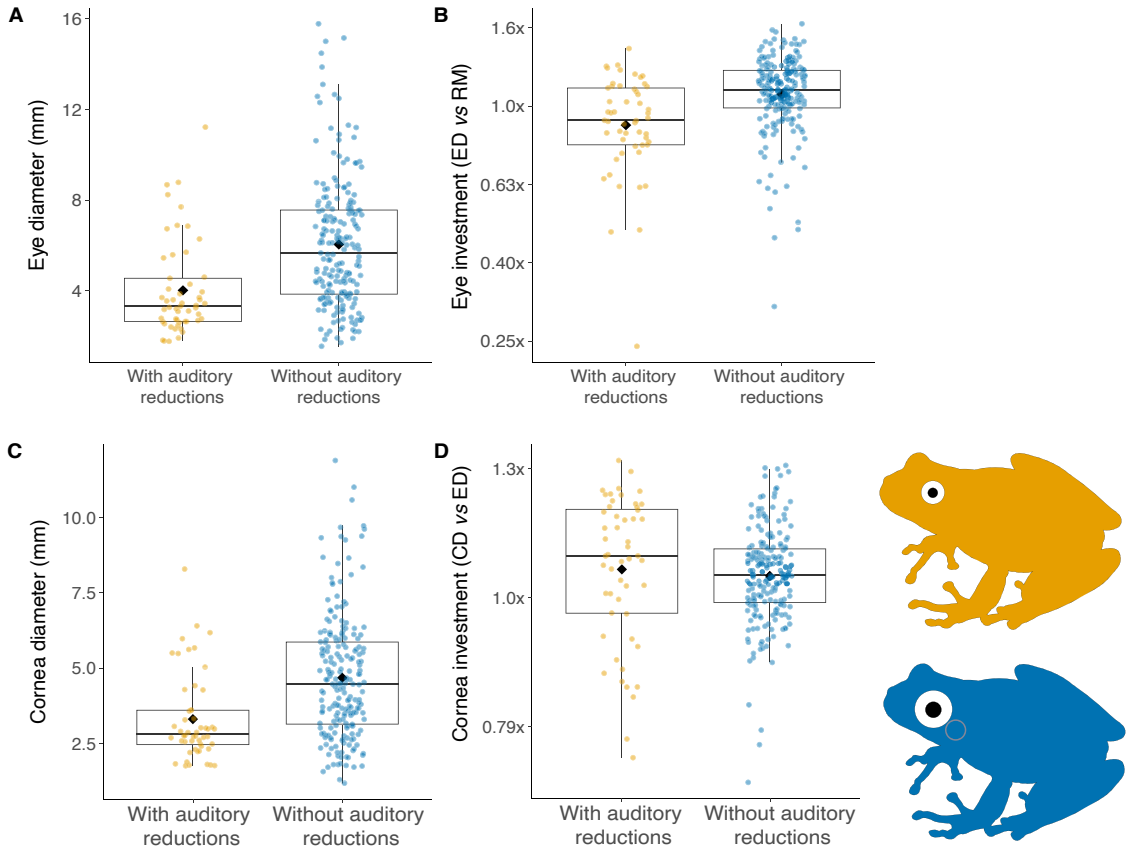

Figure 2. Visual investment across frogs with auditory reductions. (*A*) Absolute eye diameters and **(*B*)** eye investment across groups. **(*C*)** Absolute cornea diameter and (***D***) relative corneal investment. **All panels include data from all species in the dataset**.

Species with auditory loss have greater corneal investment

Given that species with auditory loss exhibit smaller eyes and reduced eye investment, we next examined corneal size and corneal investment. Across analyses, species with auditory loss consistently exhibited smaller absolute cornea diameters. In contrast, relative cornea investment tended to be higher in these species, though this difference was specific to non-fossorial taxa (Figs. 3 – 4, Figs. S2, S5).

Similar to the pattern observed in eye size, species with auditory loss exhibited significantly smaller absolute cornea diameters (mean = 3.31 mm) compared to species without auditory reduction (mean = 4.68 mm; Wilcoxon test: $W = 3061.5$, $p < 0.001$). Relative cornea investment (*i.e.*, CD *vs* ED) showed no significant difference between species with auditory loss (mean = 1.05×) and those without (mean = 1.04×) (Wilcoxon test: $W = 6286$, $p = 0.09$). Phylogenetic ANCOVA revealed a significant main effect of eye size on cornea size ($F_{1,259} = 4813.373$, $p < 0.001$), but no significant main effect of auditory loss ($F_{1,259} = 1.459$, $p = 0.228$). A two-way phylogenetic ANCOVA testing the joint effects of adult habitat and sensory loss revealed significant main effects of both auditory loss ($F_{1,250} = 23.477$, $p < 0.001$) and habitat ($F_{5,250} = 3.960$, $p = 0.002$) on absolute cornea size, but not significant interaction between them ($F_{5,250} = 0.698$, $p = 0.625$). Similarly, for relative cornea investment, both auditory loss ($F_{1,238} = 653.758$, $p < 0.001$) and habitat ($F_{5,238} = 130.628$, $p < 0.001$) had significant effects, with eye size exerting the strongest overall influence ($F_{1,238} = 5048.208$, $p < 0.001$). In addition, interaction between auditory reduction and adult habitat ($F_{5,238} = 2.899$, $p = 0.015$) was also significant.

Because the effect of auditory loss was only revealed when accounting to habitat variation, we suspected the not all species with auditory reduction exhibited the same pattern. In particular, fossorial species may be expected to be under different selective pressures and indeed several species with auditory loss are also fossorial. To further investigate this, we first excluded fossorial species and found that species with auditory loss still had significantly smaller absolute cornea diameters (mean = 3.84 mm) compared to those without auditory reduction (mean = 5.99 mm; Wilcoxon test: $W = 2567$, $p < 0.001$). In contrast, relative cornea investment was slightly, but significantly, greater in species with auditory loss (mean = 1.06×) compared to those without (mean = 1.02×; Wilcoxon test: $W = 5907$, $p = 0.011$). Phylogenetic ANCOVA revealed

significant main effects of both eye size ($F_{1,249} = 4707.502$, $p < 0.001$) and auditory loss ($F_{1,249} = 497.580$, $p < 0.001$) on cornea size. Patterns for eye size remained the same (see SI).

To further assess the effects of auditory reduction on eye and corneal scaling while controlling for the influence of habitat, we restricted the analysis to ground-dwelling species only, which was the habitat category with the highest proportion of species with auditory reductions (25 out of 53). Ground-dwelling species with auditory loss still exhibited significantly smaller eyes in both absolute (Wilcoxon test: $W = 499.5$, $p < 0.001$; mean = 3.63 mm vs. 6.17 mm) and relative terms (Wilcoxon test: $W = 638$, $p = 0.0006$; 0.97× vs. 1.1×). Phylogenetic ANCOVA again showed significant effects of body mass ($F_{1,113} = 973.875$, $p < 0.001$) and auditory loss ($F_{1,113} = 167.637$, $p < 0.001$). We also found that ground-dwelling species had significantly smaller absolute cornea diameters (mean = 3.19 mm) compared to species without auditory reduction (mean = 4.84 mm; Wilcoxon test: $W = 559.5$, $p < 0.001$). However, species with auditory loss showed significantly greater corneal investment (mean = 1.12×) than those without loss (mean = 1.05×; Wilcoxon test: $W = 1700$, $p = 0.0009$). Phylogenetic ANCOVA supported significant main effects of both eye size ($F_{1,117} = 2855.795$, $p < 0.001$) and auditory loss ($F_{1,117} = 372.209$, $p < 0.001$) on cornea size.

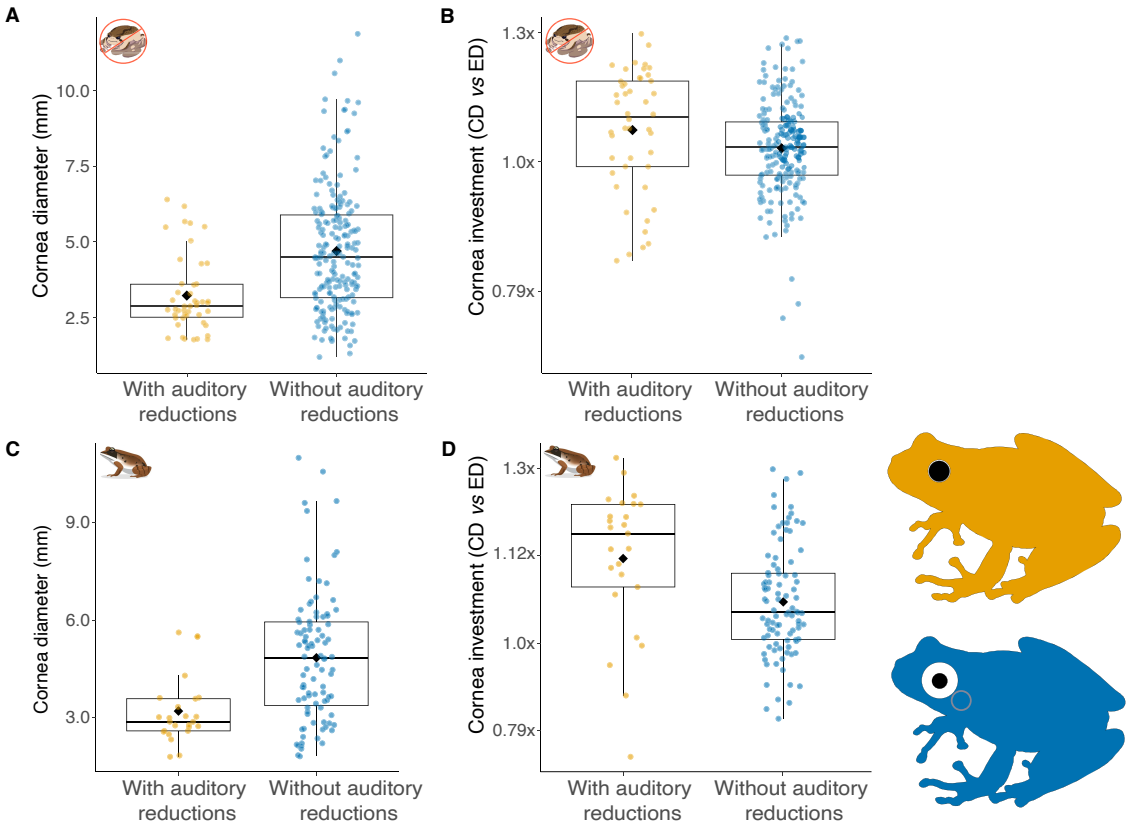

Figure 3. Cornea size and investment vary significantly across frogs with auditory reductions. (A) Absolute cornea diameter and **(B)** relative corneal investment, based on analyses **excluding fossorial species. (C)** Absolute cornea diameter and **(D)** relative corneal investment, **based on analyses restricted to ground-dwelling species.** Boxplots illustrate trait differences across sensory system conditions.

Because diurnality is overrepresented among species with sensory system reductions (16), we next tested the effects of activity period and auditory loss on eye morphology. A two-way phylogenetic ANCOVA revealed significant main effects of auditory system reduction ($F_{1,218}$ = 13.146, $p < 0.001$) and activity period ($F_{2,218}$ = 3.566, $p = 0.030$) on absolute eye size, but no significant interaction between them. Likewise, for relative eye size, both auditory loss ($F_{1,210}$ = 80.399, $p < 0.001$) and activity period ($F_{2,210}$ = 7.012, $p = 0.001$) had significant effects, with body mass exerting the strongest influence overall ($F_{1,210}$ = 772.107, $p < 0.001$). In addition, the interaction between body mass and auditory reduction ($F_{1,210}$ = 9.178, $p = 0.003$) was also significant. Similarly, a two-way phylogenetic ANCOVA revealed that both activity period ($F_{2,216}$ = 5.169, $p = 0.006$) and auditory system reduction ($F_{1,216}$ = 13.605, $p < 0.001$) significantly

affected absolute cornea size, with no significant interaction between them. For relative cornea size, significant main effects were found for body mass ($F_{1,210} = 3359.669$, $p < 0.001$), auditory loss ($F_{1,210} = 272.233$, $p < 0.001$), and activity period ($F_{2,210} = 83.356$, $p < 0.001$), but no significant interactions were detected among these factors

When restricting the analysis to diurnal species only (Fig. 4), we found that those with auditory reductions exhibited significantly smaller eyes in both absolute (Wilcoxon test: $W = 39$, $p = 0.006$; mean = 3.56 mm vs. 6.01 mm) and relative terms (Wilcoxon test: $W = 30$, $p = 0.001$; 0.89× vs. 1.25×). Phylogenetic ANCOVA confirmed that both auditory system reduction ($F_{1,25} = 77.751$, $p < 0.001$) and body mass ($F_{1,25} = 149.374$, $p < 0.001$) had significant effects on eye size. When analyzing the cornea, we found that diurnal species with auditory reductions exhibited significantly smaller corneas in absolute size (Wilcoxon test: $W = 51$, $p = 0.03$; mean = 3.08 mm vs. 4.52 mm). However, differences in relative cornea size (1.09× in species with sensory loss vs. 1.00× in those without) were not statistically significant (Wilcoxon test: $W = 141$, $p = 0.06$). Phylogenetic ANCOVA confirmed that both auditory system reduction ($F_{1,26} = 104.717$, $p < 0.001$) and body mass ($F_{1,26} = 347.899$, $p < 0.001$) had significant effects on cornea size.

Given that mating habitat was previously shown to shape independently eye and cornea morphology (24) (see Supplementary Material), we next evaluated whether this ecological variable could also help account for the variation associated with sensory system reductions. To this end, we performed two-way phylogenetic ANCOVAs, testing the combined effects of auditory loss and mating habitat, along with post hoc Wilcoxon comparisons.

Analyses revealed that absolute eye size was significantly influenced by both auditory system reduction ($F_{1,210} = 16.469$, $p < 0.001$) and mating habitat ($F_{3,210} = 9.767$, $p < 0.001$), with no evidence for an interaction between them. A similar pattern emerged for relative eye size: both auditory loss ($F_{1,202} = 118.118$, $p < 0.001$) and mating habitat ($F_{3,202} = 26.244$, $p = 0.001$) showed significant effects, while body mass had the strongest overall influence ($F_{1,202} = 896.041$, $p < 0.001$). Additionally, we detected significant interactions between body mass and auditory reduction ($F_{1,202} = 16.237$, $p < 0.001$), as well as a three-way interaction between auditory loss, mating habitat, and body mass ($F_{3,202} = 3.701$, $p = 0.013$) on eye size. For corneal morphology, both mating habitat ($F_{3,210} = 6.496$, $p < 0.001$) and auditory system reduction ($F_{1,210} = 20.083$, $p < 0.001$) had significant effects on absolute cornea size, while their interaction was not significant.

For relative cornea size, we found significant main effects of mating habitat ($F_{3,202} = 163.608$, $p < 0.001$), auditory loss ($F_{1,202} = 323.137$, $p < 0.001$), and body mass ($F_{1,202} = 3308.245$, $p < 0.001$). Furthermore, both the interaction between mating habitat and auditory loss ($F_{3,202} = 4.403$, $p = 0.005$) and the three-way interaction among mating habitat, auditory loss, and body mass ($F_{3,202} = 3.093$, $p = 0.028$) were also significant.

Because our data show that most species with sensory system reductions mate on the ground, we repeated the analyses restricted to ground-mating species (Fig. 4). Within this subset, those with auditory reductions exhibited significantly smaller eyes in both absolute (Wilcoxon test: $W = 223$, $p = 0.0003$; mean = 2.92 mm vs. 4.33 mm) and relative terms (Wilcoxon test: $W = 198$, $p < 0.001$; 0.84× vs. 1.08×). Phylogenetic ANCOVA confirmed significant effects of auditory system reduction ($F_{1,58} = 10.673$, $p < 0.001$), body mass ($F_{1,58} = 162.569$, $p < 0.001$), and their interaction ($F_{1,58} = 13.042$, $p = 0.001$) on eye size. When analyzing the cornea, we found that ground-mating species with auditory reductions had significantly smaller absolute cornea diameters (Wilcoxon test: $W = 227.5$, $p = 0.0007$; mean = 2.67 mm vs. 3.62 mm). Differences in relative cornea size were also significant (Wilcoxon test: $W = 611$, $p = 0.03$), with greater corneal investment observed in species with auditory loss (mean = 1.11×) compared to those without (mean = 1.07×). Phylogenetic ANCOVA again revealed significant effects of both auditory system reduction ($F_{1,58} = 58.594$, $p < 0.001$) and body mass ($F_{1,58} = 1170.984$, $p < 0.001$) on cornea size.

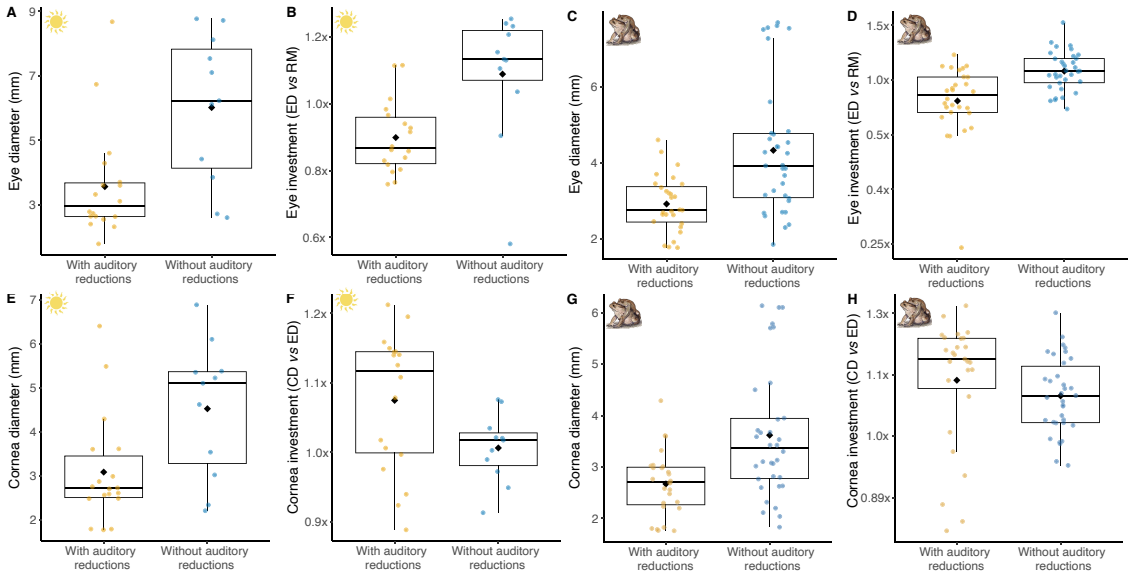

Figure 4. Eye and cornea size and investment in diurnal and ground-mating frog species. **(*A*)** Absolute eye diameter and **(*B*)** relative eye investment in diurnal species. **(*C*)** Absolute eye diameter and **(*D*)** relative eye investment in species that mate on the ground. **(*E*)** Absolute cornea diameter and **(*F*)** relative cornea investment in diurnal species. **(*G*)** Absolute cornea diameter and **(*H*)** relative cornea investment in ground-mating species. Boxplots show trait differences between species with and without auditory system reduction.

Discussion

Our results show that frog species with auditory system reduction have consistently smaller eyes compared to those without auditory loss, both in absolute diameter and relative to body size. This pattern remained consistent across analyses, including when accounting for variation in habitat type and after excluding fossorial species that are expected to have smaller eyes. We also observed significant effects of both auditory loss and habitat on eye size, prompting additional analyses focused on ground-dwelling species, which were overrepresented among species with sensory reductions. The same pattern held: ground-dwelling species with auditory loss exhibited significantly smaller eyes. Species with auditory loss also had smaller absolute cornea diameters, but relative cornea investment (*i.e.,* cornea size relative to eye size) was significantly greater when fossorial species were excluded and when analyses were restricted to ground-dwelling taxa. These findings suggest that while overall eye size is constrained in species with auditory

loss, specific eye components such as the cornea may be differentially affected under certain ecological contexts.

Why prioritize investment in the cornea rather than the entire eye?

Our results highlight that reductions in the auditory system are closely linked to ecological context, particularly habitat, in shaping evolutionary investment in eye morphology among frogs. Many species with auditory loss inhabit fossorial or terrestrial environments, where ecological constraints strongly influence the utility and maintenance of visual structures. In fossorial species, the subterranean environment imposes strong limitations on vision, resulting in rudimentary visual systems characterized by consistently smaller eyes and corneas, a feature closely linked to their predominantly fossorial lifestyle (22,24,49,50). In such habitats, where visual cues are scarce, the metabolic and spatial costs of large eyes likely outweigh their benefits. Physical limitations such as darkness, abrasive substrates, and limited cranial space likely drive the evolutionary reduction of the visual system. This pattern is not exclusive to frogs but is also observed across other vertebrates, including mammals (51,52), fish (53), reptiles (54), and caecilians (49). In these species, reliance likely shifts toward alternative sensory modalities such as chemoreception (55), mechanoreception (52), and, in some cases, bone-conducted auditory signals (27) rather than visual or airborne acoustic cues. It is likely due to these distinct evolutionary forces acting on fossorial species that we saw different scaling patterns in fossorial species with auditory reductions.

Our findings also indicate that most frogs with auditory system reductions are ground-dwelling, a pattern similarly reported by Womack and Hoke (2023). These species are frequently found in leaf litter, among low vegetation, or near lotic water bodies, microhabitats that are structurally complex and visually cluttered. Although larger eyes can enhance visual acuity and sensitivity (24,56,57), they are metabolically costly to produce and maintain (58,59), and can pose biomechanical challenges, particularly for small-bodied, hopping animals. Consistent with this, our results, and those of Womack and Hoke (2023), show that species with sensory reductions tend to be smaller in body size than those without, which may further constrain eye size due to allometric scaling. Moreover, large, protruding eyes increase cranial mass (60), raise the risk of mechanical injury from surrounding vegetation, and can hinder movement in cluttered

environments (56), likely selecting against increased investment in eye structures under these ecological contexts.

Besides adult habitat and auditory loss, other ecological factors appear to influence eye size and related structures. Our analyses show that mating habitat and activity period significantly affect eye and cornea size alongside sensory loss. Frogs that mate primarily on the ground, overrepresented among species with auditory loss in our dataset, possess the smallest eyes in both absolute and relative terms, consistent with previous findings (24). Importantly, our results also reveal that these ground-mating species display increased relative corneal investment, suggesting a reallocation of visual resources despite an overall reduction in eye size. Regarding activity period, diurnal species, also overrepresented among auditory-loss frogs (16), generally invest less in eye size compared to nocturnal or mixed-activity species, a trend consistent with broader vertebrate patterns linking increased visual investment to the need for enhanced sensitivity in low-light environments (29,61). Although no significant differences in corneal size were detected among activity periods, our data reveal a main effect of activity period on both eye and cornea dimensions.

Given these ecological and anatomical constraints, reduced eye size associated with adult habitat, reproductive habitat, and diurnal activity, we propose that an increase in relative corneal size may be the optimal adaptive response for frogs with auditory losses. This potential adaptation could compensate for sensory reductions and their already small eyes, enhancing visual capabilities while minimizing metabolic and locomotive costs, thus offering a plausible solution to the environmental challenges these species face.

Does having a larger cornea enhance the visual system?

Visual capacity is shaped by a variety of anatomical and optical factors beyond eye size. Structural differences, such as a higher rod-to-cone ratio (62), tubular-shaped eyes (56), and a larger cornea can significantly affect species-specific visual abilities (28,57). Although research on corneal size in frogs is limited, it is well-established in vertebrates more broadly that both the size and curvature of the cornea play crucial roles in determining visual sensitivity (22,57,63). The cornea's size and curvature directly limit the maximum pupillary aperture, thereby

controlling the amount of light entering the eye (57). While a larger cornea facilitates a greater pupillary aperture, enhancing retinal image brightness, this increased aperture size also broadens the field of vision, contributing to improved overall visual performance (22). To capture light rays reaching the anterior retina and extend the eye's periscopic range, the cornea must be wider than the pupil (22). Additionally, a larger cornea and greater corneal investment increase retinal image brightness, enhancing visual sensitivity by maximizing the amount of light that reaches the retina (29,64). When other factors, such as eye size and corneal transmission, are held constant, an eye with a cornea occupying a larger proportion of the anterior surface can admit more light, thus improving visual sensitivity compared to an eye with a smaller corneal proportion (64). The optical properties of the cornea-lens system are optimized to maximize image brightness within a specific light range, independent of the overall size of the eye. The cornea-to-lens ratio governs the refractive power of the cornea, with a larger cornea typically corresponding to a proportionally larger lens (22,64). Studies conducted in nocturnal mammals and birds have shown that a larger relative cornea size is often coupled with a larger lens and a posterior nodal point shift toward the retina. In these species, this configuration of the dioptric system enables the production of a brighter retinal image by efficiently utilizing available light, thereby further enhancing visual sensitivity (57,64).

Beyond lens enlargement, corneal expansion may be accompanied by structural modifications and neural adaptations that enhance visual sensitivity, although these remain unexamined in species with auditory reductions. Retinal specializations, such as visual streaks or areas of elevated cell density along the naso-temporal axis, have been observed in both the ganglion cell layer (GCL) (65–69) and the inner nuclear layer (INL) (70), suggesting adaptations for enhanced visual acuity (22,66). In *Rhinella marina* (Linnaeus, 1758), these streaks are also associated with a non-uniform distribution of photoreceptors, with peak densities along the naso-temporal axis (66). The spatial overlap between photoreceptor-rich regions and areas of high neuronal density in the GCL and INL defines a zone of acute vision, similar to the area centralis or visual streak found in other vertebrates (66). A comparable organization may exist in frogs with sensory reductions, potentially enhancing visual resolution in specific parts of the visual field.

Additional retinal adaptations, such as the slenderness and spacing of visual cells, are also critical in enhancing resolving power (22). The slenderness of visual cells (*i.e.*, rods and cones) is critical for fine detail resolution, as narrower cells can detect light with greater precision. Conversely, thicker cells impair the resolution of closely spaced points of light. Similarly, the spacing between visual cells influences the retina's ability to distinguish fine details. When cells are spaced closely, individual points of light are detected separately, enhancing resolution. However, if cells are too widely spaced, adjacent points of light may fall on neighboring cells, resulting in a blurred, indistinct image (22). In addition to enhancing precision, corneal enlargement may also be accompanied by adaptations in visual cells that improve sensitivity. One such adaptation involves the elongation of the outer segments of rod cells (22). This modification reduces the stimulation threshold, allowing rods to respond to lower light levels, thus increasing their sensitivity (22).

Finally, in frogs with reduced reliance on other sensory modalities, enhanced visual capacity may be accompanied not only by peripheral adaptations such as corneal enlargement and retinal specialization, but also by increased neural investment in brain regions dedicated to visual processing. In particular, these species may exhibit greater development of the optic tectum, the primary center for visual integration in amphibians (71). This association between peripheral and central adaptations has also been documented in other vertebrate groups, suggesting a broader pattern of coordinated investment across the visual system (72,73), but remains unstudied in frogs.

Conclusion

Frogs predominantly use acoustic communication for a wide range of social interactions, with mate attraction and selection being among the most critical functions. In species that have lost the ability to detect airborne sounds, this essential communication channel is impaired, necessitating compensatory adaptations. Contrary to our initial expectation that these species would evolve larger eyes to improve visual signaling, we found that they instead exhibit a relative enlargement of the cornea alongside an overall reduction in eye size. This corneal expansion likely enhances visual sensitivity, allowing these frogs to better utilize visual cues for social and reproductive behaviors while avoiding the metabolic and locomotor costs of larger

eyes. Such an adaptation is particularly important for small-bodied species facing anatomical constraints. Our results highlight the role of sensory compensation following auditory loss and provide new insights into the evolutionary dynamics of communication strategies in frogs.

Author Contributions

Jhael A. Ortega and Ryan K. Schott jointly conceptualized and designed the study. Jhael A. Ortega conducted all data collection and analyses, prepared the figures, and wrote the first draft of the manuscript. Ryan K. Schott provided methodological guidance and contributed to the interpretation of results. Santiago R. Ron, Kate N. Thomas, Rayna C. Bell, Matthew K. Fujita, David J. Gower, and Jeffery W. Streicher critically reviewed the manuscript and provided editorial suggestions that improved its quality.

Supervisor's Statement on Author Contributions

JAO and RKS conceived and designed the study. JAO collected new morphometric measurements. JAO collected new trait data with input from SRR. KNT, JWS, and DJG contributed morphometric measurements, and KNT, DJG, RCB, MKF, RKS, and JWS contributed trait data, from Thomas et al. (2020). JAO analyzed the data with guidance from RKS and based on a workflow written by KNT. JAO and RKS interpreted the results. JAO wrote the manuscript with edits from RKS, RCB, and SRR. All authors provided feedback and reviewed the manuscript.

Chapter III: Hearing Lost, Genome Gained: Genome Assemblies from a Frog with Auditory Reduction

Abstract

Amphibian genomes have historically been underrepresented in genomic research due to their large size and complexity, but recent advances in long-read sequencing technologies have facilitated the generation of high-quality assemblies. Here, we present the *de novo* genome assembly of *Pristimantis brevicrus*, a direct-developing frog species belonging to one of the most species-rich vertebrate genera that has lost middle ear structures at least three independent times. Using PacBio HiFi sequencing and the HiFiASM assembler, we obtained a highly contiguous assembly consisting of 884 contigs with a total length of approximately 2.17 Gb, an N50 of 12.76 Mb, and a GC content of 45.7%. Assembly quality was further validated with QUAST and Compleasm analyses, demonstrating high completeness and low ambiguity. These genomic resources represent a significant contribution to the study of anuran evolution, especially in species with reduced auditory structures, and provide a foundation for future comparative and functional genomic analyses.

Key words

Amphibian genomics; Direct development; Genome completeness; Long-read genome assembly; *Pristimantis brevicrus*; PacBio HiFi sequencing; Strabomantidae

Introduction

Amphibians are a diverse and ecologically significant vertebrate group, with over 8,000 species and global distribution (74). Their unique life histories and physiological adaptations make them important models for studies in ecology, evolution, and conservation biology (75). Despite their significance, amphibian genomic resources have lagged behind those of other vertebrates, primarily due to the large and complex nature of their genomes, which pose challenges in sequencing and assembly (75–78). Recent technological advances, particularly in long-read

sequencing and improved assembly algorithms, have substantially improved the quality and availability of amphibian reference genomes (79). These developments have resulted in a growing number of high-quality, chromosome-level genome assemblies, although many taxonomic groups remain underrepresented. Developing effective tools for genome annotation and comparative analyses remains a critical frontier for amphibian genomics (75).

In this study, we present mid-coverage genome assembly for *Pristimantis brevicrus*, an anuran species characterized by evolutionary reductions in its auditory system (74,78). Specifically, these species lack middle-ear structures such as the tympanic membrane and columella and have been described as missing vocal sacs and slits, indicating a notable sensory system modification (74). This taxon has been largely overlooked in genomic studies, making it a valuable addition to the growing repertoire of amphibian genomes. Notably, *Pristimantis* is the most species-rich genus of terrestrial vertebrates worldwide (620 species), underscoring the importance of genomic data from this lineage.

Here, we provide genome assemblies generated using Pacific Biosciences HiFi long-read sequencing technology, accompanied by assessments of assembly quality and completeness. These assemblies will serve as foundational resources to facilitate future investigations into the molecular and evolutionary mechanisms underlying sensory system reduction and diversification in amphibians.

Methodology

Specimen selection and sample collection

Pristimantis brevicrus was the species selected for his study (Fig. 1). It is characterized by the loss of middle ear structures, and according to their original descriptions, it also lacks vocal sacs and vocal slits. Specimens were collected in Ecuador from locations within their known distribution ranges. Collected individuals were transported to the Herpetology Division of the Museo de Zoología QCAZ at the Pontificia Universidad Católica del Ecuador (PUCE).

Specimens were collected and transported under the corresponding permits issued to the QCAZ museum by the Ministry of Environment, Water and Ecological Transition of Ecuador (permit

number: MAAE-DBI-CM-2022-0230). Upon arrival at the museum, individuals were euthanized following established ethical protocols. Muscle tissue from the calf and liver samples were collected and preserved in 96% ethanol at –80 °C. The specimens were fixed in formalin and stored in the museum's scientific collection. Export permits were obtained for the tissue samples, which were then transferred to Dr. Schott's laboratory (York University, Toronto, Canada), where they were stored in an ultra-low-temperature freezer until DNA extraction.

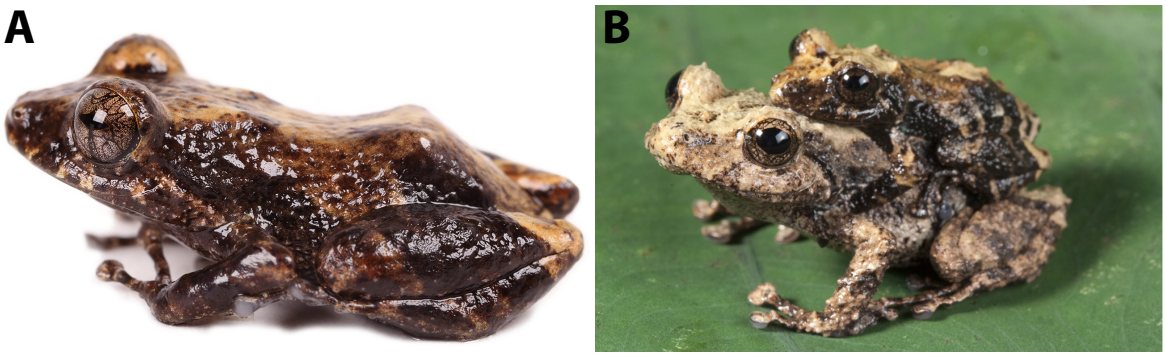

Figure 1. Representative photographs of the focal species included in this study. (*A*) Adult *Pristimantis brevicrus* in lateral view. **(*B*)** Pair of *P. brevicrus* in amplexus. Photographs by Santiago R. Ron.

DNA extraction and sequencing

High-molecular-weight genomic DNA was extracted from preserved liver tissue using the Monarch® HMW DNA Extraction Kit for Tissue (NEB, T3060G), following the manufacturer's instructions. DNA concentration was quantified with the Equalbit 1X dsDNA High Sensitivity Assay Kit (Cat. #EQ121-01) on a Qubit fluorometer, by mixing 2 µL of DNA with 198 µL of working solution per sample. DNA integrity and fragment size distribution were assessed using the Agilent TapeStation with the D5000 High Sensitivity ScreenTape Assay, diluting 1 µL of DNA in 10 µL of buffer.

Qualified DNA samples (DIN = 9.8 for both samples) were submitted for whole-genome sequencing (WGS) using Pacific Biosciences Revio long-read technology at the Lunenfeld-Tanenbaum Research Institute (Toronto, Canada). Libraries were prepared using the latest SMRT

Cell chemistry. Sequencing aimed for approximately 30× genome coverage per sample, using half a SMRT Cell for each sample.

Sequence assembly and quality control

Raw PacBio HiFi reads in BAM format were converted to FASTQ files using Samtools v1.16. *De novo* genome assemblies were generated independently for each sample using HiFiASM v0.16.1 (80), a genome assembler optimized for highly accurate long reads. Assemblies were run on the Béluga cluster (Compute Canada), using 36 CPUs and 356 GB of RAM per job to handle the computational demands of large-genome reconstruction. HiFiASM was executed with default parameters and 36 threads per sample. This approach produced high-quality, contiguous genome assemblies suitable for downstream genomic analyses.

To assess the quality of the raw sequencing data and genome assemblies, initial basic statistics were calculated using seqkit (80). Key metrics such as total number of contigs, total assembly length, contig length distribution (minimum, maximum, average), and GC content were obtained to evaluate assembly contiguity and completeness. Further quality evaluation of genome assemblies was performed using QUAST v5.2.0 (81), which provides comprehensive metrics including number of misassemblies, and contiguity indicators such as N50 and L50. The N50 represents the length of the shortest contig at which 50% of the total assembly length is covered, with higher values indicating greater assembly contiguity. The L50 is the minimum number of contigs whose combined length accounts for at least 50% of the genome assembly, where lower values reflect fewer, larger contigs. Additionally, the number of ambiguous bases per 100,000 base pairs (Ns per 100 kbp) was assessed to identify gaps or unresolved regions in the assembly; fewer Ns indicate higher sequence quality. QUAST analyses were run with parameters optimized for large genomes, using multiple CPU threads to reduce computational time.

Genome completeness was assessed using Compleasm (82), a fast reimplmenation of the popular tool BUSCO, which uses evolutionary homology to estimate assembly completeness through alignment of conserved orthologous proteins. For benchmarking, we employed the updated *tetrapoda_odb12* lineage dataset, which provides a comprehensive set of single-copy

orthologs for tetrapods. Compleasm was run with default parameters, leveraging multiple CPU threads to optimize computational efficiency. This approach allowed for robust evaluation of genome completeness, complementing the assembly quality metrics provided by QUAST. These complementary quality control steps ensured that the assembled genomes were of sufficient contiguity and completeness for subsequent comparative genomic analyses.

Results

We present the genome assembly and quality assessment results for *Pristimantis brevicrus*.

The primary genome assembly of *Pristimantis brevicrus* consisted of 884 contigs, with a total assembly length of approximately 2.17 Gb. The contig lengths varied widely, ranging from a minimum of 7,138 base pairs to a maximum of 49.4 Mb. The average contig length was approximately 2.46 Mb, indicating a generally high degree of contiguity in the assembly. These metrics provided an initial indication of assembly quality, which was further evaluated through additional analyses of genome completeness and structural integrity.

The QUAST analysis (Fig. 2, Table 1) corroborated these findings and reported an N50 value of 12.76 Mb and an N75 of 5.73 Mb, indicating strong assembly contiguity. The L50 and L75 metrics were 47 and 113 contigs, respectively. The GC content was 45.73%, consistent with typical amphibian genomes. Importantly, the assembly contained no gaps, with zero Ns per 100 kbp, highlighting the high sequence quality.

Table 1. QUAST assembly statistics for the *Pristimantis brevi*crus genome. Summary of contiguity and sequence quality metrics, including contig size distribution, total assembly length, GC content, and N/L statistics. All values are based on contigs ≥3,000 bp unless otherwise noted.

Assembly	*Pristimantis brevicrus* genome
# contigs (>= 0 bp)	884
# contigs (>= 1000 bp)	884
# contigs (>= 5000 bp)	884
# contigs (>= 10000 bp)	883
# contigs (>= 25000 bp)	806
# contigs (>= 50000 bp)	666
Total length (>= 0 bp)	2175107986
Total length (>= 1000 bp)	2175107986
Total length (>= 5000 bp)	2175107986
Total length (>= 10000 bp)	2175100848
Total length (>= 25000 bp)	2173593094
Total length (>= 50000 bp)	2168717292
# contigs	884
Largest contig	49415233
Total length	2175107986
GC (%)	45.73
N50	12759533
N75	5733901
L50	47
L75	113
# N's per 100 kbp	0.00

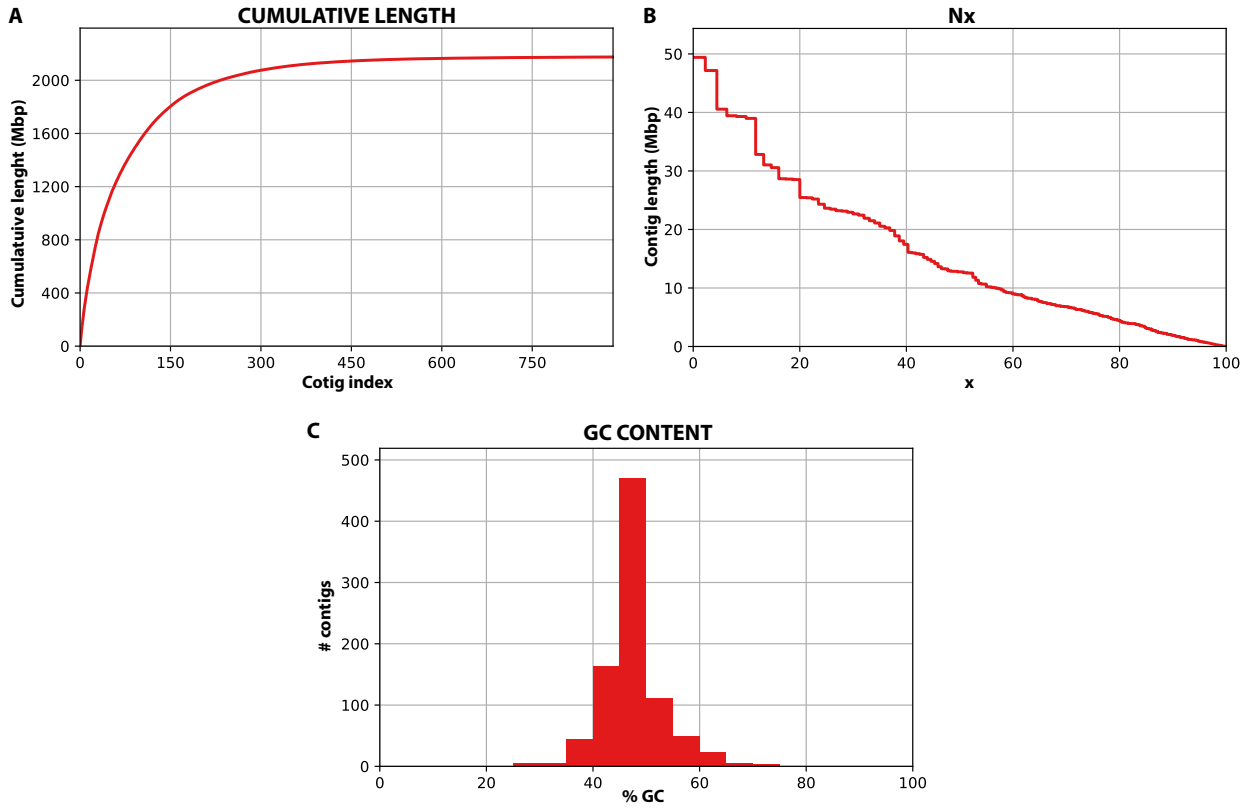

Figure 2. Genome assembly quality metrics for *Pristimantis brevicrus*, generated using QUAST v5.2.0. (*A*) Cumulative length curve of the assembly, illustrating the accumulation of total genomic content as contigs increase in size. **(*B*)** Nx plot showing contig length thresholds (e.g., N50, N75) at which x% of the total assembly length is represented by contigs of that length or longer. **(*C*)** GC content (%) distribution across contigs ordered by contig number, reflecting variation in base composition across the genome assembly.

To further evaluate genome completeness, we used Compleasm with the *tetrapoda_odb12* lineage dataset, which assesses the presence of highly conserved single-copy orthologs. The analysis identified a total of 5623 orthologous groups, of which 92.71% were complete and single-copy, and an additional 1.94% were complete but duplicated. Only 0.76% of genes were fragmented, and 4.59% were missing (Table 2). These values indicate a highly complete assembly for *Pristimantis brevicrus*, comparable to other high-quality long-read amphibian genomes.

Table 2. Compleasm-based assessment of genome completeness for *Pristimantis brevicrus*. Completeness was evaluated using Compleasm v0.2.2 against the tetrapoda_odb12 ortholog dataset, which includes 5,623 conserved single-copy orthologs. The assembly showed a high proportion of complete genes (92.71%), with low levels of duplication (1.94%) and fragmentation (0.76%). No insertions were detected, and 4.59% of genes were classified as missing.

Metric	Count	%
Complete (S)	5213	92.71%
Duplicated (D)	109	1.94%
Fragmented (F)	43	0.76%
Missing (M)	258	4.59%
Total	5623	100%

Discussion

In this study, we present a high-quality genome assembly for *Pristimantis brevicrus*, a direct-developing anuran species characterized by the evolutionary loss of middle ear structures. This assembly represents a valuable genomic resource for amphibian research, particularly given that *Pristimantis* is the most species-rich genus of terrestrial vertebrates and has been historically underrepresented in genomic studies. Moreover, *Pristimantis* belongs to the family Strabomantidae, one of the least represented anuran families in terms of available genome assemblies (75). Expanding genomic resources for this clade is therefore essential to better understand the evolutionary dynamics of highly diverse and morphologically specialized lineages within Neotropical frogs.

The *P. brevicrus* genome demonstrates excellent contiguity, with a contig N50 of 12.7 Mb, no ambiguous bases per 100 kbp, and a GC content consistent with other anurans. Compleasm analysis using the *tetrapoda_odb12* dataset recovered over 94% of conserved orthologs as complete, with low proportions of missing or fragmented genes. When compared to the 51 amphibian genome assemblies reviewed by Kosch et al. (75), the genome of *Pristimantis brevicrus* ranks among the most complete to date. More than 70% of those assemblies (36 genomes) exhibit BUSCO completeness scores (single-copy plus duplicated genes) below 90%, and 12 others range between 90.0% and 92.1%. Only three assemblies exceed 94.4%

completeness, placing *P. brevicrus* in the top tier of anuran genome quality, despite the lack of chromosome-level scaffolding. Notably, 14 of the low-completeness assemblies were produced using short-read technologies, which perform poorly in large, repeat-rich genomes like those of amphibians. These include some of the lowest completeness scores published to date, such as *Scaphiopus couchii* (0.7%), *Scaphiopus holbrookii* (2.6%), *Phrynoglossus myanhessei* (9.0%; Dicroglossidae), and *Pipa carvalhoi* (11.8%; Pipidae). Even in comparison with chromosome-level assemblies, which make up 28 of the 51 genomes analyzed, *P. brevicrus* remains highly competitive. Its completeness surpasses that of 26 chromosome-scale genomes, which range from 66.1% to 92.1%, and is only exceeded by *Xenopus tropicalis* (94.4%) and *Xenopus laevis* (96.0%), both assembled using hybrid or long-read approaches (Fig. 3).

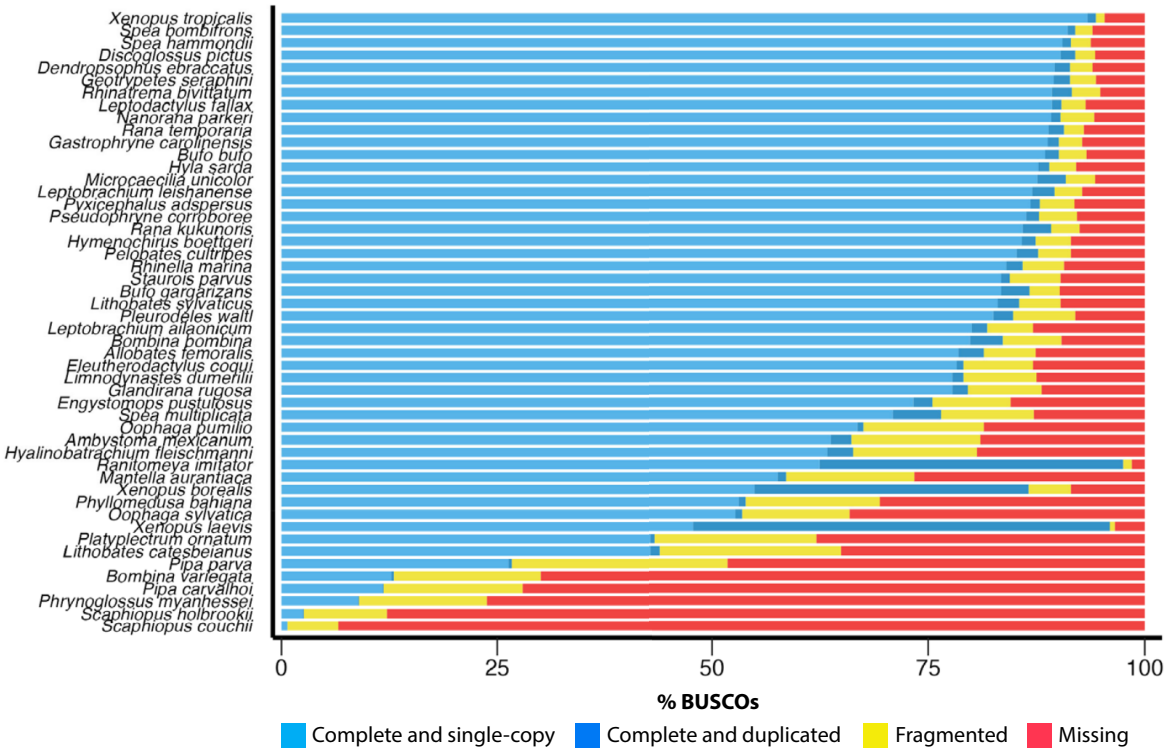

Figure 3. BUSCO (Benchmarking Universal Single-Copy Orthologs) assessment results for the 51 publicly available amphibian genome assemblies, based on the *tetrapoda_odb10* dataset. Bars indicate the proportion of complete (single-copy and duplicated), fragmented, and missing orthologs. Figure adapted from Kosch et al. (2025).

The high quality of the *P. brevicrus* genome was largely achieved through the use of PacBio HiFi long-read sequencing. This platform offers superior resolution of repetitive and structurally complex regions that often hinder assembly quality when using short-read data alone (75). This advantage has been documented in recent studies highlighting the superiority of HiFi reads for generating more contiguous and accurate assemblies in amphibians (79).

Overall, our results underscore the increasing accessibility and quality of amphibian genome assemblies afforded by long-read sequencing technologies, marking a significant step forward in characterizing the genomic diversity of this hyperdiverse vertebrate group. In particular, the use of HiFi sequencing enabled the generation of a highly complete assembly without the need for additional scaffolding data. This highlights the efficiency of the approach, not only in terms of data quality, but also in terms of time and cost, offering a practical alternative to full chromosome-level assemblies. However, it is important to acknowledge that without chromosome-level scaffolding, certain large-scale evolutionary questions, such as those involving chromosomal synteny, rearrangements, or overall genome architecture, remain inaccessible. Despite this, such resources are sufficiently robust to support a wide range of research questions, from comparative genomics to molecular evolution, and represent an important advance for amphibian genomics.

Conclusion

The *Pristimantis brevicrus* genome assembly presented here is among the most contiguous and complete amphibian genomes assembled to date using long-read sequencing technologies. The high N50 and Compleasm completeness values indicate a reliable and comprehensive genomic resource, which will facilitate studies of evolutionary adaptations associated with direct development and sensory system reduction. This genome fills critical gaps in anuran genomics by representing understudied direct-developing and earless lineages, and they set the stage for advancing our understanding of the molecular bases of key phenotypic traits in frogs.

Chapter IV: Seeing Differently: Selection on Opsin Genes in Frogs with Reduced Auditory Systems

Abstract

The loss or reduction of a sensory modality can alter selective pressures on other sensory systems, yet the molecular consequences of such cross-modal shifts remain poorly understood. Here, we test whether auditory system reduction in frogs is associated with altered evolutionary dynamics in visual opsins. We analyzed four key genes (RH1, SWS1, SWS2, and LWS) using codon-based selection models across a diverse sample of anuran species. Overall, we found strong purifying selection across all genes, consistent with their conserved visual functions. However, species with auditory reductions showed gene-specific patterns of relaxed constraint and episodic positive selection. Notably, SWS1 and LWS exhibited significant relaxation of purifying selection, and all genes showed evidence of episodic or site-specific diversifying selection. These results suggest that auditory loss is associated with localized molecular changes in visual opsins, possibly reflecting compensatory shifts in sensory ecology. Our findings highlight the potential for cross-modal interactions to shape the evolutionary trajectories of sensory genes.

Key words

Anuran auditory evolution, Middle ear reduction, Molecular adaptation, Opsin gene evolution, Sensory loss, Sensory trade-offs, Visual system compensation.

Introduction

The tympanic middle ear is a critical structure for detecting airborne sounds in frogs, underpinning acoustic communication behaviors essential for mate attraction, species recognition, and territorial interactions (1,5,7,34). Despite this functional importance, multiple anuran lineages have independently evolved reductions or complete losses of this structure, with

over 38 documented instances distributed non-randomly across the phylogeny (14,16). These losses are significantly associated with specific ecological and life-history traits including diurnality, terrestrial microhabitat use, small body size, narrow elevational ranges, and occurrence at high altitudes. Importantly, earless species often coexist with eared relatives within overlapping geographic and microhabitat ranges, indicating that environmental factors alone do not fully explain the repeated loss of auditory structures (16).

The recurrent loss of auditory capacity raises the possibility of a sensory trade-off whereby diminished hearing could be compensated by enhanced reliance on alternative communication channels. Given that anurans are generally highly visual animals, employing visual cues for various ecological functions including predator avoidance and social signaling (16,34,83), vision emerges as a strong candidate for compensatory adaptation. Prior morphological studies have identified adaptations in the visual system of earless species, prompting investigation into whether molecular adaptations in visual opsins accompany these anatomical changes.

Visual opsins form the protein component of the light-sensitive visual pigments that initiate the phototransduction cascade in photoreceptor cells (84). In vertebrates, they are expressed in rods and cones, which are specialized for scotopic (dim-light) and photopic (bright-light) vision, respectively (85). The ancestral vertebrate visual system comprised five distinct opsin classes: one rod opsin (RH1) and four cone opsins (LWS, RH2, SWS1, and SWS2), each tuned to a different spectral range (86). Most frogs retain four of these five opsins (*i.e.,* RH1, SWS1, SWS2, and LWS), with RH2 having been lost in the amphibian ancestor (9), providing broad spectral sensitivity across visual environments (85–87). Although the spectral sensitivities of rod and cone opsins are generally conserved across vertebrates, changes in opsin amino acid sequences can shift the wavelength of peak absorption (λ_{max}), a process known as spectral tuning, and enable adaptation to variable light conditions (85,88,89). Additionally, peak spectral sensitivity is influenced by the chromophore bound covalently to the opsin protein (90). Most vertebrates use a vitamin A1-derived chromophore (retinal, A1), but some species incorporate a vitamin A2-derived chromophore (3,4-didehydroretinal, A2), which shifts peak absorption toward longer wavelengths and broadens spectral sensitivity (85,90,91).

Opsin gene variation and spectral tuning are central to the adaptive evolution of vertebrate visual systems. Across taxa, shifts in opsin sequence, expression, and chromophore usage correlate with changes in ambient light, diel activity, and habitat structure. In cichlid fishes, for instance, shifts in cone opsin expression and sequence variation have evolved in response to water depth and turbidity, allowing species to maximize sensitivity to their visual environment (92,93); deep-sea fishes, such as *Diretmus argenteus*, have evolved multiple rod opsins with distinct spectral peaks to navigate dim, spectrally restricted habitats (94), and diurnal primates have duplicated and tuned long-wavelength-sensitive opsins, enhancing color vision (95). Conversely, lineages occupying persistently dim environments often show opsin gene losses, such as in coelacanths and nocturnal mammals (84,96).

Frogs also show remarkable visual system diversification. Unlike most vertebrates, they possess two spectrally distinct classes of rod photoreceptors: a dominant population expressing RH1 and a minority expressing SWS2, typically a cone opsin, within rod-like cells. Additionally, LWS is found in double cones, and single cones express either SWS1 or SWS2 (86,97). Early work in Neotropical frogs reported positive selection at multiple opsin amino acid sites associated with diurnal habits, suggesting that spectral tuning may enhance visual performance and communication under bright-light conditions (87). However, broader phylogenetic analyses have since found no consistent association between opsin evolution and diel activity (85), indicating that other ecological or phylogenetic factors may modulate selection on these genes. The evolutionary loss of the short-wavelength–sensitive opsin SWS2 in diurnal poison frogs (Dendrobatidae), first reported in *Oophaga pumilio*, has now been confirmed across the family, and may reflect relaxed selection on dim-light discrimination and increased reliance on vision under full daylight (85,87,98). Ontogenetic transitions further highlight visual plasticity: in *Lithobates sphenocephalus*, opsin gene expression shifts between aquatic tadpoles and terrestrial juveniles, enabling adaptation to stage-specific light environments (97). Similarly, chromophore usage varies ontogenetically in some species; the fully aquatic clawed frog *Xenopus laevis* relies exclusively on the A2 chromophore throughout its life cycle, while biphasic species like ranids and hylids transition from primarily A2 in tadpoles to predominantly A1 in adults, aligning with habitat-specific light environments (99).

Given the evolutionary lability of auditory structures and the ecological significance of vision in frogs, exploring the molecular evolution of visual opsins presents a promising opportunity to uncover sensory trade-offs. While previous work has identified morphological changes in the visual system of earless frogs, the extent to which these changes are mirrored at the genetic level remains unknown. Here, we investigate the molecular evolution of visual opsin genes across a diverse sample of anuran species, including both eared and earless taxa. By analyzing selection signatures, we test whether auditory loss is associated with potential adaptive shifts in visual molecular traits. We hypothesize that the loss of auditory input in earless species is associated with either relaxed purifying selection or positive selection in visual opsin genes. Such signals may occur at the gene-wide level or at specific amino acid sites, particularly those near known spectral tuning sites or residues involved in opsin kinetics. This work advances our understanding of how vertebrates reconfigure sensory systems in response to functional loss and ecological pressures.

Methodology

Extraction of opsin sequences

The assembled genome FASTA file of *Pristimantis brevicrus* was formatted into a local nucleotide BLAST database using *makeblastdb* (100) to facilitate targeted retrieval of opsin gene sequences. BLASTN searches were conducted using curated opsin reference sequences from the Terrarana clade to maximize homology detection. Searches were performed with an e-value cutoff of 1e-10 and default parameters, with results output in tabular format.

To complement opsin sequence recovery, an *in silico* target capture pipeline (101) was applied to additional sequencing data generated within our laboratory but not yet published. Reference FASTA files for each opsin gene were curated from species with available genomic or transcriptomic resources. To improve recovery across phylogenetically diverse taxa, reference sequences were grouped by evolutionary proximity into clade-specific sets. Trimmed reads were aligned to these references using *Bowtie2* (102) in local alignment mode with relaxed parameters optimized for divergent sequences. Resulting BAM files were processed with *Samtools v1.16* (103) to fix mate information, sort and index alignments, and filter mapped reads.

Consensus sequences were generated directly from filtered alignments using samtools consensus. Sequence completeness and coverage were assessed with Mosdepth v0.3.2 (104), and low-quality regions were masked using a custom Perl script.

Visual opsins sequences dataset

Independent gene matrices were assembled for each of the four visual opsin genes to create a comprehensive, phylogenetically representative dataset. Newly recovered sequences covering at least 50% of the coding region were retained. Each matrix combined these novel sequences with previously published opsin data (85,87) and additional homologs retrieved from GenBank via targeted BLAST searches using curated query files. Reference sequences for BLAST were selected based on phylogenetic proximity to optimize recovery across diverse anuran clades. Initial matrix assembly and sequence curation were performed in *Mesquite v3.51* (105). Preliminary alignments were generated with *Muscle v5.1* (106), followed by codon-aware alignment using *MACSE v2.07* (107) using the *alignSequences* function, followed by refinement with *refineAlignment*. Alignments were cleaned by replacing stop codons and masked characters with ambiguous bases to preserve reading frame integrity. Final alignments were manually inspected and adjusted in *AliView v1.3* (108) to ensure homology and codon structure accuracy.

Selection analysis

To investigate molecular signatures of selection in visual opsin genes, we performed three complementary codon-based analyses using the web-based interface of Datamonkey 2.0 (109): *FUBAR*, *RELAX*, and *BUSTED*. All analyses were run separately for each opsin gene matrix. When applicable, the foreground branches were defined as those corresponding to species with documented auditory losses (16), allowing targeted comparisons between taxa with and without such reductions (Fig. 1). For BUSTED, we first ran the model using all branches as test branches and then re-ran it specifying only the branches corresponding to auditory-loss lineages as the test set.

FUBAR (Fast Unconstrained Bayesian AppRoximation) (110) detects pervasive selection by estimating site-specific dN/dS ratios under a Bayesian framework. It identifies

codon positions evolving under consistent purifying or positive selection across the entire tree. In contrast, RELAX (111) tests whether the intensity of selection has been systematically relaxed or intensified along foreground branches compared to the background. This is particularly suited to detecting shifts in selective pressure associated with ecological or physiological changes. Finally, BUSTED (Branch-site Unrestricted Statistical Test for Episodic Diversification) (112) identifies gene-wide evidence of episodic positive selection affecting a subset of sites along foreground branches. Datamonkey default thresholds and model parameters were used unless otherwise specified.

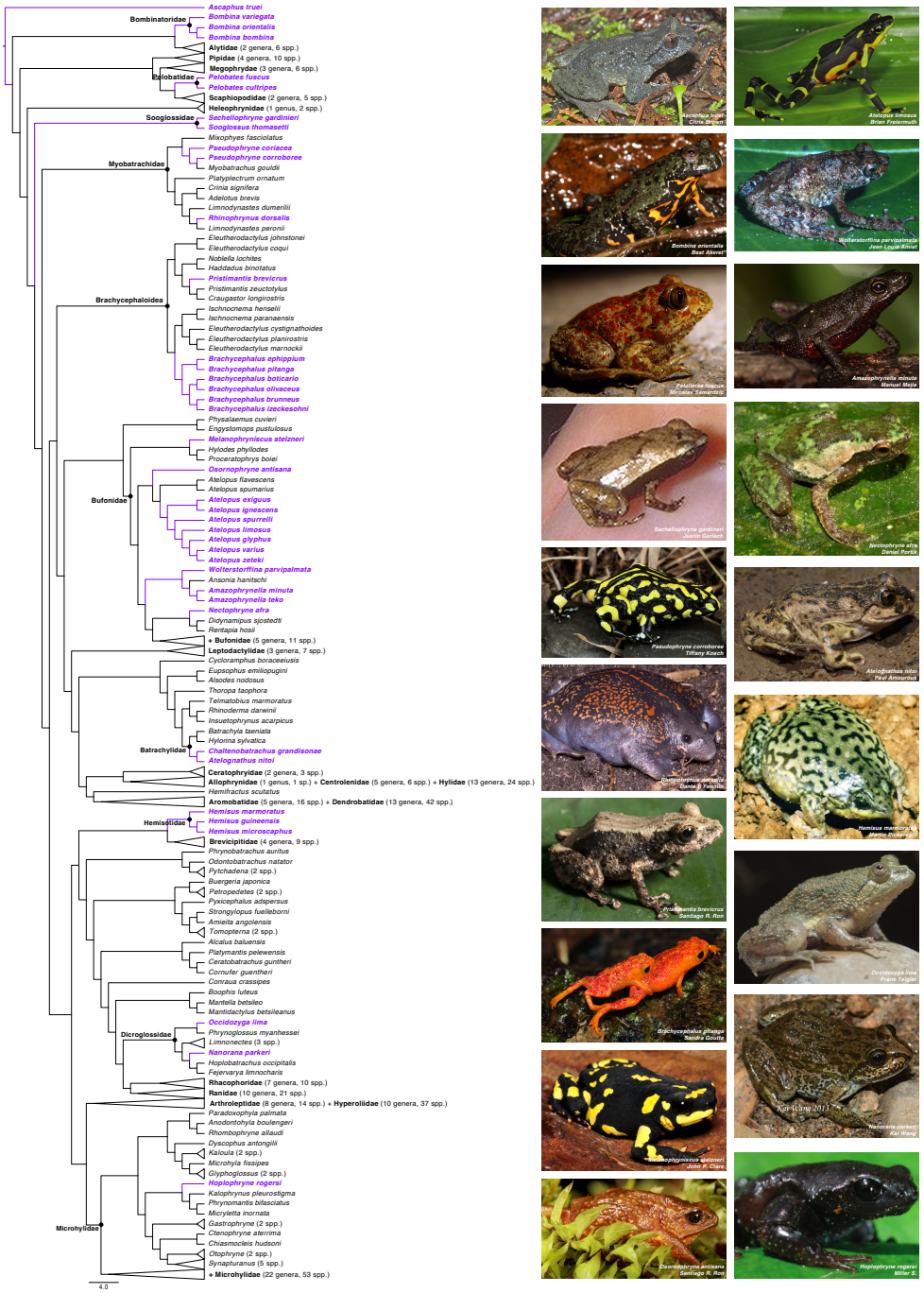

Figure 1. Phylogenetic sampling of anuran RH1 sequences, highlighting species with auditory system reductions. Maximum likelihood phylogeny inferred from the RH1 alignment (409 terminal taxa), showing broad taxonomic sampling across Anura. Branches in purple indicate species with known reductions or losses of middle ear structures. Major anuran families and genera containing only species without auditory reductions are shown as collapsed clades, labeled with family or genus names for clarity. For collapsed genera, the number of species included is indicated in parentheses; for collapsed families, both the number of genera and the

total number of species are indicated in parentheses. Representative photographs are included for each independent clade containing species with auditory loss; each image is annotated with the species' scientific name and photographer credit.

Results

Recovery of opsin sequences

We assembled four gene-specific alignments corresponding to the visual opsins RH1, SWS1, SWS2, and LWS, comprising 409, 365, 326, and 383 terminal taxa, respectively. These matrices integrate sequences from publicly available sources, high-coverage loci extracted from the *Pristimantis brevicrus* genome, and additional sequences recovered using an *in-silico* target capture approach based on unpublished data generated in our laboratory. Complete or partial coding sequences were successfully obtained for all four opsins across most major anuran clades (see Supplementary Information for full recovery metrics).

Our alignments represent the most taxonomically comprehensive opsin datasets assembled for frogs to date. For comparison, the most recent broad-scale analysis by Schott et al. (85) included 125 RH1, 118 LWS, 113 SWS1, and 113 SWS2 sequences, while the earlier study by Wan et al. (87) analyzed 103 RH1, 99 LWS, 98 SWS1, and 42 SWS2 sequences. In contrast, our alignments contain over three times more sequences for each gene, providing enhanced phylogenetic resolution and improved statistical power for detecting lineage- and site-specific evolutionary shifts. In addition to their expanded taxonomic breadth, our datasets also capture robust representation of species with auditory system reductions. Of the 383 taxa in the LWS alignment, 35 (9.14%) correspond to species with confirmed loss of middle ear structures. Similarly, 32 of 365 (8.77%) taxa in the SWS1 matrix, 39 of 409 (9.54%) in RH1, and 37 of 326 (11.35%) in SWS2 belong to lineages exhibiting auditory reduction. This extensive sampling across sensory-reduced species provides a uniquely powerful framework for testing hypotheses of compensatory molecular evolution in the visual system of frogs.

On average, gene recovery exceeded 80% across taxa, enabling robust downstream phylogenetic and selection analyses. RH1 showed the highest recovery consistency, with average completeness surpassing 90% in several clades. SWS2 also exhibited high recovery across groups, often exceeding 85%. In contrast, SWS1 and LWS showed greater variation, with some

species yielding partial or fragmented sequences. Consistent with previous reports of opsin gene loss in neotropical poison frogs, we did not recover SWS2 sequences in any members of the family Dendrobatidae, despite successful recovery of the remaining opsins from the same individuals. This pattern supports earlier findings suggesting SWS2 has been pseudogenized or entirely lost in this lineage (85,87). Similarly, SWS1 was not recovered in any arthroleptid species included in our dataset, supporting previous suggestions that this gene may have been lost in Arthroleptidae (9). Finally, we recovered full-length coding sequences for all four opsins from the *Pristimantis brevicrus* genome.

Selective patterns in visual opsins reflect predominant purifying selection and episodic adaptive events in auditory-reduced species

To investigate whether auditory system reduction influences visual gene evolution, we applied three complementary codon-based selection analyses: RELAX, BUSTED, and FUBAR, designating species with auditory system reductions as the foreground branches for BUSTED and RELAX analyses, to four anuran visual opsins. Across genes and taxa, purifying selection was pervasive as expected; however, several opsins exhibited gene- and lineage-specific signatures of relaxed constraint and episodic diversifying selection, particularly in species with reduced auditory systems.

RH1 (Table 1)— To assess patterns of selection acting on RH1, we first applied BUSTED using the entire phylogeny as the test set (Table S1). This analysis provided strong evidence for episodic diversifying selection across the tree (LRT $p = 0.000$). The unconstrained model inferred three nonsynonymous rate classes ($\omega_1 = 0.035$, $\omega_2 = 1.000$, $\omega_3 = 56.85$), with the vast majority of sites evolving under purifying selection (92.1%). Model fit improved substantially over the null model (ΔAICc = 294.1) and BUSTED identified 49 codons with evidence ratios ≥10 and over 500 (site, branch) pairs with empirical Bayes factors (EBF) >100, suggesting that adaptive evolution has affected a small number of sites distributed across the phylogeny.

To investigate whether this selection was specifically associated with sensory system reduction, we conducted a second BUSTED analysis using only foreground branches corresponding to species with auditory loss or reduction. This analysis again detected significant evidence of episodic selection (LRT $p = 0.0212$). The estimated ω classes were 0.073 (97.1%), 1.000 (1.75%), and 5.634 (1.12%), with a mean ω of 0.151 and coefficient of variation (CoV) of 3.93. Twenty-four site–branch combinations exhibited strong support for positive selection (EBF > 100), indicating localized episodes of adaptive change in lineages with reduced auditory systems.

Complementing these results, the *FUBAR* analysis identified four codon sites (*i.e.* 112, 169, 213, 333) under pervasive diversifying selection with posterior probabilities ≥ 0.9, while 308 codons were inferred to be under strong purifying selection. Sites 169 and 213, in particular, showed high non-synonymous rates relative to synonymous rates ($\beta - \alpha > 4.3$), and their Bayes factors exceeded 100,000, indicating extremely strong support for positive selection.

The *RELAX* analysis did not identify a statistically significant relaxation or intensification of selection along these foreground branches ($K = 0.80$, $p = 0.050$, $LR = 3.83$), although the result was marginal. The general descriptive model estimated three site classes, with approximately 92.78% of sites evolving under strong purifying selection ($\omega_1 \approx 0.00$), 6.49% under nearly neutral selection ($\omega_2 \approx 0.91$), and a small proportion (0.73%) under strong diversifying selection ($\omega_3 \approx 128.8$). The alternative model suggested that selection in foreground branches was slightly relaxed, with ω_3 decreasing to 24.87, though the distribution of sites among categories remained similar. Taken together, these results suggest that RH1 has experienced both episodic and pervasive positive selection in association with the reduction or loss of auditory structures in frogs, despite the absence of significant global shifts in selective pressure as assessed by RELAX.

Table 1. Summary of codon-based selection analyses for the RH1 opsin gene. This table presents the results of RELAX, BUSTED, and FUBAR analyses for the RH1 alignment (409 taxa). RELAX did not identify a statistically significant relaxation of purifying selection in test branches. BUSTED identified signatures of episodic positive selection affecting a small proportion of codons and branches in foreground lineages. FUBAR identified four codons under pervasive positive selection. These findings suggest that, despite the overall conservation of RH1, localized adaptive changes may have occurred repeatedly.

Analysis	Model	*log* L	#. param	AICc	Branch set	ω1	ω2	ω3
RELAX	General descriptive	-48836.7	1633	100977.1	Shared	0.00(92.78%)	0.9(6.49%)	128.8 (0.73%)
	RELAX alternative	-49476.8	827	100617.2	Reference	0.0 (90.37%)	1.0 (9.28%)	55.84 (0.35%)
					Test	0.01(90.37%)	1.0 (9.28%)	24.87 (0.35%)
	RELAX null	-49478.7	826	100619.0	Reference	N/A	1.0 (9.93%)	55.87 (0.33%)
					Test	N/A	1.0 (9.93%)	55.87 (0.33%)
	RELAX partitioned	-49472.4	831	100616.5	Reference	N/A	1.0 (9.78%)	60.45 (0.32%)
					Test	N/A	0.96(9.13%)	11.22 (1.12%)
BUSTED	**Model**	***log* L**	**#. params**	**AICc**	**Rate distribution**			
	Unconstrained model	−48106.1	836	97894.0	**Tested ω** 0.07299 (97.133%) 1.000 (1.7481%) 5.634 (1.1186%) Mean = 0.1514, CoV = 3.934			
	Unconstrained model				**Background ω** 0.000 (81.290%) 0.5619 (18.472%) 41.06 (0.23769%) Mean = 0.2014, CoV = 9.961			
	Unconstrained model				**Synonymous rates** 0.2994 (30.500%) 0.8976 (49.198%) 2.301 (20.301%) Mean = 1.000, CoV = 0.7059			
	Constrained model	−48109.2	835	97898.2	**Tested ω** 0.02228 (88.516%) 1.000 (6.6257%) 1.000 (4.8585%) Mean = 0.1346, CoV = 2.317			
	Constrained model				**Background ω** 0.000002 (81.927%) 0.59 (17.851%) 43.92 (0.2229%) Mean = 0.2029, CoV = 10.24			
	Constrained model				**Synonymous rates** 0.2990 (30.475%) 0.8971 (49.254%) 2.304 (20.272%) Mean = 1.000, CoV = 0.7068			

	Sites under (+) selection	Partition	α	β	β-α	Prob α>β	Prob α<β	Bayes Factor α<β
FUBAR	**169**	1	2.543	7.125	4.582	0	1.000	103393.216
	213	1	2.770	7.125	4.355	0	1.000	955945.278
	112	1	1.109	2.815	1.706	0	985	270.519
	333	1	654	1.131	477	22	920	48.212

SWS1 (Table 2)— When testing for episodic diversifying selection across all branches of the phylogeny using BUSTED (Table S2), we found strong evidence for gene-wide episodic positive selection acting on *SWS1* ($p = 0.000$). The unconstrained model partitioned codon sites into three ω categories: 93.8% of sites evolved under strong purifying selection ($\omega \approx 0.059$), 6.1% under neutral to weak selection ($\omega = 1.00$), and a very small proportion (~0.06%) under extreme diversifying selection ($\omega \approx 1392$). The mean ω across the gene was 0.997 with a high coefficient of variation (CoV = 35.1), reflecting substantial heterogeneity in selective pressures. Synonymous substitution rates showed typical variation, with mean rate normalized to 1.0. The constrained model that disallowed episodic selection fit the data significantly worse (higher AICc), supporting the presence of episodic positive selection events throughout the phylogeny.

Focusing specifically on branches with documented auditory system losses as foreground, *BUSTED* detected significant evidence for episodic diversifying selection acting on at least one site in foreground branches ($p = 0.0288$). In the unconstrained model, the distribution of ω values revealed that 38.4% of codons evolved under a low non-synonymous rate ($\omega \approx 0.065$), 60.7% under an intermediate rate ($\omega \approx 0.083$), and 0.93% under strong diversifying selection ($\omega \approx 4.75$). The mean ω was 0.1195, with a coefficient of variation of 3.76, again reflecting heterogeneous selection pressures across sites. Although only one site showed an evidence ratio (ER) ≥ 10 for positive selection, BUSTED identified 16 site–branch combinations with empirical Bayes factors (EBF) exceeding 100, highlighting multiple instances of episodic selection on foreground branches.

The *FUBAR* analysis further supported these findings by identifying one codon (site 115) under pervasive diversifying selection, with a posterior probability of 0.999 and a Bayes factor exceeding 6,800. This site exhibited a high non-synonymous rate ($\beta = 1.217$) relative to a

low synonymous rate (α = 0.252), resulting in a β – α difference of 0.965. In contrast, 312 codons were inferred to be under strong purifying selection, reinforcing the predominance of constraint across this gene.

The *RELAX* test identified a statistically significant relaxation of selective pressure in the lineages with auditory losses (K = 0.32, p = 0.000, LR = 12.75). The general descriptive model estimated that 97.9% of sites evolved under strong purifying selection ($\omega_1 \approx 0.05$), 1.99% under nearly neutral selection ($\omega_2 \approx 1.16$), and 0.11% under very strong diversifying selection ($\omega_3 \approx 874.9$). Under the alternative model, selection intensity was lower in foreground branches, with ω_3 dropping to 25.52, and purifying selection dominating nearly 88% of the sites ($\omega_1 \approx 0.00$), consistent with a widespread relaxation of constraint. Together, these results highlight that while SWS1 remains largely conserved, there are clear signatures of episodic positive selection and relaxed purifying selection associated with auditory system reduction, suggesting adaptive evolutionary changes in this visual opsin gene within these taxa.

Table 2. Summary of codon-based selection analyses for the SWS1 opsin gene. Results from RELAX, BUSTED, and FUBAR analyses are shown for the SWS1 alignment (365 taxa). RELAX models tested for shifts in selection intensity between foreground (auditory reduced) and background lineages. Partitioned models detected significant relaxation of purifying selection in test branches, evidenced by lower ω values and a shift in site proportions across rate categories. BUSTED detected episodic positive selection, with a small proportion of sites in foreground branches showing ω > 1. FUBAR identified one codon (site 115) under pervasive positive selection across the entire tree. Together, these results indicate that although SWS1 remains largely conserved, it shows clear signatures of both relaxed constraint and adaptive change in specific lineages.

Analysis	**Model**	***log* L**	**#. params**	**AICc**	**Branch set**	**ω1**	**ω2**	**ω3**
RELAX	General descriptive	-501321	1473	103244.6	Shared	0.05(97.9%)	1.16(1.99%)	874.91 (0.11%)
	RELAX alternative	-50708.4	747	102919.5	Reference	0.0(87.69%)	1.0(12.22%)	22701.93(0.09%)
					Test	0.00(87.69%)	1.00(12.22%)	25.52 (0.09%)
	RELAX null	-50714.7	746	102930.3	Reference	0.0 (87.95%)	1.0 (11.96%)	22885.58(0.09%)
					Test	0.0 (87.95%)	1.0 (11.96%)	22885.58(0.09%)
	RELAX partitioned	-50705.2	751	102921.2	Reference	0.0 (87.78%)	1.0 (12.13%)	30832.70(0.09%)
					Test	0.04 (90.8%)	0.56 (8.44%)	9.19 (0.76%)
	Model	***log* L**	**#. params**	**AICc**	**Rate distribution**			

BUSTED					**Tested ω**			
	Unconstrained model	−50073.8	101669	756	0.0647 (38.35%) 0.0831 (60.715%) 4.751 (0.93174%)			
					Mean = 0.1195, CoV = 3.758			
					Background ω			
	Unconstrained model				1.0 (5.7072%) 0.0631 (94.218%) 1.0e+4 (0.075185%)			
					Mean = 7.635, CoV = 35.90			
					Synonymous rates			
	Unconstrained model				0.6128 (52.728%) 1.193 (37.516%) 2.349 (9.7557%)			
					Mean = 1.000, CoV = 0.5203			
					Tested ω			
	Constrained model	−50076.6	101672	755	0.0522 (10.22%) 0.05957 (84.796%) 1.000 (4.9836%)			
					Mean = 0.1057, CoV = 1.938			
					Background ω			
	Constrained model				1.00 (5.7229%) 0.0629 (94.202%) 1.e+4 (0.075173%)			
					Mean = 7.634, CoV = 35.90			
					Synonymous rates			
	Constrained model				0.6117 (52.444%) 1.187 (37.548%) 2.332 (10.009%)			
					Mean = 1.000, CoV = 0.5194			
FUBAR	**Sites under (+) selection**	**Partition**	**α**	**β**	**β-α**	**Prob α>β**	**Prob α<β**	**Bayes Factor α<β**
	115	1	0.252	1.217	0.965	0.000	0.999	6885.11

SWS2 (Table 3)— The BUSTED analysis conducted on SWS2 using all branches in the phylogeny as the test set revealed strong evidence of episodic diversifying selection across the gene (LRT p = 0.000) (Table S3). The analysis included 325 sequences and 363 codon positions. According to the unconstrained model, the majority of sites evolved under strong purifying selection (ω = 0.03, 74.7%), with a subset under intermediate rates (ω = 0.32, 25.2%) and a small fraction (0.07%) experiencing very high nonsynonymous rates (ω = 205.7), indicative of episodic positive selection. In total, 35 codon sites showed evidence ratios ≥10, and 317 branch–site combinations had empirical Bayes factors (EBF) ≥100, further supporting widespread but localized episodes of diversifying selection throughout the phylogeny. These results suggest that, despite its overall conservation, SWS2 has experienced recurrent bursts of adaptive evolution across multiple anuran lineages.

When restricting the analysis to branches representing lineages with auditory system reduction, *BUSTED* detected strong evidence for episodic diversifying selection affecting a subset of sites and branches within the SWS2 phylogeny ($p < 0.0001$). The unconstrained model fit to the full alignment of 325 sequences and 363 codons showed that the majority of sites (74.2%) evolved under strong purifying selection ($\omega = 0.04562$), but a small proportion (0.1%) exhibited high non-synonymous rates ($\omega = 204.7$), consistent with adaptive episodes in a restricted number of branches. Importantly, 26 branch–site combinations exceeded an empirical Bayes factor (EBF) of 100, indicating strong lineage-specific selection signals despite the rarity of positively selected sites. Four sites showed evidence ratios ≥10 for positive selection under this model, further supporting punctuated and localized adaptive shifts in this gene.

FUBAR analyses corroborated a pattern of pervasive purifying selection across most codon sites, with 328 codons inferred to be under negative selection (posterior probability ≥ 0.9). Only one site, codon 69, showed evidence of pervasive positive selection ($\alpha = 1.21$, $\beta = 2.815$, $\beta–\alpha = 1.605$, $P[\alpha < \beta] = 0.904$, Bayes factor = 42.92). Overall, these results indicate that while SWS2 is primarily conserved, a small number of codons and branches within species lacking auditory systems have likely experienced episodic bursts of adaptive evolution.

The *RELAX* analysis did not detect significant evidence of selection intensification or relaxation acting on foreground branches ($K = 1.25$, $p = 0.259$, $LR = 1.27$). Despite this, branch-site-specific rate classes estimated under the general descriptive model suggested a small proportion of sites (0.46%) under strong diversifying selection ($\omega_3 = 206.18$), while most codons were best fit by a model of strong purifying selection ($\omega_1 = 0.00$, 94.03% of sites) or nearly neutral evolution ($\omega_2 = 0.89$, 5.51%). The partitioned descriptive model also recovered a low frequency of codons evolving under high ω ratios on foreground branches ($\omega_3 = 486.08$, 0.08%), although these estimates were not statistically supported in the formal test.

Table 3. Summary of codon-based selection analyses for the SWS2 opsin gene. Selection results are presented for the SWS2 alignment (326 taxa), analyzed using RELAX, BUSTED, and FUBAR. RELAX models include general and partitioned descriptive fits, as well as null and alternative models testing for relaxation or intensification of selection along foreground branches (K). BUSTED results include ω distributions for tested and background branches, along with synonymous rate categories, showing a small subset of sites with very high ω ratios indicative of episodic diversifying selection. FUBAR identified one codon (site 69) under pervasive positive selection across the full phylogeny. Collectively, these results suggest that while SWS2 remains strongly conserved across anurans, isolated sites and branches exhibit signatures of adaptive evolution.

Analysis	**Model**	***log* L**	**#. params**	**AICc**	**Branch set**	**ω1**	**ω2**	**ω3**
RELAX	General descriptive	-44017.6	1313	90690.8	Shared	0.0(94.03%)	0.89(5.51%)	206.18 (0.46%)
	RELAX alternative	-44657.4	667	90656.5	Reference	N/A	1 (10.56%)	72.45 (0.14%)
					Test	N/A	1 (10.56%)	214.47 (0.14%)
	RELAX null	-44658.1	666	90655.7	Reference	N/A	1 (10.56%)	75.07 (0.15%)
					Test	N/A	1 (10.56%)	75.07 (0.15%)
	RELAX partitioned	-44530.1	671	90409.9	Reference	0.00(89.18%)	0.99(10.67%)	68.87 (0.15%)
					Test	0.00(88.74%)	0.88(11.18%)	486.08 (0.08%)
BUSTED	**Model**	***log* L**	**#. params**	**AICc**	**Rate distribution**			
	Unconstrained model	−43752.0	676	88863.9	**Tested ω** 0.04562 (74.232%) 0.191 (25.660%) 204.7 (0.10745%) **Mean = 0.3029, CoV = 22.13**			
	Unconstrained model				**Background ω** 0.07801 (96.776%) 1.0 (3.1596%) 228.0 (0.064189%) Mean = 0.2534, CoV = 22.78			
	Unconstrained model				**Synonymous rates** 0.5192 (47.300%) 1.158 (42.220%) 2.533 (10.480%) Mean = 1.000, CoV = 0.6052			
	Constrained model	−43763.7	675	88885.3	**Tested ω** 0.0558 (73.709%) 0.07550 (22.777%) 1.000 (3.5143%) Mean = 0.09347, CoV = 1.853			
	Constrained model				**Background ω** 0.07766 (96.732%) 1.00 (3.2042%) 226.4 (0.063840%) Mean = 0.2517, CoV = 22.72			

	Constrained model				Synonymous rates 0.5178 (46.748%) 1.149 (42.456%) 2.500 (10.796%) Mean = 1.000, CoV = 0.6009			
FUBAR	**Sites under (+) selection**	**Partition**	**α**	**β**	**β-α**	**Prob α>β**	**Prob α<β**	**Bayes Factor α<β**
	69	1	1.21	2.815	1.605	0.000	0.904	42.918

LWS (Table 4)— BUSTED detected strong evidence of episodic diversifying selection across the LWS gene when all branches were tested (p = 0.000) (Table S4). The unconstrained model inferred that 92.5% of sites evolved under strong purifying selection (ω ≈ 0.039), 7.4% under neutrality (ω = 1), and 0.1% under strong positive selection (ω ≈ 101.3), with a mean ω of 0.220 and high variation across sites (CoV = 15.17). Compared to the constrained model (ΔAICc = 184), these results support lineage-specific selection. A total of 37 sites showed strong evidence for positive selection (ER ≥ 10), and 419 site–branch combinations had empirical Bayes factors > 100, indicating widespread but localized adaptive evolution in LWS.

When foreground branches were restricted to species with auditory system reductions, *BUSTED* still detected strong evidence of episodic diversifying selection across the gene (p < 0.0001). The unconstrained model fitted to 382 sequences and 369 codons indicated that most sites (77.5%) evolved under strong purifying selection (ω = 0.055), but a small fraction (2.3%) exhibited high non-synonymous substitution rates (ω = 4.35), consistent with episodic adaptation on certain branches. Notably, 14 sites showed evidence ratios ≥10 for positive selection, and 28 branch-site combinations had empirical Bayes factors (EBF) ≥ 100, indicating strong, lineage-specific signals of episodic selection.

FUBAR analyses supported pervasive purifying selection at 332 codon sites (posterior probability ≥ 0.9), alongside evidence for positive/diversifying selection at five codons (sites 179, 183, 235, 105, and 279), all with very high Bayes factors (up to 260,900), reinforcing the presence of adaptive evolution in these positions. Overall, these results suggest that although LWS is mostly conserved, it has experienced episodes of adaptive evolution in specific codons and branches, particularly in species with auditory system reductions.

RELAX analysis detected significant evidence of selection relaxation acting on foreground branches (K = 0.84, p = 0.043, LR = 4.11). Under the general descriptive model,

most codons were evolving under strong purifying selection ($\omega_1 = 0.00$, 91.3% of sites), while a small fraction showed nearly neutral evolution ($\omega_2 = 0.93$, 7.94%) or strong diversifying selection ($\omega_3 = 120.93$, 0.77%). The partitioned descriptive model showed a reduction of ω values in foreground branches, with $\omega_2 = 0.86$ and $\omega_3 = 6.95$, although only a small proportion of sites fell under these categories (5.81% and 2.3%, respectively).

Table 4. Summary of codon-based selection analyses for the LWS opsin gene. Results are shown for RELAX, BUSTED, and FUBAR models applied to a codon alignment of 383 anuran taxa. RELAX models include general and partitioned descriptive fits as well as null and alternative models testing for changes in selection intensity (K). BUSTED results report ω distributions and proportions across rate classes under both unconstrained and constrained models, including synonymous rate estimates. FUBAR identifies individual codon sites under pervasive diversifying selection ($\alpha < \beta$). Values are reported for each positively selected site. Results indicate strong purifying selection across most sites and branches, but with a small number of codons evolving under positive selection, particularly in foreground lineages associated with auditory system reductions.

Analysis	Model	*log* L	#. params	AICc	Branch set	ω1	ω2	ω3
RELAX	General descriptive	-48946.2	1541	101008.4	Shared	0.0(91.30%)	0.93(7.94%)	120.93 (0.77%)
	RELAX alternative	-49521.0	781	100612.7	Reference	N/A	1.0(9.39%)	37.93 (0.38%)
					Test	N/A	1.0(9.39%)	21.34 (0.38%)
	RELAX null	-49523.0	780	100614.8	Reference	N/A	1.0(9.34%)	33.86 (0.40%)
					Test	N/A	1.0(9.34%)	33.86 (0.40%)
	RELAX partitioned	-49511.9	785	100602.6	Reference	N/A	1.0(9.49%)	42.66 (0.34%)
					Test	N/A	0.86(5.81%)	6.95 (2.30%)
BUSTED	**Model**	***log* L**	**#. params**	**AICc**	**Rate distribution**			
	Unconstrained model	−48726.4	790	99041.8	**Tested ω** 0.0340 (20.142%) 0.05461 (77.526%) 4.352 (2.3324%) Mean = 0.1507, CoV = 4.309			
	Unconstrained model				**Background ω** 0.1045 (85.044%) 0.000 (14.568%) 20.06 (0.38773%) Mean = 0.1666, CoV = 7.450			
	Unconstrained model				**Synonymous rates** 0.4577 (32.682%) 0.9843 (54.730%) 2.476 (12.588%) Mean = 1.000, CoV = 0.6088			

					Tested ω			
	Constrained model	−48735.3	789	99057.5	0.01417 (6.3024%) 0.0182 (83.363%) 1.000 (10.335%)			
					Mean = 0.1194, CoV = 2.504			
					Background ω			
	Constrained model				0.1048 (84.569%) 0.00 (15.035%) 19.40 (0.39560%)			
					Mean = 0.1654, CoV = 7.334			
					Synonymous rates			
	Constrained model				0.4555 (32.471%) 0.9821 (54.770%) 2.463 (12.759%)			
					Mean = 1.000, CoV = 0.6078 Bottom of Form			
FUBAR	**Sites under (+) selection**	**Partition**	**α**	**β**	**β-α**	**Prob α>β**	**Prob α<β**	**Bayes Factor α<β**
	179	1	2.813	7.125	4.312	0	1.000	260.900.872
	235	1	1.131	2.815	1.683	0	997	1.642.512
	183	1	2.121	7.093	4.971	0	996	996.265
	105	1	1.225	2.815	1.590	0	973	155.287
	279	1	1.310	2.813	1.503	1	926	53.168

Discussion

To assess whether the reduction of the auditory system in anurans has influenced the molecular evolution of visual opsins, we conducted codon-based selection analyses across four key opsin genes (RH1, SWS1, SWS2, and LWS) using RELAX, BUSTED, and FUBAR. Our results reveal a predominant pattern of strong purifying selection across all genes, consistent with the essential and conserved roles of visual opsins in vertebrate vision. Nevertheless, we also uncovered gene- and site-specific signatures of adaptive evolution associated with auditory system reduction. BUSTED identified significant evidence of episodic diversifying selection in all four opsins, with particularly pronounced signals in SWS2 and LWS, including numerous site–branch combinations with high empirical Bayes factors. FUBAR further detected codons under pervasive diversifying selection in each gene, most notably in RH1 and LWS. RELAX analyses revealed significant relaxation of purifying selection in SWS1 and LWS, but not in RH1 or SWS2, indicating that reductions in auditory capacity may differentially modulate evolutionary pressures across the opsin repertoire. Together, these findings suggest that while purifying

selection remains the dominant force shaping opsin evolution, auditory system loss is associated with localized episodes of positive selection, potentially reflecting compensatory adaptations in the visual system.

These patterns are broadly consistent with previous research on visual opsin evolution in frogs, which has similarly highlighted the prevalence of purifying selection alongside gene- and lineage-specific episodes of adaptive change. For example, Wan et al. (87) focused on diurnality in Neotropical frogs and found codons under positive selection near known spectral tuning sites in diurnal lineages. Schott et al. (85), examining a broader array of ecological and life-history traits, including activity period, reproductive mode, and habitat use, detected relaxed selection in three of the four opsins, as well as clade-specific signals of diversifying selection. Both studies, like ours, also reported the recurrent absence of functional SWS2 in Dendrobatidae, a pattern we likewise observed. While these studies investigated different ecological axes than ours, they similarly demonstrate that visual opsins, despite being under strong purifying selection overall, can exhibit localized adaptive shifts in response to specific ecological pressures. The examples underscore a broader trend in which selection on opsins reflects the sensory demands associated with diverse ecological and behavioral strategies. Our findings extend this framework by highlighting auditory system reduction as an additional axis of sensory evolution driving gene- and site-specific molecular changes in opsin genes. In the following sections, we explore the gene-level patterns in more detail and discuss their potential functional implications.

Despite the dominant signal of strong purifying selection on *RH1*, consistent with its essential role in scotopic vision and previous findings in frogs (85), our analyses revealed clear evidence of episodic positive selection in lineages with auditory system reductions. Codon-based models identified four positively selected sites, three of which (*i.e.* 169, 213, and 333) overlap with those reported in a smaller dataset (85). Although these residues are not currently annotated as functional tuning sites, they lie in close proximity to positions known to influence spectral sensitivity and may also affect rhodopsin kinetics. Temporal resolution in scotopic vision is constrained in part by the speed of rod recovery (113). Therefore, substitutions in *RH1* that accelerate deactivation could enhance temporal resolution. Such changes may be adaptive in species with reduced auditory systems that rely more heavily on visual cues. Many of these frogs are diurnal or crepuscular and inhabit visually complex terrestrial environments, such as dense

leaf litter, where rapid visual processing could be crucial. Similar hypotheses have previously been proposed for scansorial frogs, in which enhanced visual temporal resolution could facilitate navigation and prey detection in structurally intricate arboreal habitats under dim-light conditions (85). Additionally, several species with auditory reductions are known to communicate using brief visual signals, including dynamic limb movements and transient color displays (34,83). Enhanced temporal resolution in rod photoreceptors, possibly mediated by faster *RH1* kinetics, would be advantageous in supporting such behaviors. These findings raise the possibility that *RH1* has undergone localized adaptive changes in response to altered sensory demands, potentially reflecting compensatory shifts following auditory loss. Functional validation will be necessary to determine whether the positively selected RH1 sites contribute to spectral or kinetic tuning. This could be addressed using *in vitro* expression systems combined with spectrophotometric and fluorescence-based assays, which allow direct estimation of λ_{max} and of the deactivation kinetics of the rhodopsin active state, approaches that have proven effective in other opsin systems (114).

Similar to RH1, SWS2 did not exhibit significant evidence of relaxed or intensified selection in the RELAX analysis. However, BUSTED identified episodic diversifying selection affecting specific branches within species with auditory system reductions, while FUBAR detected a small number of codons under pervasive positive selection across the entire phylogeny. Although limited in number, these signals collectively point to localized episodes of adaptive evolution within an otherwise highly conserved gene. Notably, SWS2 encodes the opsin sensitive to blue light and is expressed both in blue-sensitive cones and in the amphibian-specific blue-sensitive rod photoreceptors (86). Expression data confirm that this gene is retained and functional in species with auditory reductions. Interestingly, recent comparative analyses (85) found that SWS2 evolves under relatively weaker purifying selection in direct-developing frogs, a developmental strategy disproportionately represented among lineages lacking an auditory system (*e.g. Osornophryne*, some *Rhinella* species, Brachycephalids, and *Pristimantis*). Furthermore, studies have demonstrated that SWS2 is differentially expressed between larval and adult stages in at least one amphibian species (99) a pattern also observed in some teleost fishes (92). Together, these findings suggest a generally conserved function of SWS2 across anurans, but with potential modulation in developmental timing or tissue-specific expression that could be especially relevant in taxa undergoing sensory reorganization. Comparative expression studies

between froglets and adults in direct-developing lineages could provide critical insight into the ecological and developmental flexibility of SWS2 function in frogs with and without auditory systems.

Among the four visual opsins examined, *SWS1* and *LWS* were the only genes to exhibit significant relaxation of purifying selection in species with auditory system reduction. The case of *SWS1* is particularly intriguing: not only did it show a clear signal of relaxed selection, but also evidence of episodic diversifying selection and one codon under pervasive positive selection. This combination suggests adaptive molecular evolution in *SWS1* specifically associated with auditory system loss. Such a pattern is unexpected, as *SWS1* is typically considered highly conserved in other vertebrates, including reptiles and birds (115). Nonetheless, recent comparative analyses in amphibians have shown that *SWS1*, despite being subject to strong purifying selection overall, exhibits the highest relative degree of selection relaxation among the opsin genes (85). Its evolutionary lability in frogs may point to a previously underappreciated functional role, particularly in lineages undergoing sensory reorganization. Notably, *SWS1* is also the least characterized opsin in anurans. A differential expression study in *Lithobates sphenocephalus* estimated that it has the lowest retinal expression of all visual opsins (99). Furthermore, anatomical studies in *L. catesbeianus* and *Xenopus laevis* found that the photoreceptor class expressing *SWS1* is both small and rare (116,117). Still, the fact that this gene is expressed, and exhibits both relaxed constraint and positive selection signatures, suggests it plays a meaningful role in visual function, potentially gaining greater relevance in species with reduced auditory input. The codon identified under pervasive positive selection (site 115) is especially noteworthy, as it has been previously identified as a spectral tuning site (85), providing a promising candidate for future functional assays. Together, these findings point to *SWS1* as a potentially important, yet overlooked, component of the frog visual repertoire, particularly in species undergoing compensatory sensory evolution.

The *LWS* opsin exhibited the strongest signal of relaxed purifying selection among the four visual opsins analyzed, along with clear evidence of both episodic and pervasive positive selection. As the long-wavelength–sensitive pigment, *LWS* typically absorbs light in the red portion of the spectrum ($\lambda max \approx 550–625$ nm) (85). One plausible explanation for the observed relaxation is that red light sensitivity may be less critical in diurnal frogs, which are

disproportionately represented among species with auditory system reductions (16). Previous studies have shown that diurnal frogs exhibit anatomical and molecular adaptations that enhance sensitivity to shorter wavelengths, particularly blue and UV light, which dominate under full daylight conditions. These include reduced eye size (24,118), ocular media optimized for blue light transmission (54), and amino acid substitutions in *RH1* at known tuning sites which shift spectral sensitivity toward shorter wavelengths (87,114,119). In this context, diminished selection on LWS could reflect a visual ecology in which long-wavelength sensitivity is less essential. However, an alternative, non-exclusive interpretation arises from the strong evidence of episodic and pervasive positive selection. Multiple LWS codons were identified as targets of diversifying selection, suggesting functional optimization rather than simple decay. This may be particularly relevant for crepuscular species, also well represented among auditory-reduced taxa (16), for which ambient light is enriched in longer wavelengths (120). In such environments, enhanced red sensitivity could improve contrast detection or object discrimination under dim, reddish light conditions. Moreover, although the specific positively selected sites identified here have not yet been functionally characterized in frogs, studies in mammals indicate that amino acid changes in LWS can drive spectral tuning differences between long- and middle-wavelength–sensitive pigments (87,121–124). This raises the possibility that similar molecular changes in frogs contribute to adaptive shifts in spectral sensitivity, including in diurnal species with auditory reductions. Thus, selection on LWS may reflect divergent pressures across taxa, with relaxed constraint in diurnal lineages and adaptive enhancement in crepuscular species, both potentially linked to compensatory shifts in visual function following auditory system loss.

Taken together, our results suggest that while purifying selection remains the dominant force shaping the evolution of visual opsins in frogs, lineages with auditory system reductions show gene- and site-specific signatures of adaptive molecular change. Relaxation of selective constraint was detected only in SWS1 and LWS, whereas all four opsins showed evidence of episodic diversifying selection in at least some lineages. These patterns were most pronounced in LWS and RH1, indicating possible shifts in spectral or temporal tuning in response to changes in sensory ecology. Although the precise functional consequences of these signals remain unresolved, our findings highlight the potential for compensatory visual adaptations in frogs that have lost key components of the auditory system. Future studies combining transcriptomics, *in vitro* functional assays, and behavioral analyses will be essential to

clarify the phenotypic consequences of these molecular changes and to test whether they confer measurable advantages in visual performance or ecological fitness.

Conclusion

Taken together, our results provide preliminary evidence that reductions in the auditory system are associated with lineage-specific shifts in the molecular evolution of visual opsins in frogs. While strong purifying selection remains the predominant force across all genes, we detected consistent signals of episodic and site-specific positive selection, as well as significant relaxation of selective constraint in SWS1 and LWS. These patterns suggest that auditory system loss may drive compensatory or co-adaptive modifications in visual sensitivity and function, potentially through altered ecological reliance on visual cues. The recurrence of positive selection at or near candidate tuning sites further supports the hypothesis that such shifts could affect opsin kinetics or spectral sensitivity, though functional validation remains necessary. More broadly, this study highlights how sensory trade-offs can shape the evolutionary dynamics of deeply conserved gene families, revealing previously overlooked axes of sensory adaptation in vertebrates.

Chapter V: General Conclusions

Returning to the overarching question that motivated this research: ***How do frogs lacking auditory and/or vocal structures communicate?*** The definitive answer remains unknown. However, this thesis provides strong evidence that the visual system in anurans experiencing auditory reduction is undergoing evolutionary changes consistent with compensatory adaptation. This study represents the first comprehensive investigation of sensory trade-offs in frogs with auditory system loss, integrating morphological, genomic, and molecular evolutionary approaches to reveal the multifaceted nature of sensory evolution in these species.

Chapter one establishes a morphological framework, demonstrating that frogs with auditory system reduction have smaller eyes overall but exhibit a relatively greater investment in the cornea. This differential allocation likely enhances visual sensitivity without the energetic and biomechanical costs associated with larger eyes and under selective constraint for small body size and small eyes. Notably, these patterns are most pronounced in ground-dwelling species and are influenced by additional ecological factors, including mating habitat, body size, and activity period.

Chapter two contributes a high-quality, contiguous genome assembly of *Pristimantis brevicrus*, a direct-developing anuran with middle ear loss. This genomic resource fills a significant gap in amphibian genomics by providing one of the most complete assemblies available for an underrepresented clade. It sets a solid foundation for future comparative and functional genomic studies aimed at uncovering the genetic bases of sensory system evolution and other phenotypic adaptations in Neotropical frogs.

Chapter three reveals molecular signatures of selection in four key visual opsin genes. While purifying selection remains the dominant force, lineage-specific episodes of positive selection and relaxed constraint associated with auditory loss were detected. These patterns suggest potential adaptive modifications in spectral sensitivity and temporal processing that may compensate for reduced auditory input. The identification of amino acid sites under selection near known spectral tuning regions further supports the hypothesis that changes in opsin function contribute to sensory compensation.

Although these findings represent a major advancement in understanding sensory system interactions in anurans, they mark only the initial steps in a complex research pathway. Functional validation of candidate molecular adaptations through *in vitro* expression and spectral sensitivity assays is essential to confirm their phenotypic effects. Comprehensive studies of gene expression dynamics across developmental stages and tissues in species with and without auditory structures will clarify the ecological and developmental flexibility of these potential adaptations. Additionally, neuroanatomical and physiological investigations of retinal specializations and central visual processing centers such as the optic tectum will be necessary to understand the integrated nature of sensory compensation. Finally, behavioral and ecological research assessing how these morphological and molecular changes influence communication, predator detection, and habitat use will be critical to linking sensory evolution to organismal performance and fitness.

In summary, this thesis constitutes the foundational research exploring sensory trade-offs in frogs with auditory system reductions. It demonstrates that the visual system undergoes targeted, multi-level adaptations that likely compensate for auditory loss. These insights deepen our understanding of sensory evolution in anurans and provide a robust framework for future integrative research bridging morphology, genomics, physiology, and ecology.

References

1. Wells KD. The Ecology and Behavior of Amphibians [Internet]. University of Chicago Press; 2007 [cited 2024 Mar 12]. Available from: http://www.bibliovault.org/BV.landing.epl?ISBN=9780226893341

2. Köhler J, Jansen M, Rodríguez A, Kok PJR, Toledo LF, Emmrich M, et al. The use of bioacoustics in anuran taxonomy: theory, terminology, methods and recommendations for best practice. Zootaxa [Internet]. 2017 Apr 11 [cited 2024 Dec 12];4251(1). Available from: https://www.mapress.com/zt/article/view/zootaxa.4251.1.1

3. Toledo LF, Martins IA, Bruschi DP, Passos MA, Alexandre C, Haddad CFB. The anuran calling repertoire in the light of social context. Acta Ethologica. 2015 Jun;18(2):87–99.

4. Endler JA. Signals, Signal Conditions, and the Direction of Evolution. Am Nat. 1992 Mar;139:S125–53.

5. Gerhardt HC, Huber F, Simmons AM. *Acoustic Communication in Insects and Anurans: Common Problems and Diverse Solutions*. J Acoust Soc Am. 2003 Aug 1;114(2):559–559.

6. Kelley DB. Vocal communication in frogs. Curr Opin Neurobiol. 2004 Dec;14(6):751–7.

7. Wells KD, Schwartz JJ. The Behavioral Ecology of Anuran Communication. In: Narins PM, Feng AS, Fay RR, Popper AN, editors. Hearing and Sound Communication in Amphibians [Internet]. Springer New York; 2006 [cited 2024 Dec 12]. p. 44–86. (Springer Handbook of Auditory Research; vol. 28). Available from: http://link.springer.com/10.1007/978-0-387-47796-1_3

8. Bee MA, Gerhardt HC. Neighbour–stranger discrimination by territorial male bullfrogs (Rana catesbeiana): I. Acoustic basis. Anim Behav. 2001 Dec;62(6):1129–40.

9. Davis MS. Acoustically mediated neighbor recognition in the North American bullfrog, Rana catesbeiana. Behav Ecol Sociobiol. 1987 Sep;21(3):185–90.

10. Ryan M. ANURAN COMMUNICATION. Copeia. 2002 Feb;2001(1):252–4.

11. Simmons AM. Call recognition in the bullfrog, *Rana catesbeiana* : Generalization along the duration continuum. J Acoust Soc Am. 2004 Mar 1;115(3):1345–55.

12. Barry TH. The ontogenesis of the sound-conducting apparatus of Bufo angusticeps Smith. Morphol Jahrb. 1956;97:477–544.

13. Helff OM. Studies on Amphibian Metamorphosis. III. The Influence of the Annular Tympanic Cartilage on the Formation of the Tympanic Membrane. Physiol Zool. 1928 Oct;1(4):463–95.

14. Pereyra MO, Womack MC, Barrionuevo JS, Blotto BL, Baldo D, Targino M, et al. The complex evolutionary history of the tympanic middle ear in frogs and toads (Anura). Sci Rep. 2016 Sep 28;6(1):34130.

15. Sedra SN, Michael MI. The ontogenesis of the sound conducting apparatus of the egyptian toad, bufo regularis reuss, with a review of this apparatus in salientia. J Morphol. 1959 Mar;104(2):359–75.

16. Womack MC, Hoke KL. Convergent anuran middle ear loss lacks a universal, adaptive explanation. Brain Behav Evol [Internet]. 2023 Nov 1 [cited 2023 Nov 16]; Available from: https://karger.com/doi/10.1159/000534936

17. Von May R, Lehr E, Rabosky DL. Evolutionary radiation of earless frogs in the Andes: molecular phylogenetics and habitat shifts in high-elevation terrestrial breeding frogs. PeerJ. 2018 Feb 22;6:e4313.

18. Mason MJ, Narins PM. Vibrometric studies of the middle ear of the bullfrog *Rana catesbeiana* I. The extrastapes. J Exp Biol. 2002 Oct 15;205(20):3153–65.

19. Gutierrez EDA, Schott RK, Preston MW, Loureiro LO, Lim BK, Chang BSW. The role of ecological factors in shaping bat cone opsin evolution. Proc R Soc B Biol Sci. 2018 Apr 11;285(1876):20172835.

20. Emer SA, Grace MS, Mora CV, Harvey MT. Pit organ-based infrared discrimination sensitivity and signal transduction in the Burmese python (Python molurus bivitattus). Behav Brain Res. 2022 Jul;429:113910.

21. Martínez-Martínez CA, Martins HOJ, Kobal ROAC, Cordeiro GD, Hrncir M, Alves-dos-Santos I. Unique morphological and morphometric traits of nocturnal bee antennae. Apidologie. 2024 Dec;55(6):78.

22. Walls GL. The vertebrate eye and its adaptive radiation [by] Gordon Lynn Walls. [Internet]. Bloomfield Hills, Mich.,: Cranbrook Institute of Science,; 1942 [cited 2024 Dec 12]. Available from: http://www.biodiversitylibrary.org/bibliography/7369

23. Mason MJ, Narins PM. Seismic sensitivity in the desert golden mole (Eremitalpa granti): A review. J Comp Psychol. 2002;116(2):158–63.

24. Thomas KN, Gower DJ, Bell RC, Fujita MK, Schott RK, Streicher JW. Eye size and investment in frogs and toads correlate with adult habitat, activity pattern and breeding ecology. Proc R Soc B Biol Sci. 2020 Sep 30;287(1935):20201393.

25. Land MF, Nilsson DE. Animal eyes. 2nd ed. Oxford: Oxford university press; 2012. (Oxford animal biology series).

26. Brooke MDL, Hanley S, Laughlin SB. The scaling of eye size with body mass in birds. Proc R Soc Lond B Biol Sci. 1999 Feb 22;266(1417):405–12.

27. Castiglione GM, Chiu YLI, Gutierrez EDA, Van Nynatten A, Hauser FE, Preston M, et al. Convergent evolution of dim light vision in owls and deep-diving whales. Curr Biol. 2023 Nov;33(21):4733-4740.e4.

28. Hall MI. Comparative analysis of the size and shape of the lizard eye. Zoology. 2008 Jan;111(1):62–75.

29. Kirk E. Effects of activity pattern on eye size and orbital aperture size in primates. J Hum Evol. 2006 Aug;51(2):159–70.

30. Liu Y, Ding L, Lei J, Zhao E, Tang Y. Eye size variation reflects habitat and daily activity patterns in colubrid snakes. J Morphol. 2012 Aug;273(8):883–93.

31. Mitkus M, Potier S, Martin GR, Duriez O, Kelber A. Raptor Vision. In: Oxford Research Encyclopedia of Neuroscience [Internet]. Oxford University Press; 2018 [cited 2024 Dec 12]. Available from: http://oxfordre.com/neuroscience/view/10.1093/acrefore/9780190264086.001.0001/acrefore-9780190264086-e-232

32. Schmitz L, Wainwright PC. Nocturnality constrains morphological and functional diversity in the eyes of reef fishes. BMC Evol Biol. 2011;11(1):338.

33. Werner YL, Seifan T. Eye size in geckos: Asymmetry, allometry, sexual dimorphism, and behavioral correlates. J Morphol. 2006 Dec;267(12):1486–500.

34. Hödl W, Amézquita A. Visual signaling in anuran amphibians. In: Anuran communication. Ryan, M.J. Washington, DC: Smithsonian Inst. Press.; 2001. p. 121–41.

35. Bajger J. Diversity of defensive responses in populations of Fire Toads (Bombina bombina and Bombina variegata). Herpetologica. 1980;36:133–7.

36. Edmunds M. Visual Signaling in Anuran Amphibians. In: Anuran communication. Ryan MJ. Washington, USA: Smithsonian lust. Press; 2001. p. 121–41.

37. Hinsche G. Vergleichende untersuchungen zum sogenannten Unkenreflex. Biol Zentralblatt. 1926;46:296–305.

38. Myers C. The distribution and behavior of a tropical horned frog, Cerathyla panamensis Stejneger. Herpetologica. 1966;22:68–71.

39. Duellman WE, Lehr E. Terrestrial-breeding frogs (Strabomantidae) in Peru. Munster, Germany: Nature und Tier Verlag.; 2009.

40. Portik DM, Streicher JW, Wiens JJ. Frog phylogeny: A time-calibrated, species-level tree based on hundreds of loci and 5,242 species. Mol Phylogenet Evol. 2023 Nov;188:107907.

41. Paradis E, Claude J, Strimmer K. APE: Analyses of Phylogenetics and Evolution in R language. Bioinformatics. 2004 Jan 22;20(2):289–90.

42. Kim J, Sanderson MJ. Penalized Likelihood Phylogenetic Inference: Bridging the Parsimony-Likelihood Gap. Syst Biol. 2008 Oct 1;57(5):665–74.

43. Paradis E. Molecular dating of phylogenies by likelihood methods: A comparison of models and a new information criterion. Mol Phylogenet Evol. 2013 May;67(2):436–44.

44. Sanderson MJ. Estimating Absolute Rates of Molecular Evolution and Divergence Times: A Penalized Likelihood Approach. Mol Biol Evol. 2002 Jan 1;19(1):101–9.

45. Orme D, Freckleton R, Thomas G, Petzoldt T, Fritz S, Isaac N, et al. caper: Comparative Analyses of Phylogenetics and Evolution in R [Internet]. 2011 [cited 2025 Jun 6]. p. 1.0.3. Available from: https://CRAN.R-project.org/package=caper

46. R Core Team. R: a language and environment for statistical computing. Vienna, Austria: R Foundation for Statistical Computing. 2019;

47. Warton DI, Duursma RA, Falster DS, Taskinen S. smatr 3– an R package for estimation and inference about allometric lines. Methods Ecol Evol. 2012 Apr;3(2):257–9.

48. Revell LJ. phytools: an R package for phylogenetic comparative biology (and other things). Methods Ecol Evol. 2012 Apr;3(2):217–23.

49. Mohun SM, Davies WL, Bowmaker JK, Pisani D, Himstedt W, Gower DJ, et al. Identification and characterization of visual pigments in caecilians (Amphibia: Gymnophiona), an order of limbless vertebrates with rudimentary eyes. J Exp Biol. 2010 Oct 15;213(20):3586–92.

50. Mohun SM, Wilkinson M. The eye of the caecilian *Rhinatrema bivittatum* (Amphibia: Gymnophiona: Rhinatrematidae). Acta Zool. 2015 Apr;96(2):147–53.

51. Borghi CE, Giannoni SM, Roig VG. Eye reduction in subterranean mammals and eye protective behavior in Ctenomys. Mastozool Neotrop. 2002;9:123–34.

52. Catania K. Mole senses. Curr Biol. 2009;29(17):R825–8.

53. Eagderi S, Adriaens D. Cephalic morphology of *Pythonichthys macrurus* (Heterenchelyidae: Anguilliformes): specializations for head-first burrowing. J Morphol. 2010 Sep;271(9):1053–65.

54. Yovanovich CAM, Pierotti MER, Rodrigues MT, Grant T. A dune with a view: the eyes of a neotropical fossorial lizard. Front Zool. 2019 Dec;16(1):17.

55. Martín J, Raya García E, Ortega J, López P. How to maintain underground social relationships? Chemosensory sex, partner and self recognition in a fossorial amphisbaenian. Bartos L, editor. PLOS ONE. 2020 Aug 19;15(8):e0237188.

56. Thomas RJ, Székely T, Powell RF, Cuthill IC. Eye size, foraging methods and the timing of foraging in shorebirds. Funct Ecol. 2006 Feb;20(1):157–65.

57. Lisney TJ, Iwaniuk AN, Kolominsky J, Bandet MV, Corfield JR, Wylie DR. Interspecifc variation in eye shape and retinal topography in seven species of galliform bird (Aves: Galliformes: Phasianidae). J Comp Physiol A. 2012 Oct;198(10):717–31.

58. Laughlin SB, De Ruyter Van Steveninck RR, Anderson JC. The metabolic cost of neural information. Nat Neurosci. 1998 May;1(1):36–41.

59. Moran D, Softley R, Warrant EJ. The energetic cost of vision and the evolution of eyeless Mexican cavefish. Sci Adv. 2015 Sep 4;1(8):e1500363.

60. Laughlin SB. Towards the cost of seeing. Nervous Systems and Behaviour. Vis Res. 1995;36:1529–41.

61. Garamszegi LZ, Møller AP, Erritzøe J. Coevolving avian eye size and brain size in relation to prey capture and nocturnality. Proc R Soc Lond B Biol Sci. 2002 May 7;269(1494):961–7.

62. Waldvogel JA. The Bird's Eye View. Am Sci. 1990 Agosto;78(4):342–53.

63. Martin GR. Schematic Eye Models in Vertebrates. In: Ottoson D, Autrum H, Perl ER, Schmidt RF, Shimazu H, Willis WD, editors. Progress in Sensory Physiology [Internet].

Berlin, Heidelberg: Springer Berlin Heidelberg; 1983 [cited 2024 Dec 12]. p. 43–81. (Progress in Sensory Physiology; vol. 4). Available from: http://link.springer.com/10.1007/978-3-642-69163-8_2

64. Kirk EC. Comparative morphology of the eye in primates. Anat Rec A Discov Mol Cell Evol Biol. 2004 Nov;281A(1):1095–103.

65. Bousfield JD, Pessoa VF. Changes in ganglion cell density during post-metamorphic development in a neotropical tree frog Hyla raniceps. Vision Res. 1980 Jan;20(6):501–10.

66. Zhang Y, Straznicky C. The morphology and distribution of photoreceptors in the retina of Bufo marinus. Anat Embryol (Berl) [Internet]. 1991 Jan [cited 2025 Apr 19];183(1). Available from: http://link.springer.com/10.1007/BF00185840

67. Dunlop SA, Beazley LD. Changing retinal ganglion cell distribution in the frog *Heleioporus eyrei*. J Comp Neurol. 1981 Oct 20;202(2):221–36.

68. Nguyen VS, Straznicky C. The development and the topographic organization of the retinal ganglion cell layer in Bufo marinus. Exp Brain Res [Internet]. 1989 Apr [cited 2025 Apr 19];75(2). Available from: http://link.springer.com/10.1007/BF00247940

69. Pushchin II, Zyumchenko NE. Retinal ganglion cell topography and spatial resolving power in the oriental fire-bellied toad *Bombina orientalis*. J Integr Neurosci. 2015 Dec;14(04):521–34.

70. Zhu B, Hiscock J, Straznicky C. The changing distribution of neurons in the inner nuclear layer from metamorphosis to adult: a morphometric analysis of the anuran retina. Anat Embryol (Berl) [Internet]. 1990 Jul [cited 2025 Apr 19];181(6). Available from: http://link.springer.com/10.1007/BF00174630

71. Dong W, Lee RH, Xu H, Yang S, Pratt KG, Cao V, et al. Visual Avoidance in *Xenopus* Tadpoles Is Correlated With the Maturation of Visual Responses in the Optic Tectum. J Neurophysiol. 2009 Feb;101(2):803–15.

72. Yopak KE, Lisney TJ. Allometric Scaling of the Optic Tectum in Cartilaginous Fishes. Brain Behav Evol. 2012;80(2):108–26.

73. Barton RA. Visual specialization and brain evolution in primates. Proc R Soc Lond B Biol Sci. 1998 Oct 22;265(1409):1933–7.

74. AmphibiaWeb. University of California, Berkeley, CA, USA; 2025. Available from: https://amphibiaweb.org

75. Kosch TA, Crawford AJ, Lockridge Mueller R, Wollenberg Valero KC, Power ML, Rodríguez A, et al. Comparative analysis of amphibian genomes: An emerging resource for basic and applied research. Mol Ecol Resour. 2025 Jan;25(1):e14025.

76. Hotaling S, Kelley JL, Frandsen PB. Toward a genome sequence for every animal: Where are we now? Proc Natl Acad Sci. 2021 Dec 28;118(52):e2109019118.

77. Sun YB, Zhang Y, Wang K, Laboratory of Ecology and Evolutionary Biology, Yunnan University, Kunming, Yunnan 650091, China, State Key Laboratory of Genetic Resources and Evolution, Kunming Institute of Zoology, Chinese Academy of Sciences, Kunming, Yunnan 650223, China, Sam Noble Oklahoma Museum of Natural History and Department of Biology, University of Oklahoma, Norman, Oklahoma 73072, USA. Perspectives on studying molecular adaptations of amphibians in the genomic era. Zool Res. 2020;41(4):351–64.

78. Womack MC, Steigerwald E, Blackburn DC, Cannatella DC, Catenazzi A, Che J, et al. State of the Amphibia 2020: A Review of Five Years of Amphibian Research and Existing Resources. Ichthyol Herpetol [Internet]. 2022 Nov 3 [cited 2023 Dec 20];110(4). Available from: https://bioone.org/journals/ichthyology-and-herpetology/volume-110/issue-4/h2022005/State-of-the-Amphibia-2020--A-Review-of-Five/10.1643/h2022005.full

79. Rhie A, McCarthy SA, Fedrigo O, Damas J, Formenti G, Koren S, et al. Towards complete and error-free genome assemblies of all vertebrate species. Nature. 2021 Apr 29;592(7856):737–46.

80. Cheng H, Concepcion GT, Feng X, Zhang H, Li H. Haplotype-resolved de novo assembly using phased assembly graphs with hifiasm. Nat Methods. 2021 Feb;18(2):170–5.

81. Gurevich A, Saveliev V, Vyahhi N, Tesler G. QUAST: quality assessment tool for genome assemblies. Bioinformatics. 2013 Apr 15;29(8):1072–5.

82. Huang N, Li H. compleasm: a faster and more accurate reimplementation of BUSCO. Marschall T, editor. Bioinformatics. 2023 Oct 3;39(10):btad595.

83. Lindquist ED, Hetherington TE. Semaphoring in an earless frog: the origin of a novel visual signal. Anim Cogn. 1998 Oct;1(2):83–7.

84. Bowmaker JK. Evolution of vertebrate visual pigments. Vision Res. 2008 Sep;48(20):2022–41.

85. Schott RK, Fujita MK, Streicher JW, Gower DJ, Thomas KN, Loew ER, et al. Diversity and Evolution of Frog Visual Opsins: Spectral Tuning and Adaptation to Distinct Light Environments. Crandall K, editor. Mol Biol Evol. 2024 Apr 2;41(4):msae049.

86. Davies WIL, Collin SP, Hunt DM. Molecular ecology and adaptation of visual photopigments in craniates. Mol Ecol. 2012 Jul;21(13):3121–58.

87. Wan Y, Navarrete M, O'Connell L, Uricchio L, Roland A, Maan M, et al. Selection on visual opsin genes in diurnal Neotropical frogs and loss of the *SWS2* opsin in poison frogs [Internet]. Evolutionary Biology; 2023 [cited 2023 Nov 16]. Available from: http://biorxiv.org/lookup/doi/10.1101/2022.10.18.510514

88. Hagen JFD, Roberts NS, Johnston RJ. The evolutionary history and spectral tuning of vertebrate visual opsins. Dev Biol. 2023 Jan;493:40–66.

89. Yokoyama S. Evolution of Dim-Light and Color Vision Pigments. Annu Rev Genomics Hum Genet. 2008 Sep 1;9(1):259–82.

90. Corredor VH, Hauzman E, Gonçalves ADS, Ventura DF. Genetic characterization of the visual pigments of the red-eared turtle (Trachemys scripta elegans) and computational predictions of the spectral sensitivity. J Photochem Photobiol. 2022 Dec;12:100141.

91. Carleton KL, Escobar-Camacho D, Stieb SM, Cortesi F, Marshall NJ. Seeing the rainbow: mechanisms underlying spectral sensitivity in teleost fishes. J Exp Biol. 2020 Apr 15;223(8):jeb193334.

92. Carleton KL, Parry JWL, Bowmaker JK, Hunt DM, Seehausen O. Colour vision and speciation in Lake Victoria cichlids of the genus *Pundamilia*. Mol Ecol. 2005 Dec;14(14):4341–53.

93. Hofmann CM, O'Quin KE, Marshall NJ, Cronin TW, Seehausen O, Carleton KL. The Eyes Have It: Regulatory and Structural Changes Both Underlie Cichlid Visual Pigment Diversity. Noor MAF, editor. PLoS Biol. 2009 Dec 22;7(12):e1000266.

94. Musilova Z, Cortesi F, Matschiner M, Davies WIL, Patel JS, Stieb SM, et al. Vision using multiple distinct rod opsins in deep-sea fishes. Science. 2019 May 10;364(6440):588–92.

95. Hunt DM, Dulai KS, Cowing JA, Julliot C, Mollon JD, Bowmaker JK, et al. Molecular evolution of trichromacy in primates. Vision Res. 1998 Nov;38(21):3299–306.

96. Yokoyama S, Zhang H, Radlwimmer FB, Blow NS. Adaptive evolution of color vision of the Comoran coelacanth (*Latimeria chalumnae*). Proc Natl Acad Sci. 1999 May 25;96(11):6279–84.

97. Schott RK, Perez L, Kwiatkowski MA, Imhoff V, Gumm JM. Evolutionary analyses of visual opsin genes in frogs and toads: Diversity, duplication, and positive selection. Ecol Evol. 2022 Feb;12(2):e8595.

98. Siddiqi A, Cronin TW, Loew ER, Vorobyev M, Summers K. Interspecific and intraspecific views of color signals in the strawberry poison frog *Dendrobates pumilio*. J Exp Biol. 2004 Jun 15;207(14):2471–85.

99. Schott RK, Bell RC, Loew ER, Thomas KN, Gower DJ, Streicher JW, et al. Transcriptomic evidence for visual adaptation during the aquatic to terrestrial metamorphosis in leopard frogs. BMC Biol. 2022 Dec;20(1):138.

100. Camacho C. Building a BLAST database with your (local) sequences [Internet]. Bethesda (MD): National Center for Biotechnology Information (US); 2008. Available from: https://www.ncbi.nlm.nih.gov/books/NBK569841/

101. Schott RK, Panesar B, Card DC, Preston M, Castoe TA, Chang BS. Targeted capture of complete coding regions across divergent species. Genome Biol Evol. 2017 Jan 30;evx005.

102. Langmead B, Salzberg SL. Fast gapped-read alignment with Bowtie 2. Nat Methods. 2012 Apr;9(4):357–9.

103. Danecek P, Bonfield JK, Liddle J, Marshall J, Ohan V, Pollard MO, et al. Twelve years of SAMtools and BCFtools. GigaScience. 2021 Jan 29;10(2):giab008.

104. Pedersen BS, Quinlan AR. Mosdepth: quick coverage calculation for genomes and exomes. Hancock J, editor. Bioinformatics. 2018 Mar 1;34(5):867–8.

105. Maddison W, Maddison D. Mesquite: a modular system for evolutionary analysis. [Internet]. 2025. Available from: http://www.mesquiteproject.org

106. Edgar RC. High-accuracy alignment ensembles enable unbiased assessments of sequence homology and phylogeny [Internet]. 2021 [cited 2025 Jun 26]. Available from: http://biorxiv.org/lookup/doi/10.1101/2021.06.20.449169

107. Ranwez V, Harispe S, Delsuc F, Douzery EJP. MACSE: Multiple Alignment of Coding SEquences Accounting for Frameshifts and Stop Codons. Murphy WJ, editor. PLoS ONE. 2011 Sep 16;6(9):e22594.

108. Larsson A. AliView: a fast and lightweight alignment viewer and editor for large datasets. Bioinformatics. 2014 Nov 15;30(22):3276–8.

109. Weaver S, Shank SD, Spielman SJ, Li M, Muse SV, Kosakovsky Pond SL. Datamonkey 2.0: A Modern Web Application for Characterizing Selective and Other Evolutionary Processes. Mol Biol Evol. 2018 Mar 1;35(3):773–7.

110. Murrell B, Moola S, Mabona A, Weighill T, Sheward D, Kosakovsky Pond SL, et al. FUBAR: A Fast, Unconstrained Bayesian AppRoximation for Inferring Selection. Mol Biol Evol. 2013 May 1;30(5):1196–205.

111. Wertheim JO, Murrell B, Smith MD, Kosakovsky Pond SL, Scheffler K. RELAX: Detecting Relaxed Selection in a Phylogenetic Framework. Mol Biol Evol. 2015 Mar;32(3):820–32.

112. Murrell B, Weaver S, Smith MD, Wertheim JO, Murrell S, Aylward A, et al. Gene-Wide Identification of Episodic Selection. Mol Biol Evol. 2015 May;32(5):1365–71.

113. Fortenbach CR, Kessler C, Peinado Allina G, Burns ME. Speeding rod recovery improves temporal resolution in the retina. Vision Res. 2015 May;110:57–67.

114. Castiglione GM, Chang BS. Functional trade-offs and environmental variation shaped ancient trajectories in the evolution of dim-light vision. eLife. 2018 Oct 26;7:e35957.

115. Gemmell NJ, Rutherford K, Prost S, Tollis M, Winter D, Macey JR, et al. The tuatara genome reveals ancient features of amniote evolution. Nature. 2020 Aug 20;584(7821):403–9.

116. Hisatomi O, Kayada S, Taniguchi Y, Kobayashi Y, Satoh T, Tokunaga F. Primary structure and characterization of a bullfrog visual pigment contained in small single cones. Comp Biochem Physiol B Biochem Mol Biol. 1998 Mar;119(3):585–91.

117. Starace DM, Knox BE. Cloning and expression of aXenopusShort Wavelength Cone Pigment. Exp Eye Res. 1998 Aug;67(2):209–20.

118. Ortega JA, Thomas KN, Ron SR, Bell RC, Fujita MK, Gower DJ, et al. Eyes wide open: Frogs with reduction of auditory communication ability show lower eye, but higher corneal, investment. In prep;

119. Lin SW, Kochendoerfer GG, Carroll KS, Wang D, Mathies RA, Sakmar TP. Mechanisms of Spectral Tuning in Blue Cone Visual Pigments. J Biol Chem. 1998 Sep;273(38):24583–91.

120. Whitcher C, Ron SR, Ayala-Varela F, Crawford A, Herrera-Alva V, Castillo-Urbina E, et al. Evidence for ecological tuning of novel anuran biofluorescent signals [Internet]. Evolutionary Biology; 2023 Jul [cited 2023 Dec 20]. Available from: http://biorxiv.org/lookup/doi/10.1101/2023.07.25.550432

121. Asenjo AB, Rim J, Oprian DD. Molecular determinants of human red/green color discrimination. Neuron. 1994 May;12(5):1131–8.

122. Hiramatsu C, Radlwimmer FB, Yokoyama S, Kawamura S. Mutagenesis and reconstitution of middle-to-long-wave-sensitive visual pigments of New World monkeys for testing the tuning effect of residues at sites 229 and 233. Vision Res. 2004 Sep;44(19):2225–31.

123. Yokoyama R, Yokoyama S. Convergent evolution of the red- and green-like visual pigment genes in fish, Astyanax fasciatus, and human. Proc Natl Acad Sci. 1990 Dec;87(23):9315–8.

124. Yokoyama S, Radlwimmer FB. The Molecular Genetics and Evolution of Red and Green Color Vision in Vertebrates. Genetics. 2001 Aug 1;158(4):1697–710.

Supplementary Information

Supplementary Information Chapter I: Eyes wide open: Frogs with loss of auditory communication ability show evidence of increased investment in vision

Jhael A. Ortega[1,2], Kate N. Thomas[3,4], Santiago R. Ron[2], Rayna C Bell[5,6], Matthew K Fujita[3], David J Gower[4], Jeffery W Streicher[4], Ryan K. Schott*[1]

[1]Department of Biology and Centre for Vision Research, York University, Toronto, Ontario, Canada
[2]Museo de Zoología, Escuela de Biología, Pontificia Universidad Católica del Ecuador, Quito, Pichincha, Ecuador
[3]Department of Biology, Amphibian and Reptile Diversity Research Center, University of Texas at Arlington, Arlington, USA
[4]Department of Life Sciences, Natural History Museum, London, UK
[5]Department of Herpetology, California Academy of Sciences, San Francisco, USA
[6]Department of Vertebrate Zoology, National Museum of Natural History, Smithsonian Institution, Washington DC USA
*Corresponding author email: schott@yorku.ca

Supplemental Results

Scaling relationships: Anuran corneas scale hypoallometrically with eye and body size

For the analysis between anuran ED *vs.* RM, PGLS revealed a strong positive correlation, with a slope of 0.8532 ($p < 2.2e\text{-}16$, ±0.02735 SE) and a phylogenetic λ of 0.958 (95% CI: 0.92–0.98), indicating significant phylogenetic signal. The model explained 79.05% of the variance

($R^2 = 0.7905$, $p < 2.2e-16$). Similarly, OLS regression showed a slope of 0.8789 ($p < 2e-16$, (±0.0323 SE) and $R^2 = 0.741$ ($p < 2.2e-16$), further confirming the positive relationship between the traits. SMA analysis resulted in a slope of 1.0087 (95% CI: 0.9583–1.0619) and $R^2 = 0.741$ ($p < 2.22e-16$), indicating a near-isometric relationship between root mass and eye size, **with no significant deviation from isometry** ($p = 0.7379$).

Similarly, for the analysis between anuran ED *vs.* SVL, PGLS analysis revealed a significant positive correlation ($R^2 = 0.8204$, $p < 2.2e-16$), with a slope of 0.8554 (±0.0247 SE) and a strong phylogenetic signal ($\lambda = 0.953$; 95% CI: 0.913–0.976). OLS regression yielded a similar result, estimating a slope of 0.898 ($p < 2e-16$, ±0.0289 SE) with $R^2 = 0.7857$ ($p < 2.2e-16$). SMA analysis produced a slope of 0.9865 (95% CI: 0.941–1.0341) and $R^2 = 0.7857$ ($p < 2.22e-16$). A test of whether the SMA slope deviates from 1 yielded a p-value of 0.5719, indicating **no significant deviation from isometry**.

For the relationship between CD *vs.* ED, PGLS analysis revealed a significant positive correlation ($R^2 = 0.9491$, $p < 2.2e-16$), with a slope of 0.8859 ($p < 2.2e-16$, ± 0.0127 SE). The phylogenetic signal was moderate, with a λ value of 0.674 (95% CI: 0.452–0.815, $p < 2.2e-16$). OLS regression produced a similar slope of 0.8871 ($p < 2.2e-16$, ± 0.0118 SE), with $R^2 = 0.9556$ ($p < 2.2e-16$), further supporting the observed correlation. SMA analysis estimated a slope of 0.9074 (95% CI: 0.8844–0.9311) and $R^2 = 0.9556$, ($p < 2.2e-16$) significantly lower than 1 ($p < 2.22e-16$) **indicating negative allometry in corneal investment relative to eye size**.

For the relationship between CD *vs*. RM, PGLS analysis revealed a significant positive correlation between cornea size and root mass ($R^2 = 0.7661$, $p < 2.2e-16$), with a slope of 0.7788 ($p < 2.2e-16$, ± 0.0269 SE). The phylogenetic signal was also strong with a λ of 0.949 (95% CI: 0.903–0.974, $p < 2.2e-16$). OLS analysis produced similar results, with a slope of 0.7637 ($p < 2.2e-16$, ± 0.0326 SE), $R^2 = 0.6812$ ($p < 2.2e-16$), supporting the negative allometric relationship. SMA analysis estimated a slope of 0.8893 (95% CI: 0.8388–0.9428), with an R^2 of 0.6812 and significatively lower than 1 (p-value < 2.22e-16), further confirming the **negative allometric scaling between cornea size and root mass.**

Regarding the relationship between CD *vs.* SVL, the PGLS analysis revealed a significant positive correlation ($R^2 = 0.8204$, $p < 2.2e-16$), with a slope of 0.7894 ($p < 2.2e-16$, ± 0.0229 SE), indicating a negative allometric relationship between these variables. The λ value was 0.958 (95% CI: 0.92–0.98, $p < 2.2e-16$), indicating a strong phylogenetic signal. The OLS analysis also

showed a negative allometric relationship, with a slope of 0.7935 ($p < 2.2e-16$, ± 0.0285 SE), $R^2 = 0.7481$, and $p < 2.2e-16$. Similarly, the SMA analysis estimated a slope of 0.8671 (95% CI: 0.8260–0.9102), with an R^2 of 0.7481 and a p-value < 2.22e-16, confirming the **negative allometric relationship between cornea size and SVL.**

Finally, in the relationship between SVL *vs.* RM, the PGLS analysis revealed a significant positive correlation ($R^2 = 0.935$, $p < 2.2e-16$), with a slope of 0.9894 ($p < 2.2e-16$, ± 0.0136 SE), consistent with an isometric scaling pattern. The λ value was 0.879 (95% CI: 0.743–0.945, $p < 2.2e-16$), indicating a strong phylogenetic signal. OLS results showed a slope of 0.9845 ($p < 2.2e-16$, ± 0.0128 SE) and $R^2 = 0.9577$ ($p < 2.2e-16$). SMA analysis estimated a slope of 1.006 (95% CI: 0.9809–1.0317), $R^2 = 0.9577$, and not significantly different from 1 ($p = 0.6388$), indicating **no significant deviation from isometry.**

Species with auditory reductions exhibit reduced absolute and relative eye size

Analysis restricted to fossorial species

Given the strong influence of habitat, and the fact that several species with auditory loss are also fossorial, we repeated the analyses excluding fossorial species to determine whether the effect persisted independently of ecological specialization. After removing fossorial taxa, the pattern remained consistent: species with auditory loss still had significantly smaller eyes (Fig. S3), with mean absolute eye diameter of 3.84 mm compared to 5.99 mm (Wilcoxon test: $W = 2423$, $p < 0.001$), and lower relative eye size (0.92× vs. 1.03×; Wilcoxon test: $W = 2916$, $p < 0.001$). Phylogenetic ANCOVA further supported significant effects of both body mass ($F_{1,247} = 1319.110$, $p < 0.001$) and auditory loss ($F_{1,257} = 8.664$, $p = 0.004$).

Analysis analyzing the effect of sensory reductions and life history strategy

When considering life-history strategy, a two-way phylogenetic ANCOVA revealed that only auditory system reduction had a significant effect on absolute eye size ($F_{1,235} = 25.118$, $p < 0.001$), while neither life-history strategy ($F_{1,235} = 3.190$, $p = 0.075$) nor its interaction with auditory loss ($F_{1,235} = 0.706$, $p = 0.401$) were significant. For relative eye size, significant main effects were found for auditory system reduction ($F_{1,231} = 117.813$, $p < 0.001$), life-history strategy ($F_{1,231} = 8.788$, $p = 0.003$), and body mass ($F_{1,231} = 950.204$, $p < 0.001$). Additionally,

significant two-way interactions were detected between auditory loss and life-history strategy ($F_{1,231} = 9.275$, $p = 0.003$), auditory loss and body mass ($F_{1,231} = 4.258$, $p = 0.040$), and life-history strategy and body mass ($F_{1,231} = 4.000$, $p = 0.047$), whereas the three-way interaction was not significant ($F_{1,231} = 0.002$, $p = 0.967$). When examining absolute cornea size, auditory system reduction had a significant main effect ($F_{1,235} = 27.159$, $p < 0.001$), while life-history strategy ($F_{1,235} = 2.014$, $p = 0.157$) and its interaction with auditory loss ($F_{1,235} = 0.481$, $p = 0.489$) were not significant. Regarding relative cornea investment, strong main effects were observed for life-history strategy ($F_{1,231} = 82.253$, $p < 0.001$), auditory system reduction ($F_{1,231} = 537.440$, $p < 0.001$), and eye size ($F_{1,231} = 3778.520$, $p < 0.001$). However, none of the interaction terms reached statistical significance, including those between auditory reduction and life-history strategy ($F_{1,231} = 0.006$, $p = 0.938$), life-history strategy and eye size ($F_{1,231} = 0.010$, $p = 0.922$), auditory reduction and eye size ($F_{1,231} = 1.545$, $p = 0.215$), or the three-way interaction ($F_{1,231} = 0.139$, $p = 0.709$).

Given the apparent overrepresentation of direct developers among species with sensory system reductions, we next assessed whether this life history strategy could help explain the observed variation. To do so, we restricted our analyses to species without a free-living larval stage and examined differences in eye and corneal morphology within this subset.

When restricting the analysis to species without a free-living larval stage, we found that those with auditory reductions exhibited significantly smaller eyes in absolute size (Wilcoxon test: $W = 82$, $p = 0.0001$; mean = 2.79 mm vs. 4.77 mm), but not in relative size (Wilcoxon test: $W = 158$, $p = 0.05$; 0.95× vs. 1.05×). Phylogenetic ANCOVA showed that both auditory system reduction ($F_{1,45} = 10.128$, $p = 0.003$) and body mass ($F_{1,45} = 189.947$, $p < 0.001$) had significant effects on eye size, while their interaction was not significant ($F_{1,45} = 0.153$, $p = 0.697$). When examining the cornea, species without a free-living larva and with auditory reductions exhibited significantly smaller absolute cornea sizes (Wilcoxon test: $W = 95$, $p = 0.0006$; mean = 2.55 mm vs. 3.95 mm). However, differences in relative cornea size (1.1× in species with sensory loss vs. 1.08× in those without) were not statistically significant (Wilcoxon test: $W = 313$, $p = 0.14$). Phylogenetic ANCOVA confirmed significant effects of both auditory system reduction ($F_{1,46} = 88.595$, $p < 0.001$) and body mass ($F_{1,46} = 1078.942$, $p < 0.001$) on cornea size.

Other ecological factors influence anuran eye and cornea size and investments independently of auditory reductions

Adult Habitat influences Eye and Corneal Investment

Eye absolute size (Kruskal–Wallis $\chi^2 = 34.626$, df = 5, $p < 0.0001$) and eye investment (Kruskal–Wallis $\chi^2 = 61.743$, df = 5, $p < 0.0001$) showed significant differences across habitat categories. Consistent with the findings of Thomas et al., semi-aquatic species exhibited the largest absolute eye size (mean = 8.14 mm), followed by ground-dwelling (5.6 mm), scansorial (5.18 mm), fossorial (5.1 mm), aquatic (4.9 mm), and subfossorial species, which had the smallest eyes (mean = 4.2 mm). Regarding eye investment, scansorial (1.16×) and semi-aquatic species (1.17×) exhibited the highest levels of eye investment, followed by ground-dwelling species (1.07×). The lowest values were observed in subfossorial (0.89×), aquatic (0.71×), and fossorial species (0.64×). The phylogenetic ANCOVA found that both body mass ($F_{1,248} = 1188.555$, $p < 0.0001$) and adult habitat ($F_{5,248} = 10.812$, $p < 0.0001$) had significant positive effects on eye size. Additionally, the interaction between mass and adult habitat ($F_{5,248} = 2.775$, $p = 0.019$) also significantly influenced eye size.

Adult habitat significantly influenced both absolute and relative cornea size (Kruskal–Wallis $\chi^2 = 37.78$, df = 5, $p < 0.0001$; $\chi^2 = 26.06$, df = 5, $p < 0.0001$). Semi-aquatic species had the largest corneas (mean = 6.13 mm), followed by ground-dwelling (4.50 mm), scansorial (4.22 mm), fossorial (3.88 mm), aquatic (3.58 mm), and subfossorial species (3.30 mm). For relative cornea investment, ground-dwelling species showed the highest values (1.07×), followed by scansorial (1.06×), semi-aquatic (1.03×), subfossorial (1.00×), aquatic (0.94×), and fossorial species (0.92×). Phylogenetic ANCOVA confirmed significant effects of eye size ($F_{1,250} = 5743.22$, $p < 0.0001$), adult habitat ($F_{5,250} = 4.68$, $p = 0.001$), and their interaction ($F_{5,250} = 2.68$, $p = 0.022$) on absolute cornea size.

Mating habitats affect Eye and Corneal Investment

Eye absolute size (Kruskal–Wallis $\chi^2 = 60.755$, df = 3, p = < 0.0001) and eye investment (Kruskal–Wallis $\chi^2 = 35.983$, df = 3, p = < 0.0001) also showed significant differences across mating habitats categories. Species that mate on the ground have the smallest eyes (mean = 3.69 mm), followed by species that mate on plants (5.26 mm), lentic water species (6.31 mm), and

those that mate in lotic water have the largest eyes (7.71 mm). A similar pattern is observed for eye investment, where species that mate on the ground show the lowest investment (0.96x), followed by those that mate in lentic water (0.98x), on plants (1.16x), and the highest investment is found in species that mate in lotic water (1.19x). In the phylogenetic ANCOVA, both root mass ($F_{1,210} = 847.820$, $p < 0.0001$) and mating habitat ($F_{3,210} = 5.841$, $p = 0.001$) had significant positive effects on eye size. However, the interaction between eye size and mating habitat was not significant ($F_{3,210} = 1.356$, $p = 0.26$).

Mating habitat also significantly affected corneal traits (absolute: $\chi^2 = 47.22$, df = 3, $p < 0.0001$; relative: $\chi^2 = 29.49$, df = 3, $p < 0.0001$). Species mating on the ground had the smallest corneas (mean = 3.19 mm), followed by those mating on plants (4.25 mm), in lentic water (4.77 mm), and in lotic water (5.95 mm). In contrast, ground-mating species exhibited the highest cornea investment (1.09×), followed by lotic (1.05×), plant (1.04×), and lentic (1.00×) species. Phylogenetic ANCOVA showed that both eye size ($F_{1,213} = 3870.02$, $p < 0.0001$) and mating habitat ($F_{3,213} = 3.89$, $p = 0.01$) significantly influenced cornea size.

Activity Period influences Eye and Cornea Investment

Absolute eye size differed slightly but significantly among activity period categories (Kruskal–Wallis $\chi^2 = 6.234$, df = 2, $p = 0.04$), with exclusively diurnal species having the smallest eyes (mean = 4.49 mm), followed by exclusively nocturnal species (mean = 5.46 mm), and species with mixed activity patterns (both diurnal and nocturnal) showing the largest eyes (mean = 6.04 mm). In contrast, relative eye investment did not differ significantly among activity categories (Kruskal–Wallis $\chi^2 = 5.800$, df = 2, $p = 0.055$). However, in both studies, the phylogenetic ANCOVA detected significant effects of body size ($F_{1,218} = 725.837$, $p < 0.0001$) and activity period ($F_{2,218} = 14.22$, $p < 0.0001$) on eye size.

Activity period did not significantly affect corneal traits (Kruskal–Wallis: absolute: $\chi^2 = 5.57$, df = 2, $p = 0.062$; relative: $\chi^2 = 1.13$, df = 2, $p = 0.57$). However, phylogenetic ANCOVA revealed significant effects of activity period ($F_{2,218} = 83.67$, $p < 0.0001$) and eye size ($F_{2,218} = 3635.08$, $p < 0.0001$) on absolute cornea size.

Life History strategies affect Corneal Investment but not Eye Investment

We found significant differences in absolute eye size (Wilcoxon test: W = 6839.5, p < 0.0001), but not in eye investment (Wilcoxon test: W = 5118, p = 0.2838), across life history strategies. Species with free-living larvae had larger absolute eye sizes (mean = 6.06 mm) than those without (mean = 4.21 mm). Although no differences were found in relative investment, the phylogenetic ANCOVA revealed a significant main effect only of body size ($F_{1,235}$ = 930.451, p < 0.0001).

Life history strategy significantly influenced corneal dimensions. Species with free-living larvae had larger absolute corneas (mean = 4.73 mm) than those without (3.55 mm) (Wilcoxon test: W = 6521.5, $p < 0.0001$). However, cornea investment was higher in species without free-living larvae (1.10× vs. 1.03×) (Wilcoxon test: W = 2834, $p < 0.0001$). These patterns were supported by phylogenetic ANCOVA (eye size: $F_{1,236}$ = 5002.12, $p < 0.0001$; life history: $F_{1,236}$ = 14.14, $p < 0.0001$).

Sexual Dichromatism does not influence Eye or Corneal Investment

We found no significant differences in either absolute eye size (Wilcoxon test: W = 3616.5, p = 0.12) or relative eye size (Wilcoxon test: W = 4061, p = 0.7) between species with and without sexual dichromatism. Sexual dichromatism had no significant effect on either absolute (Wilcoxon test: W = 3691, $p = 0.2$) or relative cornea size (Wilcoxon test: W = 4531, $p = 0.4$). Phylogenetic ANCOVA results were consistent, with no detectable effect of dichromatism on cornea size ($F_{1,217}$ = 0.75, $p = 0.39$).

Supplemental References

AmphibiaWeb.org

Andersson, Lars Gabriel (1903) (https://www.biodiversitylibrary.org/part/28991)

Biju, S. D., S. Garg, K. V. Gururaja, Y. S. Shouche, and S. A. Walujkar. 2014. DNA barcoding reveals unprecedented diversity in Dancing Frogs of India (Micrixalidae, Micrixalus): a

taxonomic revision with description of 14 new species. Ceylon Journal of Science. Biological Sciences 43: 1－87.

Bioweb.bio

Boulenger, G. A. 1882. Catalogue of the Batrachia Salientia s. Ecaudata in the Collection of the British Museum. Second Edition. London: Taylor and Francis.

Boulenger, G. A. 1897. Descriptions of new lizards and frogs from Mount Victoria, Owen Stanley Range, New Guinea, collected by Mr. A. S. Anthony. Annals and Magazine of Natural History, Series 6, 19: 6–13.

Boulenger, G. A. 1903. Descriptions of three new batrachians from Tonkin. Annals and Magazine of Natural History, Series 7, 12: 186–188.

Boulenger, G. A. 1905. Descriptions of new West-African frogs of the genera Petropedetes and Bulua. Annals and Magazine of Natural History, Series 7, 15: 281–283.

Boulenger, G. A. 1909. Descriptions of three new frogs discovered by Dr. P. Krefft in Usambara, German East Africa. Annals and Magazine of Natural History, Series 8, 4: 496–497.

Chan, K. O., M. A. Muin, M. S. S. Anuar, J. Andam, N. Razak, and M. A. Aziz. 2019. First checklist on the amphibians and reptiles of Mount Korbu, the second highest peak in Peninsular Malaysia. Check List. The Journal of Biodiversity Data 15: 1055–1069 (https://doi.org/10.15560/15.6.1055).

Chuaynkern, Y., et al. 2010. A revision of species in the subgenus Nidirana Dubois, 1992, with special attention to the identity of specimens allocated to Rana adenopleura Boulenger, 1909, and Rana chapaensis (Bourret, 1937) (Amphibia: Anura: Ranidae) from Thailand and Laos. Raffles Bulletin of Zoology 58: 291–310.

Coloma, L. A., and W. E. Duellman. 2025. Amphibians of Ecuador. Volume 2. Pipidae, Telmatobidae, Microhylidae, Dendrobatidae, Ranidae, Bufonidae, and Hylidae. Boca Raton, FL: CRC Press.

de Sá, R. O., T. Grant, A. Camargo, W. R. Heyer, M. L. Ponssa, and E. L. Stanley. 2014. Systematics of the Neotropical genus Leptodactylus Fitzinger, 1826 (Anura: Leptodactylidae): Phylogeny, the relevance of non-molecular evidence, and species accounts. South American Journal of Herpetology 9(Spec. Issue 1): 1–128.

Du Preez, L. H., and V. C. Carruthers. 2017. Frogs of Southern Africa: A Complete Guide. Cape Town, South Africa: Struik Nature.

Dubois, A. 1980. Notes sur la systematique et la repartition des amphibiens anoures de Chine et des regions avoisinantes IV. Classification generique et subgenerique des Pelobatidae Megophryinae. Bulletin Mensuel de la Société Linnéenne de Lyon 49: 469–482.

Duellman, W. E., & Lynch, J. D. (1969). Descriptions of Atelopus Tadpoles and Their Relevance to Atelopodid Classification. Herpetologica, 25(4), 231–240. http://www.jstor.org/stable/3891213

Duellman, W. E., and E. Lehr. (2009). Terrestrial-breeding frogs (Strabomantidae) in Peru. Münster, Germany: Nature und Tier Verlag.

Dunn, E. R. 1948. American frogs of the family Pipidae. American Museum Novitates 1384: 1–13 (http://digitallibrary.amnh.org/handle/2246/4379).

Elliot, L., H. C. Gerhardt, and C. Davidson. 2009. The Frogs and Toads of North America. A Comprehensive Guide to Their Identification, Behavior, and Calls. Boston and New York: Houghton Mifflin Harcourt.

Fouquet, A., K. Leblanc, A.-C. Fabre, M. T. Rodrigues, M. Menin, E. A. Courtois, M. Dewynter, M. Hölting, R. Ernst, P. L. V. Peloso, and P. J. R. Kok. 2021. Comparative osteology of the fossorial frogs of the genus Synapturanus (Anura, Microhylidae) with the description of three new species from the Eastern Guiana Shield. Zoologischer Anzeiger 293: 46–73 (https://doi.org/10.1016/j.jcz.2021.05.003).

Gillespie, G., E. Ahmad, and A. Shia. 2021. Field Guide to the Frogs of the Lower Kinabatangan Region, Sabah. Sabah, Malaysia: Hutan.

Günther, A. C. L. G. 1873. Description of two new species of frogs from Australia. Annals and Magazine of Natural History, Series 4, 11: 349–350.

Heyer, W. R. 1971. Mating calls of some frogs from Thailand. Fieldiana. Zoology 58: 61–82., Dubois, A., A. Ohler, and R. A. Pyron. 2021. New concepts and methods for phylogenetic taxonomy and nomenclature in zoology, exemplified by a new ranked cladonomy of recent amphibians (Lissamphibia). Megataxa 5: 1–738 (https://doi.org/10.11646/megataxa.5.1.1).

Heyer, W. R. 1971. Mating calls of some frogs from Thailand. Fieldiana. Zoology 58: 61–82.

Inger, R. F. 1966. The systematics and zoogeography of the Amphibia of Borneo. Fieldiana. Zoology 52: 1–402.

Inger, R. F. 1970. A new species of frog of the genus Rana from Thailand. Fieldiana. Zoology 51: 169–174.

Inger, R. F., and J. D. Romer. 1961. A new pelobatid frog of the genus Megophrys from Hong Kong. Fieldiana. Zoology 39: 533–538.

Kok, P. J. R., and M. Kalamandeen. 2008. Introduction to the Taxonomy of the Amphibians of Kaieteur National Park, Guyana. Abc Taxa: A Series of Manuals Dedicated to Capacity Building in Taxonomy and Collection Management, volume 5. Brussels, Belgium: Belgian Development Corporation.

Matsui, M. 1997. Call characteristics of Malaysian Leptolalax with a description of two new species (Anura: Pelobatidae). Copeia 1997: 158–165.

Meneses, C. G., C. D. Siler, P. A. Alviola, J. B. Balatibat, J. C. T. Gonzalez, C. A. Natividad, and R. M. Brown. 2022. Amphibian and reptile diversity along a ridge-to-reef elevational gradient on a small isolated oceanic island of the central Philippines. Check List. The Journal of Biodiversity Data 18: 941–984 (https://doi.org/10.15560/18.5.941).

Mkonyi (2020) (https://doi.org/10.1080/00222933.2020.1728410)

Mueses-Cisneros et al. (2012) (10.11646/zootaxa.3447.1.2)

Nunes-de-Almeida, C. H. L., C. L. de Assis, R. N. Feio, and L. F. Toledo. 2016. Redescription of the advertisement call of five species of Thoropa (Anura, Cycloramphidae), including recordings of rare and endangered species. PLoS (Public Library of Science) One 11(9: e0162617): 1–12 (doi:10.1371/journal.pone.0162617).

Ohler, A. 2003. Revision of the genus Ophryophryne Boulenger, 1903 (Megophryidae) with description of two new species. Alytes. Paris 21: 23–42.

Ortega-Andrade, H. M., Rojas-Soto, O. R., Espinosa de los Monteros, A., Valencia, J. H., Read, M., & Ron, S. R. (2017). Revalidation of Pristimantis brevicrus (Anura, Craugastoridae) with taxonomic comments on a widespread Amazonian direct-developing frog. Herpetological Journal, 31(2), 81–97.

Parker, H. W. 1934. A Monograph of the Frogs of the Family Microhylidae. London: Trustees of the British Museum.

Peters, J. A. (1973). The frog genus Atelopus in Ecuador (Anura: Bufonidae). Smithsonian Contributions to Zoology 145:1-49.

Poyarkov, N. A., Jr., T. V. Duong, N. L. Orlov, S. I. Gogoleva, A. B. Vassilieva, L. T. Nguyen, V. D. H. Nguyen, S. N. Nguyen, J. Che, and S. Mahony. 2017. Molecular, morphological and acoustic assessment of the genus Ophryophryne (Anura, Megophryidae) from Langbian Plateau, southern Vietnam, with description of a new species. ZooKeys 672: 49–120.,

Smith, M. A. 1921. New or little-known reptiles and batrachians from southern Annam (Indo-China). Proceedings of the Zoological Society of London 1921: 423–440.

Springer, L. E., and C. M. Schalk. 2016. Lepidobatrachus laevis. Catalogue of American Amphibians and Reptiles 904: 1–16.

Stuart, S. N., Hoffmann, M., Chanson, J., Cox, N., Berridge, R., Ramani, P., Young, B. E. (2008). Threatened Amphibians of the World. Lynx Edicions. España 160.

Stuart, S. N., M. Hoffmann, J. Chanson, N. Cox, R. Berridge, P. Ramani, and B. Young eds., . 2008. Threatened Amphibians of the World. Barcelona, Spain; International Union for the

Conservation of Nature, Gland. Switzerland; Conservation International, Arlington, Virginia, U.S.A.: Lynx Editions.

Stuart, S. N., M. Hoffmann, J. Chanson, N. Cox, R. Berridge, P. Ramani, and B. Young eds., . 2008. Threatened Amphibians of the World. Barcelona, Spain; International Union for the Conservation of Nature, Gland. Switzerland; Conservation International, Arlington, Virginia, U.S.A.: Lynx Editions.

Sumarli, A. X. Y., L. L. Grismer, M. S. S. Anuar, M. A. Muin, and E. S. H. Quah. 2015. First report on the amphibians and reptiles of a remote mountain, Gunung Tebu in northeastern Peninsular Malaysia. Check List. The Journal of Biodiversity Data 11(4, Art. 1679): 1–16.

Thomas, K. N., Gower, D. J., Bell, R. C., Fujita, M. K., Schott, R. K., & Streicher, J. W. (2020). Eye size and investment in frogs and toads correlate with adult habitat, activity pattern and breeding ecology. Proceedings of the Royal Society B: Biological Sciences, 287(1935), 20201393. https://doi.org/10.1098/rspb.2020.1393

Tyler, M. J., M. M. Davies, and A. A. Martin. 1981. Australian frogs of the leptodactylid genus Uperoleia Gray. Australian Journal of Zoology, Supplemental Series 29 (79): 1–64.

Weygoldt, P. 1976. Beobachtungen zur Biologie und Ethologie von Pipa (Hemipipa) carvalhoi Mir. Rib. 1937. (Anura, Pipidae). Zeitschrift für Tierpsychologie 40: 80–99.

Wogan, G. O. U., K. S. Lwin, H. Win, and T. Thin. 2004. The advertisement call of Brachytarsophrys feae (Boulenger 1887) (Anura: Megophryidae). Proceedings of the California Academy of Sciences 55: 251–254.

Womack, M. C., & Hoke, K. L. (2023). Convergent anuran middle ear loss lacks a universal, adaptive explanation. Brain, Behavior and Evolution. https://doi.org/10.1159/000534936

Supplemental Tables

Table S1. Specimens measured in this study and in Thomas et al. (2020). (INDEPENDET FILE)

Table S2. Species included in this study, including those from Thomas et al. (2020). The table presents the ecological traits analyzed and the character states for each species. **(INDEPENDET FILE)**

Table S3. Overview of sampling effort. The table includes all extant anuran families sampled in this study. **(INDEPENDET FILE)**

Supplemental Figures

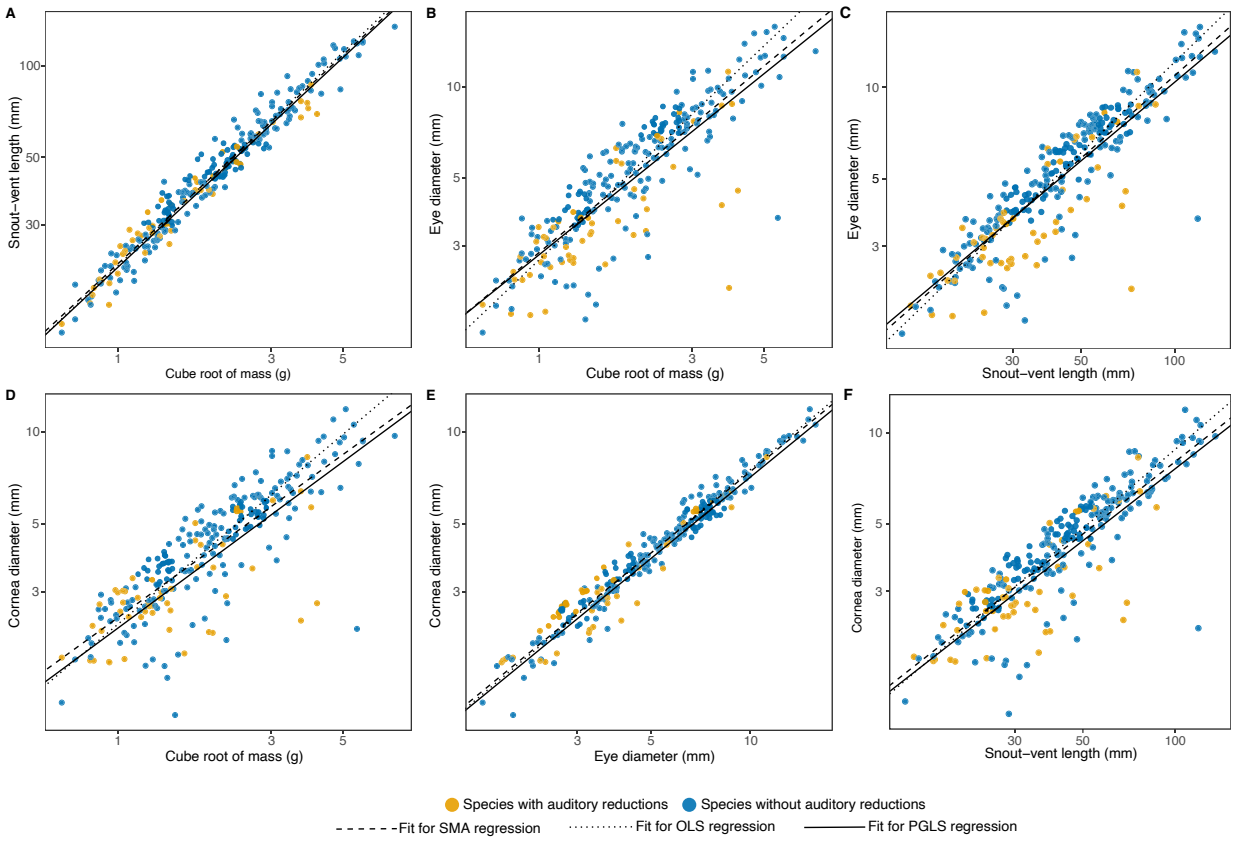

Figure S 1. Scaling of eyes and corneas of different frog species. (*A*) Snout–vent length (SVL) scales isometrically with the cube root of body mass (RM), reflecting the high correlation between these two-size metrics. **(*B*)** Eye diameter (ED) scales isometrically with RM and **(*C*)** SVL. **(*D*)** Corneal diameter (CD) shows negative allometry with RM, **(*E*)** ED, **(*F*)** and SVL. Fitted lines for each analysis are shown. Species are color-coded based on the condition of their sensory systems.

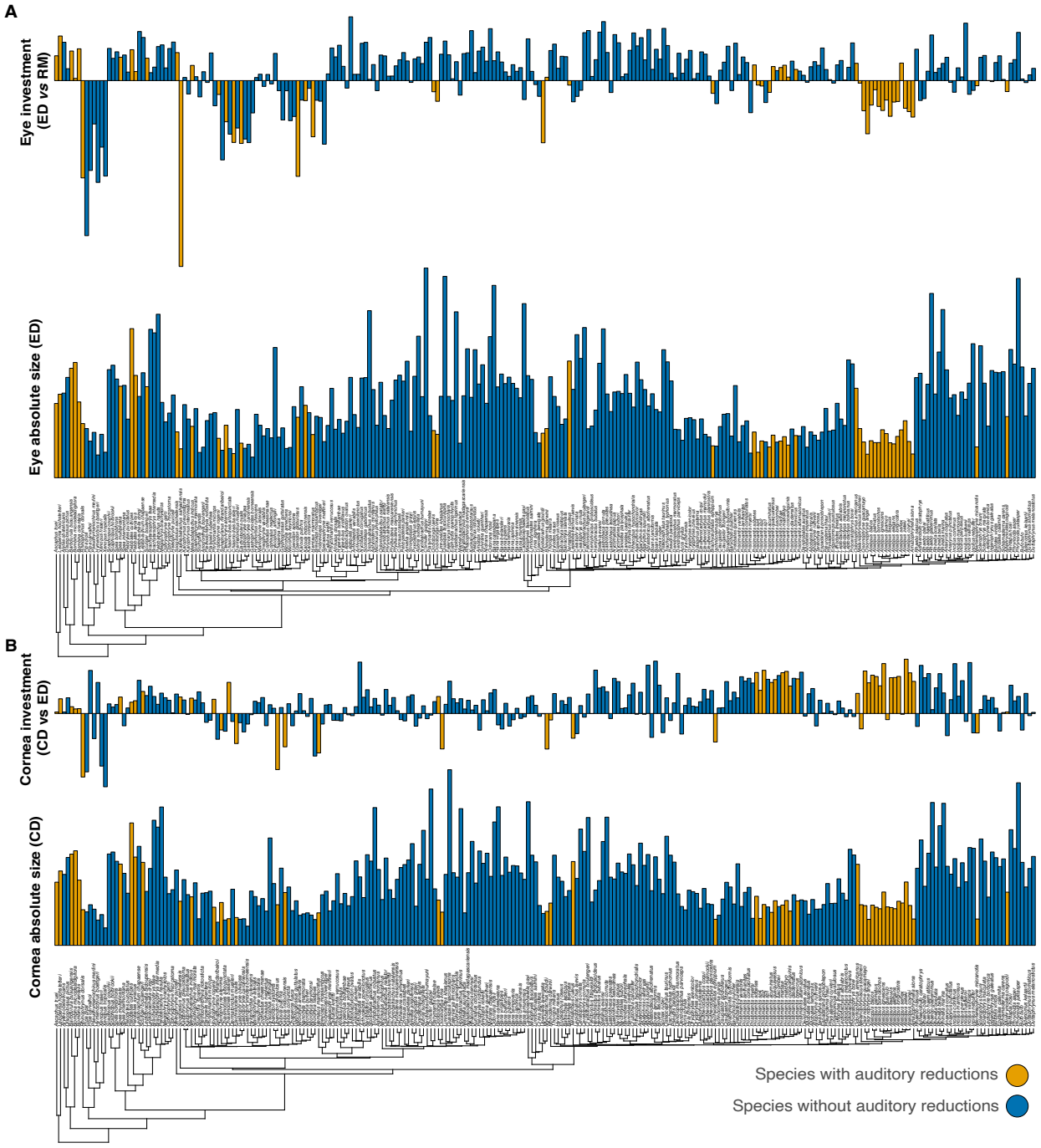

Figure S 2. Species with auditory loss exhibit reduced visual investment, having significantly smaller absolute and relative eye sizes than species without loss. (*A*) Phylogeny, adapted from Portik et al. (2023), shows species means for absolute eye diameter (ED) and relative eye investment (ED *vs* RM) and **(*B*)** species mean values for absolute cornea diameter (CD) and relative corneal investment (CD vs ED). Analyses were performed using the full dataset, including all species regardless of habitat.

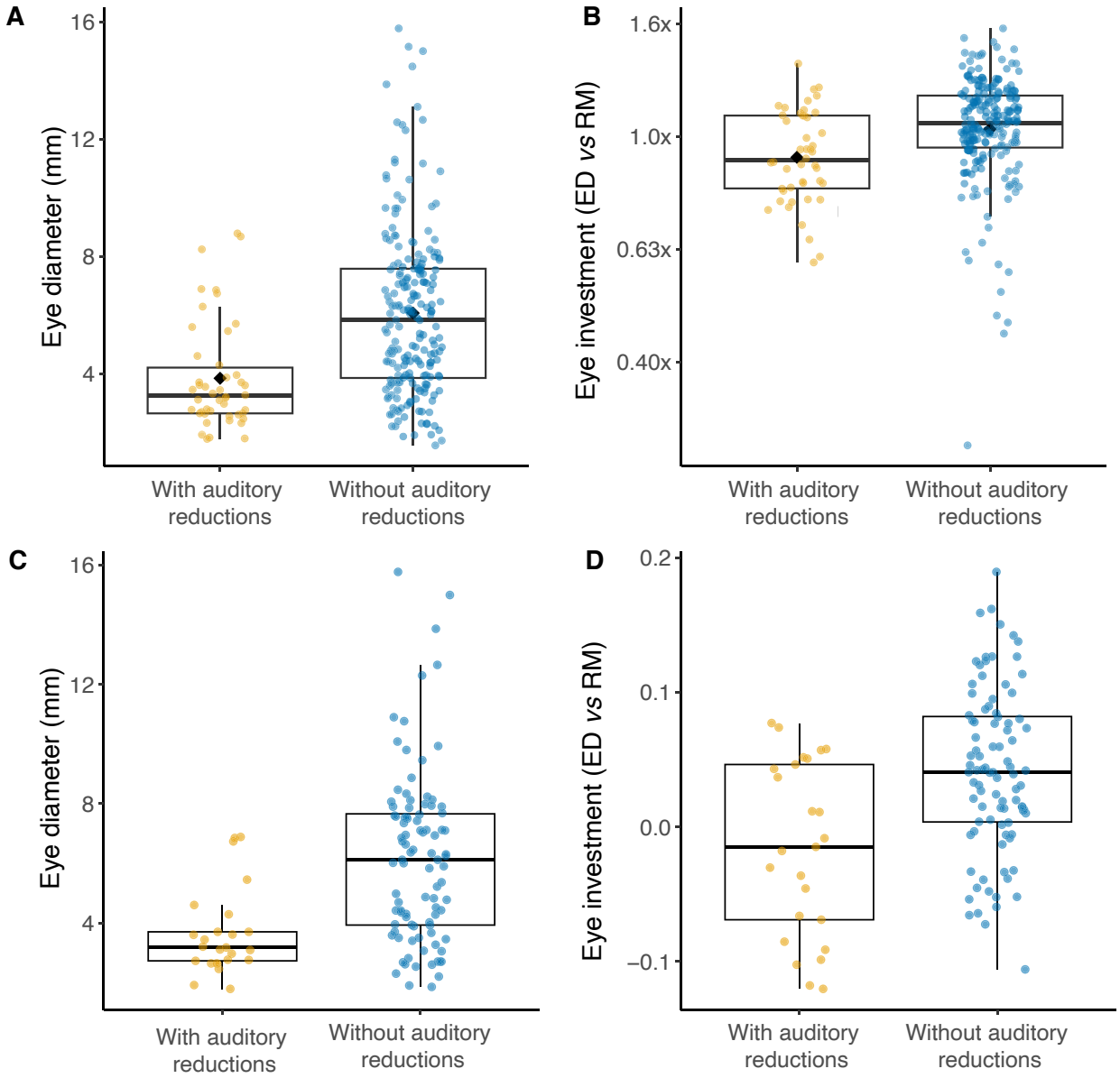

Figure S 3. Eye size differences between species with and without auditory reduction. (*A*) Absolute eye diameter and **(*B*)** relative eye size (scaled by body mass) for species excluding fossorial taxa. **(*C*)** Absolute eye diameter and **(*D*)** relative eye size for ground-dwelling species only. Boxplots compare species with auditory reduction to those without. Across analyses, species with auditory loss exhibit significantly smaller eyes and reduced relative eye investment.

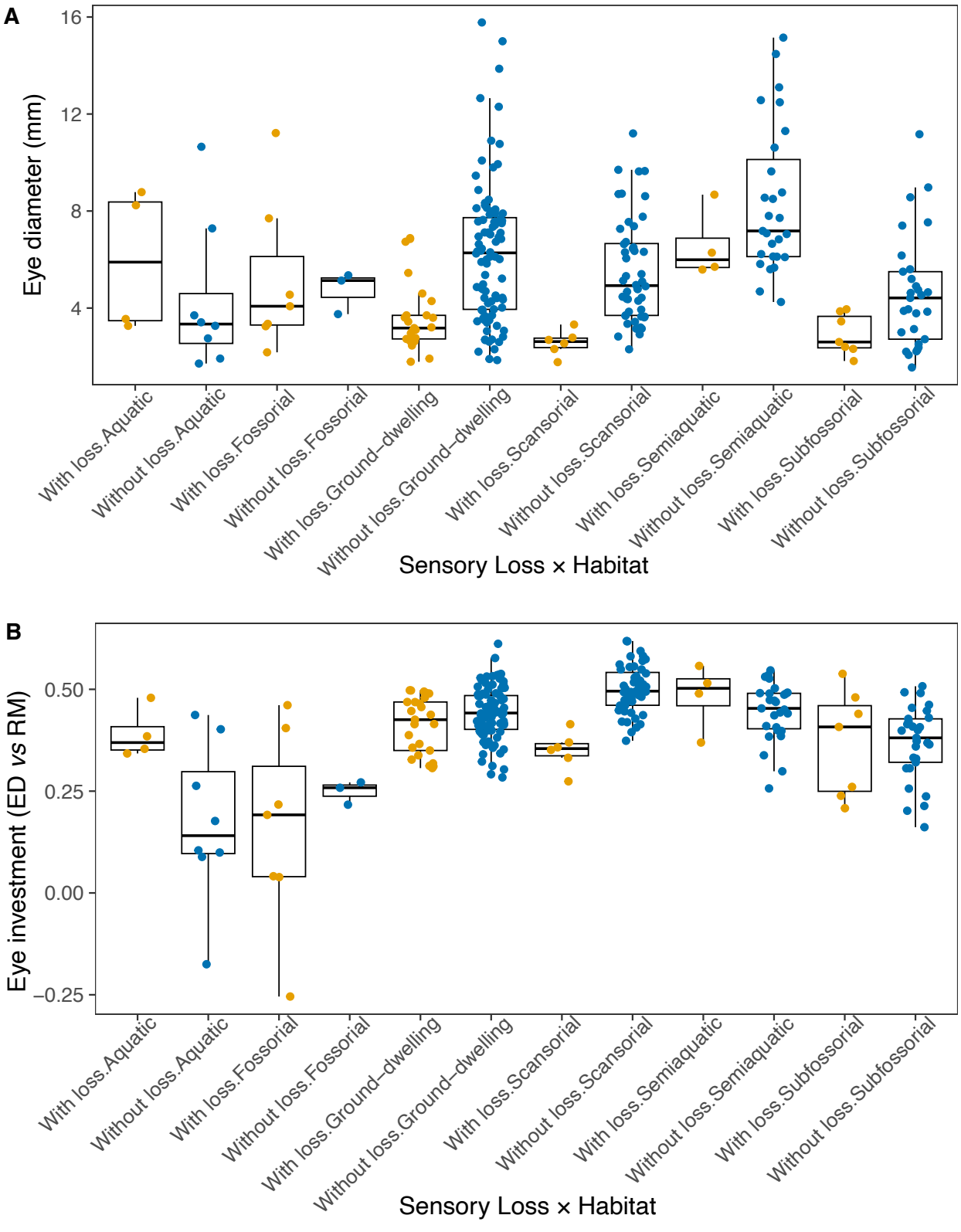

Figure S 4. Effects of auditory system loss and adult habitat on eye morphology. (*A*) Absolute eye diameter and **(*B*)** relative eye size (scaled by body mass), derived from two-way

phylogenetic ANCOVA analyses. Each boxplot displays the distribution of species values within each habitat category, separated by auditory system status. Auditory loss is associated with reduced eye size and investment across most habitats. All analyses include all species in the dataset.

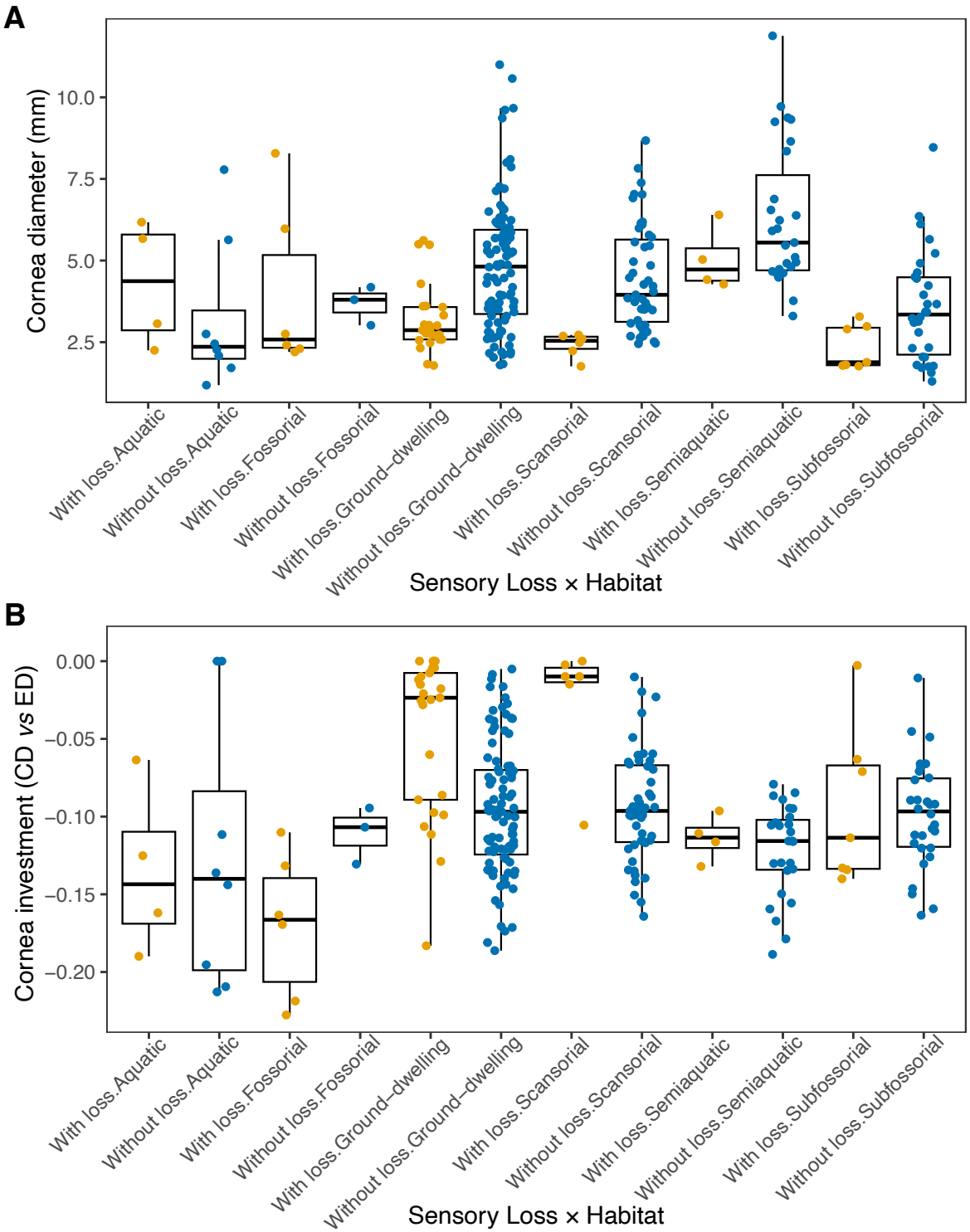

Figure S 5. Absolute and relative cornea size across habitats and auditory system conditions. (*A*) Absolute cornea diameter and **(*B*)** relative corneal investment (CD *vs* ED), derived from two-way phylogenetic ANCOVA analyses. Each boxplot shows the distribution of species values within each habitat category, separated by auditory system status. Auditory loss is

associated with reduced cornea size and slightly increased corneal investment across most habitats. All analyses include all species in the dataset.

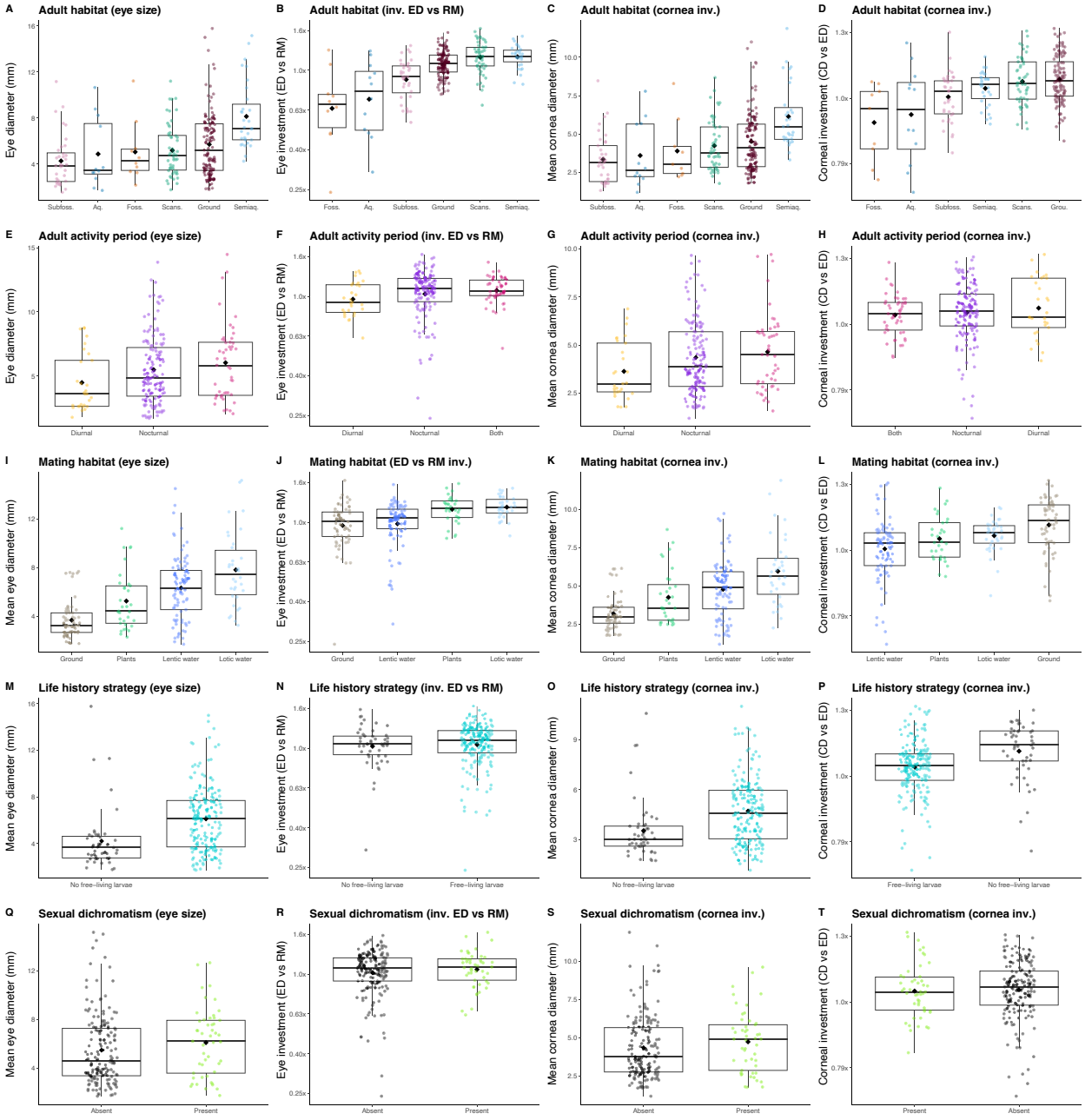

Figure S 6. Cornea and eye absolute size and investment differ significantly across ecological variables. Utilizing different (A–D) adult habitats, (E–H) activity period, (I—L), mating habitat, (M–P) life history strategy, and (Q–T) presence of absence of sexual dichromatism. All analyses include all species in the dataset.

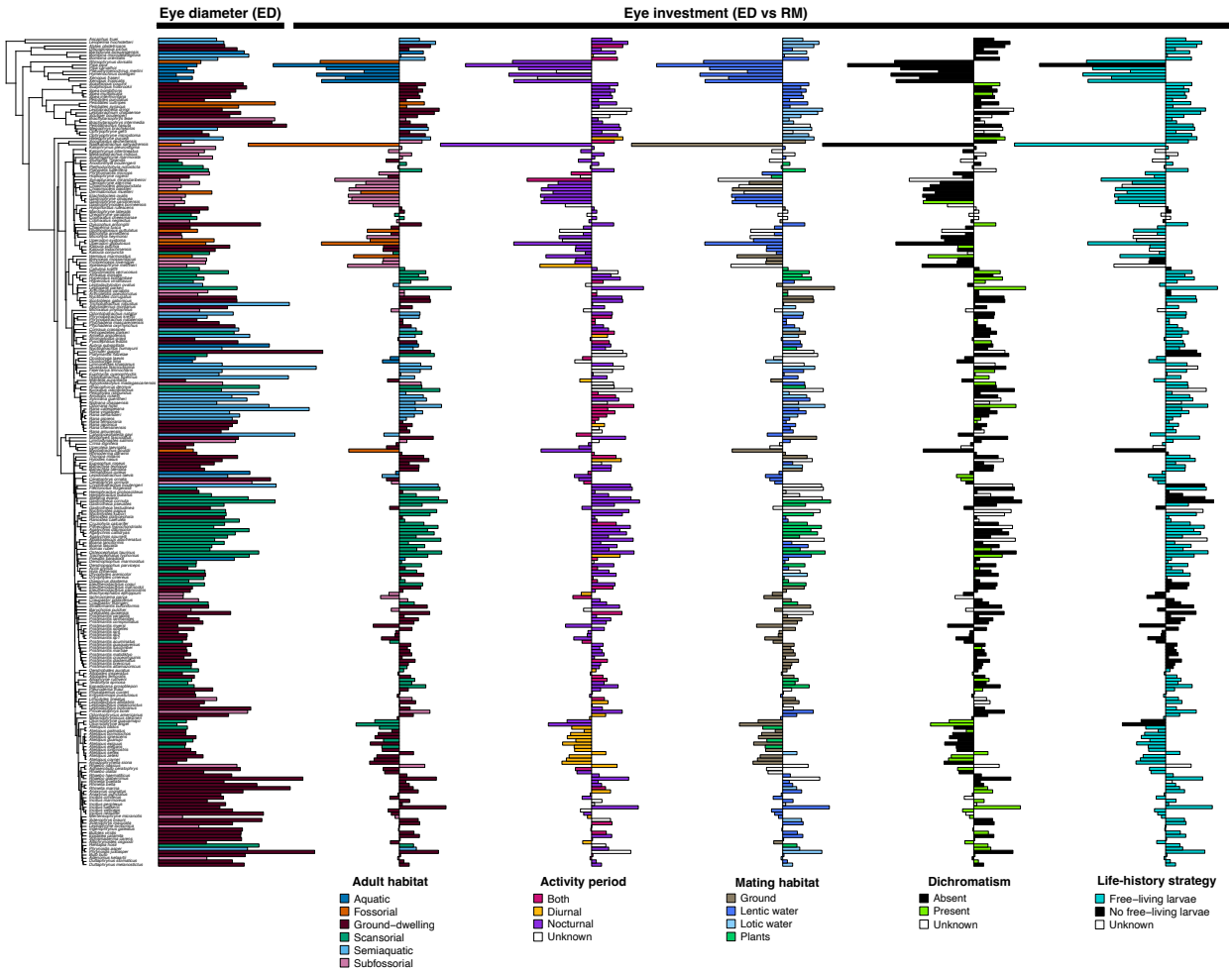

Figure S 7. Eye size and investment vary significantly across anurans with auditory and vocal reductions. Phylogeny adapted from Portik et al. 2023 shows species means for absolute eye diameter (ED) and relative eye investment (ED x RM). All analyses include all species in the dataset.

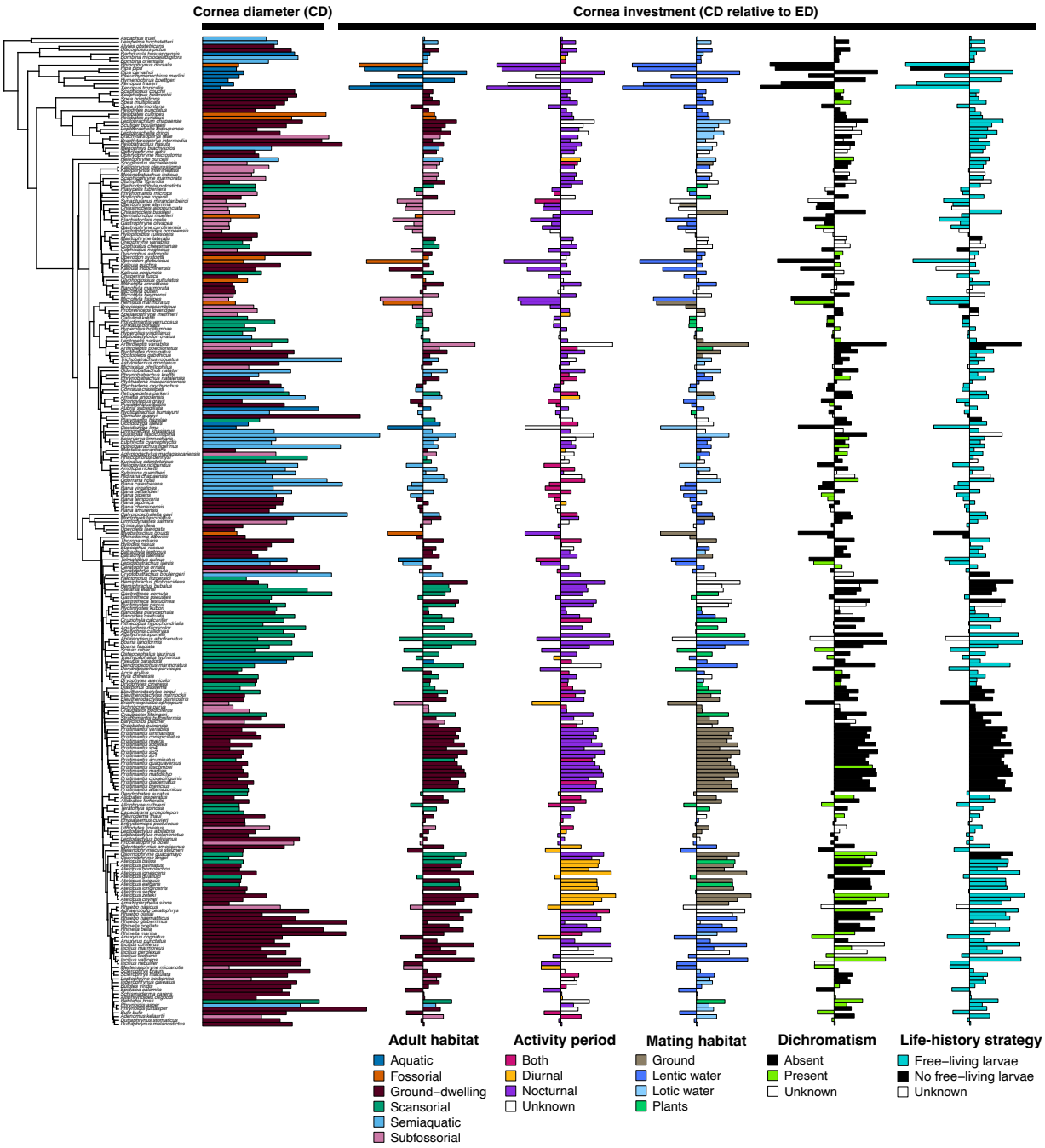

Figure S 8. Cornea size and investment vary significantly across anurans with auditory and vocal reductions. Phylogeny adapted from Portik et al. 2023 shows species means for absolute cornea diameter (CD) and relative cornea investment (CD x ED). All analyses include all species in the dataset.

Supplementary Information Chapter III: Seeing Differently: Selection on Opsin Genes in Frogs with Reduced Auditory Systems

Jhael A. Ortega[1,2], Ryan K. Schott*[1]

[1]Department of Biology and Centre for Vision Research, York University, Toronto, Ontario, Canada

[2]Museo de Zoología, Escuela de Biología, Pontificia Universidad Católica del Ecuador, Quito, Pichincha, Ecuador

Supplemental Results

All four visual opsin genes (RH1, SWS1, SWS2, and LWS) were fully recovered from the *Pristimantis brevicrus* genome assembly. Each gene was retrieved as a complete coding sequence with high-confidence matches to Terrarana reference sequences. In contrast, recovery from the in silico target capture approach varied across taxa and genes.

Opsin gene recovery within the Afrotrachia clade showed variable success across both genes and species. Coverage values, expressed as the percentage of the coding region retrieved, averaged 79.9% across all species and genes. Among the four opsins, **SWS2** exhibited the highest average coverage (82.6%), with many species recovering near-complete sequences (>90%), while **RH1** and **SWS1** showed intermediate coverage averages of 81.5% and 75.0%, respectively. The **LWS** gene had the lowest average coverage (~64.2%), with several species exhibiting partial or fragmented sequences. Notably, some species, such as *Afrixalus dorsimaculatus* and *Afrixalus fulvovittatus*, consistently yielded nearly complete sequences (>98%) across most opsins, indicating efficient capture and assembly in these taxa. In contrast, other species, including *Breviceps fichus* and *Callulina kisiwamsiyu*, had more limited recovery, particularly for SWS1 and LWS. These patterns reflect heterogeneity in sequence recovery across the Afrotrachia clade, likely influenced by factors such as sequence divergence from reference sets, genomic complexity, and data quality. Overall, the substantial number of

sequences covering at least 50% of each gene's coding region enabled robust comparative analyses of opsin evolution within this group.

Opsin gene recovery within the Archeobatrachia clade was generally high, with an average coverage of 83.8% across all genes and species. The rhodopsin gene (**RH1**) showed the most consistent and complete recovery, with an average coverage exceeding 92%, and several species (e.g., *Alytes muletensis*, *Xenopus pygmaeus*) displaying nearly complete sequences. The short-wavelength sensitive genes (**SWS1** and **SWS2**) also exhibited strong recovery, averaging 74.6% and 84.0%, respectively, though some species had partial or fragmented sequences, such as *Insuetophrynus acarpicus* and *Ascaphus truei*. The long-wavelength sensitive gene (**LWS**) showed slightly lower average coverage (~84.2%) with some variation among species. Species such as *Bombina orientalis* and *Pelobates fuscus* demonstrated particularly robust opsin sequence recovery across all genes. Overall, these results indicate a high success rate of opsin gene retrieval in Archeobatrachia, suitable for downstream comparative and evolutionary analyses.

Opsin gene recovery within the Hyloidea clade was generally strong, with an overall average coverage of approximately 86.0% across all genes and species. The long-wavelength sensitive gene (LWS) exhibited an average recovery of 84.2%, with most species showing high coverage near or above 80%, although some species such as *Hylodes phyllodes* showed lower recovery (~27.3%). The rhodopsin gene (RH1) demonstrated the highest consistency, with an average coverage of 90.4%, and many species achieving near-complete sequence recovery (close to 100%), including *Anaxyrus terrestris* and *Pristimantis zeuctotylus*. The short-wavelength sensitive genes showed variable recovery; SWS1 averaged 82.1%, with some species like *Cycloramphus boracei* and *Hemifractus scutatus* showing lower coverage (~21.9% and ~55.8%, respectively). SWS2 exhibited the highest average coverage among the short-wavelength genes at 87.2%, with broad recovery across species but some instances of lower coverage, such as in *Rulyrana flavopunctata* (~36.4%). Despite this variation, most species yielded substantial portions of opsin gene sequences, supporting their utility for comparative evolutionary analyses within Hyloidea. Overall, the results indicate a successful and robust recovery of opsin genes across multiple Hyloidea taxa, with RH1 and SWS2 showing particularly high recovery consistency.

Opsin gene recovery within the Microhylidae clade was generally high, with an average coverage of approximately 87.3% across all genes and species analyzed. The long-wavelength sensitive gene (LWS) showed robust recovery, averaging 83.6%, with most species presenting coverage above 80%. However, some species such as *Scaphiophryne marmorata* and *Oreophryne penelopeia* exhibited somewhat lower recovery values (23.2% and 24.6%, respectively). The rhodopsin gene (RH1) exhibited the most consistent and complete recovery across the clade, with an average coverage close to 94.6%, and many species, including *Austrochaperina robusta* and *Callulops doriae*, showing near-complete sequences (above 99%). The short-wavelength sensitive genes showed slightly more variability: SWS1 had an average coverage of 82.2%, with some species such as *Scaphiophryne marmorata* and *Oreophryne lemur* showing lower recovery (40.8% and 47.4%, respectively), while other taxa displayed near-complete sequences (close to 100%). SWS2 had the highest average coverage among the short-wavelength opsins at 88.7%, with broad recovery across most species, though a few taxa showed moderate to low coverage (e.g., *Oreophryne inornata* at 24.1%). Overall, these results indicate a successful recovery of opsin genes across diverse Microhylidae species, with RH1 and SWS2 demonstrating particularly high coverage and consistency.

Opsin gene recovery within the Natatanura clade was generally high, with an average coverage of approximately 85.1% across all genes and species. The rhodopsin gene (RH1) exhibited the most consistent and complete recovery, with an average coverage of 90.6%. Many species, including *Amieita angolensis*, *Conraua crassipes*, and *Odorrana* spp., showed near-complete RH1 sequences, while a few taxa such as *Hylarana albolabris* displayed lower coverage or fragmented sequences. The short-wavelength sensitive genes SWS1 and SWS2 demonstrated variable recovery. SWS2 had a high average coverage of 84.6%, with strong recovery across most species, including *Mantella betsileo* and *Theloderma* spp. However, some species, such as *Chiromantis rufescens* and *Philautus parvulus*, showed lower coverage. SWS1 recovery was more heterogeneous, averaging 79.8%, with several species like *Amieita angolensis* and *Hylorina sylvatica* showing nearly complete sequences, but other taxa exhibiting partial or missing data. The long-wavelength sensitive gene (LWS) presented an average recovery of 85.3%, with most species showing robust coverage. Nonetheless, some species had incomplete sequences or gaps, such as *Meristogenys orphnocnemis* and *Platymantis pelewensis*.

The recovery of opsin genes within the Ranoidea clade showed generally high but variable completeness across species. Rhodopsin (RH1) sequences were recovered at an average completeness of approximately 86.5%, with many taxa exhibiting nearly complete sequences (e.g., *Afrixalus dorsimaculatus*, *Amolops cremnobatus*, *Callulina* spp.). However, some specimens presented lower coverage or partial absences. Short-wavelength sensitive opsins (SWS1 and SWS2) exhibited heterogeneous recovery patterns. SWS2 had an average completeness of around 82.7% and was broadly recovered across most species, whereas SWS1 showed a lower average completeness (~71.1%) and was more inconsistently recovered, with some taxa (such as certain *Hyperolius* and *Cophixalus* species) showing fragmented or missing sequences. The long-wavelength sensitive opsin gene (LWS) demonstrated a mean recovery of approximately 80.3%, with variability among species. Overall, LWS and SWS2 genes were more consistently recovered than SWS1.

The recovery of opsin genes in Sooglosidae species showed generally high completeness, with some variation among species and genes. Long-wavelength sensitive opsin (LWS) was recovered with an average completeness of approximately 87.5%, with *Sooglossus thomasetti* and *Sechellophryne gardinieri* showing the highest completeness (>97%), while *Staurois latopalmatus* exhibited lower coverage (~53.7%). Rhodopsin (RH1) sequences were overall well recovered with a mean completeness of about 91.9%, although *Heleophryne regis* showed relatively lower completeness (~61.7%). Short-wavelength sensitive opsins showed more variation: SWS1 averaged 78.0% completeness, with *Staurois latopalmatus* at the lower end (~37.8%), and SWS2 averaged 80.0%, with similar low recovery in *Heleophryne regis*(~45.3%) and *Staurois latopalmatus* (~49.4%).

The recovery percentages of opsin genes in the Strabomantidae family show considerable variation across species. The SWS2 gene is recovered with high completeness in species such as *Acris blanchardii* and *Brachycephalus pitanga*, both exceeding 99%, whereas in *Haddadus binotatus* recovery drops significantly to just over 42%. On average, the recovery of SWS2 across the studied species is approximately 82.6%, reflecting generally good but uneven coverage. Similarly, the SWS1 gene exhibits high recovery in *Acris blanchardii* and *Brachycephalus pitanga* with nearly complete sequences, but again decreases in some species such as *Haddadus binotatus*, which shows less than 50% recovery. The mean recovery across

species for SWS1 is about 82%, demonstrating variability but an overall solid representation For the RH1 gene, recovery levels are mostly high across species, with perfect or near-perfect recovery in *Craugastor augusti*, *Noblella lochites*, and *Acris blanchardii*. This gene has the highest mean recovery of the four opsins, at nearly 89%, indicating its sequences are well captured in most taxa sampled. In contrast, the LWS gene shows greater disparity among species. While *Acris blanchardii* and *Noblella lochites* again show almost complete recovery above 99%, other species such as *Ischnocnema parva* have lower recovery, falling below 50%. Overall, LWS has an average recovery of around 74%, which is noticeably lower than RH1 and reflects more challenges in recovering this gene consistently across the family.

Supplemental Tables

Table S 1. Results of the BUSTED analysis for episodic diversifying selection in the RH1 gene using all branches of the phylogenetic tree as test branches. The table includes log-likelihood (Log(L)), corrected Akaike Information Criterion (AICc), number of parameters (Params), and estimates of nonsynonymous (ω) and synonymous substitution rates with their respective site proportions and coefficients of variation (CoV). The likelihood ratio test indicated significant evidence of episodic diversifying selection ($p < 0.0001$), suggesting adaptive episodes affecting specific sites and branches within RH1.

Model	Log (L)	AIC-c	Params.	Rate distribution
Unconstrained model	−48104.4	97880.4	831	**Tested ω** 0.03495 (92.051%) 1.000 (7.7697%) 56.85 (0.17980%) Mean = 0.2121, CoV = 11.40
Unconstrained model				**Synonymous rates** 0.3045 (31.270%) 0.9078 (48.924%) 2.326 (19.806%) Mean = 1.000, CoV = 0.7097
Constrained model	−48252.4	98174.5	830	**Tested ω** 0.000 (87.214%) 1.000 (11.751%) 1.000 (1.0347%) Mean = 0.1279, CoV = 2.612
Constrained model				**Synonymous rates** 0.3034 (30.444%) 0.9023 (50.060%) 2.339 (19.497%) Mean = 1.000, CoV = 0.7085

Table S 2. Results of the BUSTED analysis for episodic diversifying selection in the SWS1 gene using all branches of the phylogenetic tree as test branches. The table includes log-likelihood (Log(L)), corrected Akaike Information Criterion (AICc), number of parameters (Params), and estimates of nonsynonymous (ω) and synonymous substitution rates with their respective site proportions and coefficients of variation (CoV). The likelihood ratio test indicated significant evidence of episodic diversifying selection ($p < 0.0001$), suggesting adaptive episodes affecting specific sites and branches within SWS1.

Model	Log (L)	AIC-c	Params	Rate distribution
Unconstrained model	−50088.1	101687	751	**Tested ω** 0.05896 (93.816%) 1.000 (6.1204%) 1392 (0.063234%) Mean = 0.9967, CoV = 35.10
Unconstrained model				**Synonymous rates** 0.6112 (52.183%) 1.185 (37.696%) 2.317 (10.121%) Mean = 1.000, CoV = 0.5171
Constrained model	−50181.7	101872	750	**Tested ω** 0.03664 (90.874%) 1.000 (9.1046%) 1.000 (0.021814%) Mean = 0.1246, CoV = 2.227
Constrained model				**Synonymous rates** 0.6111 (51.143%) 1.176 (38.249%) 2.241 (10.609%) Mean = 1.000, CoV = 0.5025

Table S 3. BUSTED analysis results for episodic diversifying selection in the SWS2 gene, using all branches in the phylogeny as test branches. Reported values include the log-likelihood (Log L), corrected Akaike Information Criterion (AICc), number of estimated parameters (Params), and distributions of nonsynonymous (ω) and synonymous substitution rates across codon classes. The likelihood ratio test indicated strong evidence of episodic diversifying selection ($p < 0.0001$), with a small proportion of sites evolving under high nonsynonymous rates on a subset of branches, consistent with punctuated adaptive evolution in this gene.

Model	Log (L)	AIC-c	Params	Rate distribution
Unconstrained model	−43756.1	88861.8	671	**Tested ω** 0.02989 (74.699%) 0.3199 (25.229%) 205.7 (0.072427%) Mean = 0.2520, CoV = 21.95
Unconstrained model				**Synonymous rates** 0.5188 (47.159%) 1.156 (42.271%) 2.524 (10.569%) Mean = 1.000, CoV = 0.6041
Constrained model	−43833.3	89014.3	670	**Tested ω** 0.04698 (76.607%) 0.05692 (16.484%) 1.000 (6.9089%) Mean = 0.1145, CoV = 2.108
Constrained model				**Synonymous rates** 0.5005 (42.880%) 1.092 (43.641%) 2.291 (13.479%) Mean = 1.000, CoV = 0.5789

Table S 4. BUSTED analysis results for episodic diversifying selection in the LWS gene, considering all branches in the phylogeny as test branches. The table includes log-likelihood (Log(L)), corrected Akaike Information Criterion (AICc), number of parameters (Params), and estimates of nonsynonymous (ω) and synonymous substitution rates, with site proportions and coefficients of variation (CoV). The likelihood ratio test indicates significant evidence for episodic diversifying selection ($p < 0.0001$), suggesting adaptive evolution at specific sites and branches within the LWS gene.

Model	Log (L)	AIC-c	Params.	Rate distribution
				Tested ω
Unconstrained model	−48717.2	99013.3	785	1.000 (7.3882%) 0.03944 (92.503%) 101.3 (0.10854%)
				Mean = 0.2204, CoV = 15.17
				Synonymous rates
Unconstrained model				0.4586 (33.607%) 0.9883 (53.629%) 2.475 (12.764%)
				Mean = 1.000, CoV = 0.6133
				Tested ω
Constrained model	−48810.2	99197.3	784	1.000 (10.477%) 0.01059 (88.619%) 1.000 (0.90414%)
				Mean = 0.1232, CoV = 2.551
				Synonymous rates
Constrained model				0.4515 (32.573%) 0.9729 (53.783%) 2.416 (13.643%)
				Mean = 1.000, CoV = 0.6100